In vivo characterization of genetic factors involved in *Xmrk* driven melanoma formation in Medaka (*Oryzias latipes*): a closer look at *braf, Stat5* and *c-myc*

In vivo Charakterisierung genetischer Faktoren mit Einfluss auf Xmrk induzierte Melanome in Medaka (*Oryzias latipes*): Untersuchung von *braf, Stat5* und *c-myc*.

Doctoral thesis for a doctoral degree at the Graduate School of Life Sciences, Julius-Maximilians-Universität Würzburg

Submitted by

Luciana Alcantarino Menescal
from
Belém (Brazil)

Würzburg, 2012

Submitted on: ....

Members of the Promotionskomitee:

Chairperson: Alexander Buchberger

Primary supervisor: Prof. Dr. Dr. Manfred Schartl

Supervisor (Second): Prof. Dr. Stefan Gaubatz

Supervisor (Third): Prof. Dr. Christoph Winkler

Date of public defence: ....

Date of receipt of certificates: ....

AFFIDAVIT

I hereby confirm that my PhD thesis entitled "In vivo characterization of genetic factors involved in Xmrk driven melanoma formation in Medaka (Oryzias latipes): a closer look at braf, Stat5 and c-myc" is the result of my own work. I did not receive any help or support from commercial consultants. All sources and/or materials applied are listed and specified in the thesis.

Furthermore, I confirm that this thesis has not yet been submitted as part of another examination process neither in identical nor in similar form.

Place, Date   Signature

ACKNOWLEDGEMENTS

INDEX

SUMMARY

Melanoma arises from the malignant transformation of melanocytes and is one of the most aggressive forms of human cancer. In fish of the genus *Xiphophorus,* melanoma development, although very rarely, happens spontaneously in nature and can be induced by interspecific crossing. The oncogenic receptor tyrosine kinase, Xmrk, is responsible for melanoma formation in these fishes. Since *Xiphophorus* are live-bearing fishes and therefore not compatible with embryonic manipulation and transgenesis, the Xmrk melanoma model was brought to the medaka (*Oryzias latipes*) system. *Xmrk* expression under the control of the pigment cell specific *mitf* promoter leads to melanoma formation with 100% penetrance in medaka. Xmrk is an orthologue of the human epidermal growth factor receptor (EGFR) and activates several downstream signaling pathways. Examples of these pathways are the direct phosphorylation of BRAF and Stat5, as well as the enhanced transcription of C-myc. BRAF is a serine-threonine kinase which is found mutated at high frequencies in malignant melanomas. Stat5 is a transcription factor known to be constitutively activated in fish melanoma. C-myc is a transcription factor that is thought to regulate the expression of approximately 15% of all human genes and is involved in cancer progression of a large number of different tumors.

To gain new *in vivo* information on candidate factors known to be involved in melanoma progression, I identified and analysed BRAF, Stat5 and C-myc in the laboratory fish model system medaka. BRAF protein motifs are highly conserved among vertebrates and the results of this work indicate that its function in the MAPK signaling is maintained in medaka. Transgenic medaka lines carrying a constitutive active version of BRAF (V614E) showed more pigmented skin when compared to wild type. Also, some transiently expressing BRAF V614E fishes showed a disrupted eye phenotype. In addition, I was able to identify two Stat5 copies in medaka, named Stat5ab/a and Stat5ab/b. Sequence analysis revealed a higher similarity between both Stat5 sequences when compared to either human Stat5a or Stat5b. This suggests that the two Stat5 copies in medaka arose by an independent duplication processes. I cloned these two Stat5 present in medaka, produced constitutive active and dominant negative gene versions and successfully established transgenic lines carrying each version under the control of the MITF promoter. These lines will help to elucidate questions that are still remaining in Stat5 biology and its function in melanoma progression, like the role of Stat5 phosphorylation on tumor invasiveness.

In a third project during my PhD work, I analysed medaka C-myc function and indentified two copies of this gene in medaka, named *c-myc17* and *c-myc20*, according to the chromosome where they are located. I produced conditional transgenic medaka lines carrying the *c-myc17* gene coupled to the hormone binding domain of the estrogen receptor to enable specific transgene activation at a given time point. Comparable to human C-myc, medaka C-myc17 is able to induce proliferation and apoptosis *in vivo* after induction. Besides that, C-myc17 long-term activation led to liver hyperplasia.

In summary, the medaka models generated in this work will be important to bring new *in vivo* information on genes involved in cancer development. Also, the generated transgenic lines can be easily crossed to the melanoma developing *Xmrk* medaka lines, thereby opening up the possibility

to investigate their function in melanoma progression. Besides that, the generated medaka fishes make it possible to follow the whole development of melanocytes, since the embryos are transparent and can be used for high throughput chemical screens.

ZUSAMMENFASSUNG

Melanome entstehen durch die krankhafte Transformation von Melanozyten und sind eine der aggressivsten Krebsarten beim Menschen. In Fischen der Gattung *Xiphophorus* können, wenn auch sehr selten, spontan Melanome entstehen oder durch spezielle Artenkreuzungen induziert werden. Grundlage für das Entstehen der Melanome in diesen Fischen ist die Rezeptortyrosinkinase Xmrk. Da alle Xiphophorus-Arten lebendgebärend sind und keine Manipulationen an Embryonen vorgenommen werden können, wurde ein Xmrk Melanommodell für Medaka (*Oryzias latipes*) etabliert. Die Expression von *Xmrk* in Pigmentzellen dieser Fischart resultiert mit 100%iger Penetranz in Melanomen. Das Xmrk ist ein Ortholog des menschlichen „epidermal growth factor" (EGFR) und aktiviert verschiedene nachgeschaltete Signalwege. Beispiele für diese Aktivierungen sind die Phosphorylierung von BRAF, Stat5 und die erhöhte Expression von c-myc. BRAF ist eine Serin-Threoninkinase, welche oft in malignen Melanomen mutiert ist. Stat5 ist ein Transkriptionsfaktor, welcher dauerhaft in Fischtumoren aktiviert ist. C-myc ist ein Transkriptionsfaktor, welcher etwa 15% aller menschlichen Gene sowie die Entstehung vieler menschlicher Tumore reguliert.

Um neue Einsichten in die Funktion der Kanidatengene im Prozess der Melanomentstehung *in vivo* zu erlangen, habe ich Orthologe von BRAF, Stat5 und C-myc bei Medaka identifiziert und analysiert. Die Domänen des BRAF Proteins sind hoch konserviert in allen Vertebraten. Weiterhin deuten die Ergebnisse meiner Arbeit auf eine Beibehaltung der Funktionen im MAPK Signalweg hin. Transgene Medakalinien, welche eine dauerhaft aktive Version des BRAF Gens (V614E) exprimieren, weisen einerseits eine stärkere Hautpigmentierung auf. Weiterhin treten in diesen Fischen Veränderungen der Augen auf. In einem weiteren Projekt meiner Arbeit gelang es mir, zwei Kopien des Stat5 Gens im Medaka zu identifizieren, Stat5ab/a und Stat5ab/b. Sequenzanalysen zeigten eine höhere Übereinstimmung zwischen den beiden Genkopien, als zwischen denen von Medaka und Menschen. Dieses Ergebnis deutet darauf hin, dass die beiden Medaka Gene durch eine unabhängige Duplikation entstanden. In meiner Arbeit habe ich beide Gene des Medakas kloniert und jeweils eine konstitutiv aktive und eine dominant negative Version der Gene hergestellt. Weiterhin konnte ich erfolgreich für jede Genversion eine transgene Medakalinie etablieren, welche die verschiedenen Genvarianten unter der Kontrolle des pigmentzellspezifischen Promoters des *mitf* Gens exprimieren. Diese Linien werden in Zukunft helfen, den Einfluss von Stat5 Signalen auf den Prozess der Melanomverbreitung und dessen Invasivität zu erklären.

In einem dritten Projekt meiner Doktorarbeit untersuchte ich das Vorkommen und die Funktion der C-myc Gene des Medakas. Ich konnte zwei Genkopien identifizieren, *c-myc17* und *c-myc20*, welche auf unterschiedlichen Chromosomen lokalisiert sind. Ich konnte induzierbare, stabil transgene Linien herstellen, welche ein Fusionsprotein aus C-myc17 und der Hormonbindungsdomäne des Östrogenrezeptors von Maus exprimiert. Diese Linie ermöglichte eine induzierbare Aktivität des Transgens. Vergleichbar zum menschlichen MYC ist C-myc17 fähig, nach Aktivierung Proliferation und Apoptose *in vivo* auszulösen. Dauerhafte Aktivierung über einen längeren Zeitraum führt in diesen Linien zu Hyperplasie in Leber.

Die verschiedenen Fischmodelle, die während dieser Arbeit generiert wurden, werden essentiell sein, um neue Einsichten in die Rolle diese Faktoren während der Krebsentwicklung *in vivo* zu erlangen. Weiterhin ermöglichen diese transgenen Linien durch einfaches Auskreuzen auf Xmrk Linien, deren Einfluss auf die Verbreitung von Melanomen zu untersuchen. Letztendlich sind mit diesen Linien auch Untersuchungen der Entwicklung von Pigmentzellen über Zeit möglich, da die Embryonen transparent sind und sich für chemisches Hochdurchsatz-Screening eignen.

1. INTRODUCTION

1.1 Melanoma

Skin cancer is the third most common human cancer, and its global incidence is rising every year. There are an estimated 2-3 million cases of skin cancer in the world every year and although melanoma only accounts for 132,000 cases, it is responsible for most skin cancer deaths (World Health Organization). If melanoma is diagnosed early it can be cured by surgical procedures. However, metastatic malignant melanoma often does not respond to therapies and has a poor prognosis (Smalley, 2009).

Melanoma arises from the malignant transformation of melanocytes, specialized pigment cells found predominantly in the skin and eyes (White and Zon, 2008). Both genetic and environmental factors are believed to contribute to melanoma genesis (Gray-schopfer *et al*, 2007). Accounting for environmental factors, ultraviolet (UV) light exposure has a causal role in melanoma initiation (Maddodi and Setaluri, 2008). In response to UV light-induced DNA damage in keratinocytes, melanocytes synthesize melanin, which is a protective pigment. Extreme UV exposure (sunburn) can lead to massive keratinocyte population death, but melanocytes survive due to their efficient DNA damage repair response and therefore have the chance to accumulate mutations (Gilchrest *et al*, 1999). However, the underlying mechanisms that cause a normal melanocyte to become a malignant melanoma are only partly understood.

Several types of malignant melanoma can be determined. The most incident is the cutaneous melanoma which comprises about 91% of all melanomas (Netscher *et al*., 2011). Other melanoma types like uveal (ocular) and mucosal account for about 5% and 1,5% of the cases, respectively (Patrick *et al*, 2007; Triozzi *et al*, 2008).

1.1.1 Melanocytes

Melanocytes are pigment-synthesizing cells of the neural-crest lineage that provide skin tone, hair colour and protection from ultraviolet radiation (Thomas and Erickson, 2008). Melanin, the principal component of the melanocyte, helps to protect from high levels of reactive oxygen species and direct UV radiation that would otherwise damage DNA in skin cells (White and Zon, 2008). Melanocytes in mammals and birds produce two chemically distinct types of melanin pigment: the brown/black eumelanin and the yellow/reddish pheomelanin (Meredith and Sarna, 2006). Melanin pigments in fishes are essentially eumelanic (Ito and Wakamatsu, 2003).

During normal development, a strict program of subsequent transcription factor activation results in normal differentiation of melanocytes from neural crest cells (for a complete description see Hirobi *et al*, 2011). Factors like the microphthalmia-associated transcription factor (Mitf), the paired domain and homeodomain containing transcription factor Pax3, and the Sry-related transcription factor Sox10 play key roles in the switch from neural crest to melanocyte genesis. Loss of any of the three results in failure of melanoblast development (Thomas and Erickson,

2008). Although Pax3 and Sox10 are necessary for melanoblast specification, it is Mitf that is referred as the master regulator of melanocyte development (Steingrímsson *et al*, 2004). Loss of Mitf function results in almost complete loss of melanocytes in mice and zebrafish (Lister *et al*, 1999). Mitf regulates the melanocyte lineage by activating several pigment-producing genes, such as *dct* and *tyrosinase* (Yasumoto *et al*, 1994).

1.1.2 The genetics of human melanoma

Evidence for an increasing number of genetic factors contributing to melanoma genesis was found in different studies. Linkage-analysis studies of families with a high incidence of melanoma identified two susceptibility genes: CDKN2A and CDK4 (Nobori *et al*, 1994). Also, a pigmentation-associated predisposition to skin cancer has been indicated by the association of the melanocortin-1 receptor (MC1R) variation polymorphism leading to red hair, fair skin inability to tan and tendency to freckle with skin cancers (Palmer *et al*., 2000). The MC1R and its ligand, the α-melanocyte-stimulating hormone (α-MSH), comprise key determinants of the pigmentary process (Chin, 2003). The result of their signalling cascade activates the protein kinase A (PKA), which then translocates to the nucleus where it phosphorylates CREB, a family of transcription factors that induce the expression of genes containing CRE sequences in their promoters, like *mitf*.

MITF is considered the master regulator of melanocyte lineage and therefore, not surprisingly, plays also a role in melanoma (Levy *et al*, 2006). Using primary melanoma tissue microarrays, MITF was found to be amplified in 10-20% of the cases, with a higher incidence in metastatic melanomas (Garraway *et al*., 2005). Due to its essential role in melanocyte biology, MITF protein levels must be under strict control. Gray-Schopfer *et al* (2007) propose that MITF regulates distinct functions in melanocytic cells at different levels of expression. High levels predispose cells to cell cycle arrest and differentiation, while low levels lead to cell cycle arrest and apoptosis; intermediate levels favour proliferation.

The Ras/Raf/MEK/MAPK pathway, also known as MAPK (mitogen-activated protein kinase) pathway, has a key role in the proliferation of most solid tumours, including melanoma (Fecher *et al*, 2008). The most commonly mutated component of the MAPK pathway is BRAF, which is mutated in 50 to 70% of all human melanomas (Davies *et al*., 2002). Another important oncogene in melanoma, found mutated in 15% to 30% of melanomas, is NRAS (Gray-Schopfer *et al*, 2007). BRAF and NRAS mutations are mutually exclusive; they are not both found mutated in the same cancer (Chin *et al*, 2006).

Another signalling pathway that is important for melanoma is the PTEN/PI3K/AKT pathway (Wu *et al*, 2003). Activation of the PI3K/AKT pathway in melanoma occurs through either growth factors or the loss of expression and/or mutation of negative pathway regulator (Smalley, 2009). PTEN encodes a negative regulator of the PI3K pathway, and allelic loss or mutation of PTEN has been described in 5-15% of melanoma specimens and metastasis (Guldberg*et al*, 1997).

Besides these, several studies have implicated deregulated Notch signalling in patients with melanoma (Hoek *et al*., 2004; Liu *et al*., 2006; Qin *et al*., 2004). Mutation in Beta-catenin, the central activator of Wnt signalling, is very rare in melanoma (Pollock and Hayward, 2002). However, overexpression of Wnt5a, a member of the noncanonical Wnt pathway, might play an important role in melanoma invasion and metastasis (Bittner *et al*., 2000; Dissanayake *et al*., 2008). In addition, autocrine activation of HGF/SF-MET signalling pathway has been shown in melanoma, stimulating proliferation and motility of human melanocytes in culture (Li *et al*., 2001).

In summary, recent investigations identified key signals in melanogenesis and melanoma progression, but the detailed interplay between the different pathways *in vivo* is still unknown.

1.1.3 Melanoma models in mammals

Exposure to ultraviolet radiation in opossums (*Monodelphis domestica)* induced melanomas, leading to a variety of hyperplastic and neoplastic skin lesions (Kusewitt *et al*, 1991). Also, melanomas have been reported in guinea pigs and hamsters after exposure to chemical carcinogens. These tumours metastasize and show similarities in histopathology with human melanoma (Bardeesy *et al*, 2000).

In mice, several melanoma models have been generated (Becker *et al* 2010). SV40T antigen expressed under the control of the tyrosinase promoter, which targeted the transgene to melanocytes led to melanoma formation after UV light exposure, particularly ocular melanoma (Bradl *et al*, 1991). Initiation of melanoma using chemical carcinogens like 7,12-dimethylbenz(a)anthracene (Berkelhammer *et al*, 1982) and dimethylbenzanthracene (Kligman and Elenitsas, 2001) or combination of chemical and UV radiation (Strickland *et al*, 2000) have also been successfully applied.

In addition, several mouse (*Mus musculus*) models that spontaneously develop melanoma have been established. For example, mice with activated RAS and deletion of both INKA4a cooperate to accelerate melanoma development (Chin *et al*, 1997). Also, mice develop spontaneous melanoma after RAS activation in a p53 negative background (Bardeesy *et al*, 2001). Besides these, BRAF V600E cooperates with the loss of the tumour suppressor PTEN to induce metastatic melanoma Dankort *et al*, 2009). Another model using BRAF to induce melanoma in mice was generated by Dhomen *et al* (2009). In this study the inducible expression of BRAF V600E in mouse melanocytes stimulates skin hyperpigmentation, the appearance of senescent nevi, and the development of melanoma.

1.1.4 Melanoma models in fish

As mentioned above with focus on melanoma, mammalian models are widely used in cancer research due to their evolutionary relatedness with humans, with comparable cell lineage and differentiation pathways (Cheon and Orsulic, 2011). However, fish models that mimic human

diseases and cancer are extensively used in the scientific field nowadays (Stoletov and Klemke, 2008). Advantages of fish models, specially two teleost species – zebrafish (*Danio rerio*) and medaka (*Oryzias latipes*) - in research include: their high fecundity, their short breeding cycles to produce large numbers of progeny, their technically easy exposure to carcinogenesis, and the possibility to follow well-defined stages of the disease *in vivo* over time (Patton *et al*, 2010). Furthermore, in terms of genomic, these teleost dispose of a variety of genetic tools including detailed gene map and genome sequence (Flicek *et al*., 2011) and a large variety of mutants (Amsterdam and Hopkins, 2006; Patton and Zon, 2001), including pigmentation mutants (Lynn Lamoreux *et al*, 2005; Parichy, 2006). Also innovative experimental tools, such as morpholinos (Nasevicius and Ekker, 2000), efficient transgenic animal production (Kawakami, 2005; Thermes *et al*, 2002), high throughput screening of mutants (Amsterdam and Hopkins, 2006; Furutani-Seiki *et al*., 2004; Patton and Zon, 2001), and screening of small molecules (Zon and Peterson, 2005) are available. Therefore fishes are widely used as disease models or in cancer research (Mione and Trede, 2010).

Today, a number of melanoma fish models are available showing similar histopathology with human melanoma (Patton *et al*, 2010). A constantly activated version of the human oncogene BRAF (BRAF V600E) driven by the *mitfa* promoter drives non tumorigenic ectopic melanocytic lesions in zebrafish (Patton *et al*, 2005). However, to develop malignant melanoma, these fishes need to carry an additional inactivating mutation in *p53,* demonstrating that at least one additional genetic mutation is required for melanoma formation by overexpression of BRAF V600E. The p53 gene is the most frequently mutated gene in human cancer and p53 from zebrafish shares strong sequence and functional homology with human (Berghmans *et al*., 2005). The melanoma in these fishes appeared by 16 weeks of age, was highly invasive and showed genomic instability.

In addition, constitutive activation of NRAS under the mitfa promoter in a p53 negative background also leads to melanoma formation in zebrafish (Dovey *et al*, 2009). Melanomas in these fishes are variably pigmented and share features with human melanoma. Another melanoma model in zebrafish was driven by constitutive expression of HRAS oncogene without the need for a second inactivating mutation in tumour suppressors. Fishes carrying human HRASV12 expressed under the *mitfa* promoter (Michailidou *et al*., 2009) develop melanoma after 16 weeks. By contrast, expression of HRAS-V12 under the control of another pigment cell specific promoter, *kita*, leads to early onset and highly penetrant melanoma after 4 weeks in zebrafish (Santoriello *et al*., 2010). This difference may be due to the higher levels of HRASV12 expression driven by the *kita* and/or to different cell specificity of the *kita* and *mitf* promoters. In contrast to the BRAF V600E and NRAS-Q61K models, HRAS-V12 show ectopic melanocyte patterns during early embryogenesis that can rapidly become melanoma within a few weeks of development.

1.1.5 The *Xmrk* melanoma model

In fish of the genus *Xiphophorus,* melanoma development happens spontaneously in nature and can be induced by interspecific crossing (Meierjohann *et al*, 2004). The classical crossing experiment involves *X. maculates* which carries a dominant tumour inducing locus (*Tu* for tumour) and a *Tu*-repressing regulatory locus (*R*), and *X. helleri* which lacks both loci (Fig. 1, Gordon, 1947). As both loci are located on different chromosomes, it is possible to separate them through selective breeding. According to Mendelian inheritance, a cross between these two *Xiphophorus* species produces heterozygous hybrids. Further crosses of these hybrids with *X. helleri* result in 25% of fishes carrying the tumour gene but lacking the repressor (Meierjohann and Schartl, 2006). These fishes develop melanoma with 100% of penetrance.
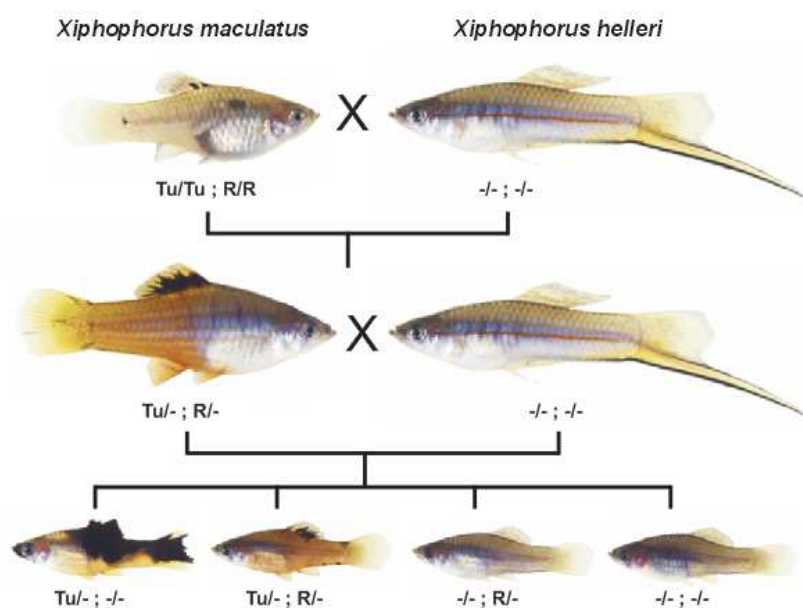
Fig. 1. Crossing experiment leading to spontaneous melanoma formation. Adapted from (Meierjohann and Schartl, 2006). *Xiphophorus maculatus* bears the tumorigenic (*Tu*) and the repressor (*R*) loci, while *Xiphophorus helleri* lacks both. An intercross between these two species produces a generation of heterozygous hybrids in both loci. A second generation (result from a cross of this heterozygous hybrids and the wild type *X. Helleri*) produces 25% of fishes bearing the Tu locus and lacking the repressor resulting in fishes that develop spontaneously melanoma.

The receptor tyrosine kinase gene *Xmrk* (*Xiphophorus* melanoma receptor kinase) was identified by positional cloning as the oncogenic determinant encoded by the *Tu* locus (Wittbrodt *et al*, 1989). Disruption of this gene leads to loss of function with respect to melanoma formation (Schartl *et al*, 1999). Xmrk is apparently restricted to the genus *Xiphophorus* (Weis and Schartl, 1998). The Xmrk repressor present in locus *R* could not be identified up to now. Xmrk is an orthologue of the human EGF receptor (Gómez *et al*, 2004). While the EGF receptor is inactive in absence of the respective ligand and signals only after growth factor binding, Xmrk is constitutively active independent of ligand activation (Wittbrodt *et al*, 1992). The oncogenic properties of Xmrk derive from two amino acid changes in the extracellular domain in comparison to the EGF receptor. These mutations result in the formation of cysteine bridges between two receptors monomers, which leads to constitutive activation of Xmrk (Gómez *et al*, 2001).

Xiphophorus are live-bearing fishes and, therefore, are not compatible with embryo manipulation and transgenesis comparable to other laboratory fish species. Hence, the *Xmrk* melanoma model was brought to the medaka system (Schartl *et al*., 2010). To induce expression of *Xmrk* in pigment cells of medaka, a stable transgenic fish line was generated in which the tumorigenic coding sequence of *Xmrk* is expressed under the control of the medaka *mitfa* promoter (Fig. 2). While in *Xiphophorus* tumorigenic activation of *Xmrk* results only in melanoma formation, in medaka the expression of *Xmrk* under the *mitfa* promoter results in melanoma as well as in pigment cell tumours arising from xanthophores and erythrophores (Schartl *et al*., 2010). Conclusively, *Xmrk* is a powerful and dominant oncogene driving melanoma formation, not only necessary but also sufficient for tumour formation.
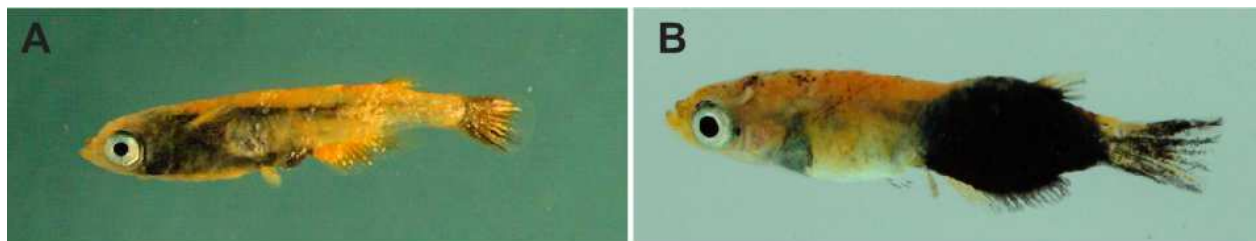
Fig. 2. Mitf:*Xmrk* transgenic medakas bearing melanoma. (A) Medaka fish bearing exophytic xanthoerythrophoromas. (B) Medaka fish bearing invasive extracutaneus melanoma. Pictures were taken by Manfred Schartl.

Interestingly, the genetic background seems to play a role in melanoma formation in medaka. The *Carbio* strain developed almost exclusively exophytic xanthoerythrophoromas, and invasiveness was only observed at terminal stages (Fig. 2A). In the *HB32C* strain, almost all tumours were invasive extracutaneus melanoma (Fig. 2B). In the albino (*i-3*) genetic background, transgenic fishes showed hyperpigmentation of xanthophores that rarely developed into tumours (Schartl *et al*., 2010).

1.1.6 Medaka as a model organism

Medaka (*Oryzias latipes)* is a small (2-4 cm long), freshwater teleost fish originating from Southeast Asia. They can be easily maintained and bred under laboratory conditions. Males and females can be distinguished due to their distinct dorsal and anal fins (Wittbrodt *et al*, 2001). Spawning is under strict control of light, temperature and food availability. Under laboratory conditions, fish are kept under a light cycle corresponding to summer conditions (14h light 10h dark). Water temperatures between 25 to 28°C are standard under laboratory conditions. Medakas are fed with synthetic diets and brine shrimp (Shima and Mitani, 2004).

Medaka fishes have external fertilization similar to zebrafish (*Danio rerio*), but in contrast to these, their eggs are kept attached to the female belly for several hours. Also, medaka fishes have a large number of offspring per week, as each female lays between 10-50 eggs per day (Takeda and Shimada, 2010). Besides that, the laid eggs have a fast embryonic development when compared to mammals. Additionally, embryos have optical clearance allowing close tracing of

development (Wittbrodt *et al.*, 2001). Early development is synchronous, and the fully transparent embryos are easily staged under the microscope according to a set of morphological criteria (Iwamatsu, 2004). All these features made Medaka one of the most famous fish model organism in science nowadays.

1.2 Oncogenic signalling of Xmrk

To be fully tumorigenic, a potential cancer cell must show uncontrolled cell proliferation, anti-apoptosis signalling, as well as inhibition of differentiation, the ability to migrate and invade other tissues and induce vascularisation (Cree, 2011). Normally, the route to a malignant tumour involves multiple steps to achieve all the requirements mentioned above. However, the single step of *Xmrk* expression leads to malignant melanoma formation in medaka fishes (Schartl *et al.*, 2010). Downstream signalling of *Xmrk* has been well studied *in vitro* and explains the reason for this: *Xmrk* signalling is involved in many of the tumorigenic events necessary for cancer formation and maintenance (Fig. 3, Meierjohann and Schartl, 2006).
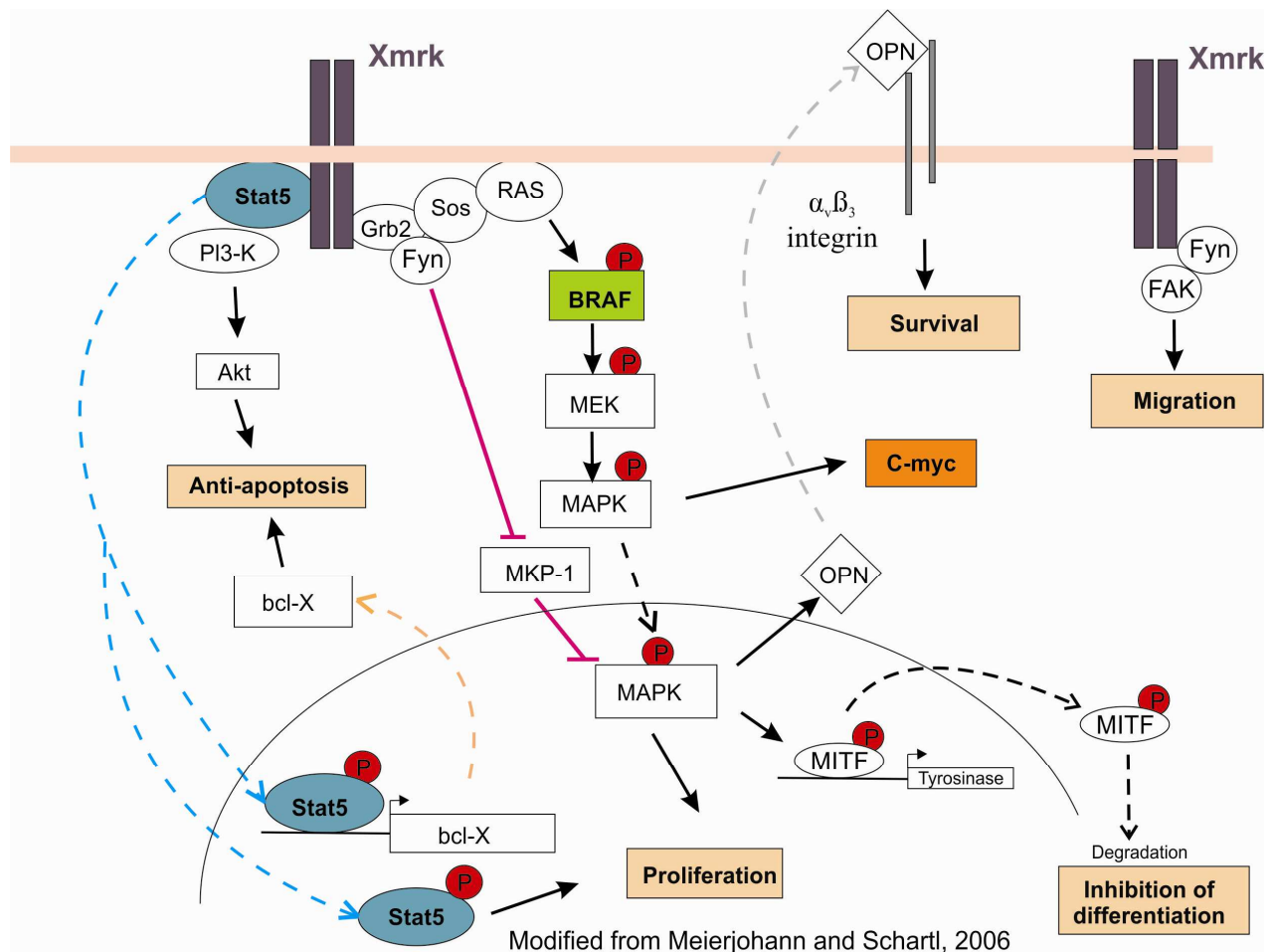
Fig. 3. Schematic representation of the *Xmrk* signalling cascade.

As a growth factor receptor, *Xmrk* is placed at the top of many signal transduction pathways (Fig. 3). Like other receptor tyrosine kinases, it possesses a carboxy-terminus which contains specific substrate binding sites (Meierjohann *et al*, 2004). Certain phosphorylated tyrosine residues serve

as sites for adapter proteins with src homology (Wellbrock and Schartl, 1999). The resulting association of these proteins is followed by the induction of the RAS-RAF-MAPK (mitogen-activated protein kinase, section 1.3) pathway, which affects proliferation, survival and differentiation. Accordingly, PSM cells, which are derived from malignant *Xiphophorus* melanoma, exhibit permanently elevated levels of phosphorylated BRAF, MEK and ERK (Wellbrock and Schartl, 1999). The src kinase fyn is also associated with the C-terminus of Xmrk and enhances the MAPK signalling cascade by inhibiting MKP-1 (Wellbrock *et al*, 2002). PI3K is another protein that binds to phosphorylated tyrosine residues of Xmrk. It becomes activated and induces anti-apoptotic signals via its downstream effector Akt (Wellbrock and Schartl, 2000).

The transcription factor Stat5 (signal transducer and activator of transcription 5, section 1.4) is activated by *Xmrk* (Baudler *et al*, 1999) and promotes both proliferation (Morcinek *et al*, 2002) and, in cooperation with the phosphatidylinositol 3-kinase (PI3-K), anti-apoptotic events (Hassel *et al*, 2008). While other Stat proteins bind to phosphorylated tyrosine residues of the intracellular part of receptor tyrosine kinases, an unusual tyrosine-phosphate-independent type of binding of Stat5 to Xmrk was found (Morcinek *et al*, 2002). After this interaction, phosphorylated Stat5 translocates to the nucleus where it activates specific target genes like the anti-apoptotic protein bcl-x.

Recent studies have suggested that c-myc (section 1.5) overexpression correlates with overall survival in melanomas (Schlagbauer-Wadl *et al*., 1999). An unpublished work performed in Manfred Schartl's laboratory detected higher *c-myc* expression after *Xmrk* activation in Melan A cells (internal communication).

1.3 BRAF

1.3.1 RAF kinase family

BRAF (also known as proto-oncogene B-Raf or v-Raf murine sarcoma viral oncogene homolog B1) is a serine-threonine kinase, and together with ARAF and CRAF, forms the RAF kinase family in mammals (reviewed in Chong *et al*, 2003). The RAF proteins participate in the ERK/MAPK signalling cascade, which connects extracellular signals to transcription regulation, mediating cell growth, survival and differentiation (Robinson and Cobb, 1997).

RAF proteins share three conserved regions: CR1 (which bears a RAS-binding domain (RBD) and a Cystein-rich domain (CRD)) and CR2 are both regulatory and present in the N-terminus. Also, CR3 is present in the C-terminus and encompasses the kinase domain. CR3 contains two regions important for RAF activation: the activation segment and the negatively charged regulatory region (N-region, Fig. 4).
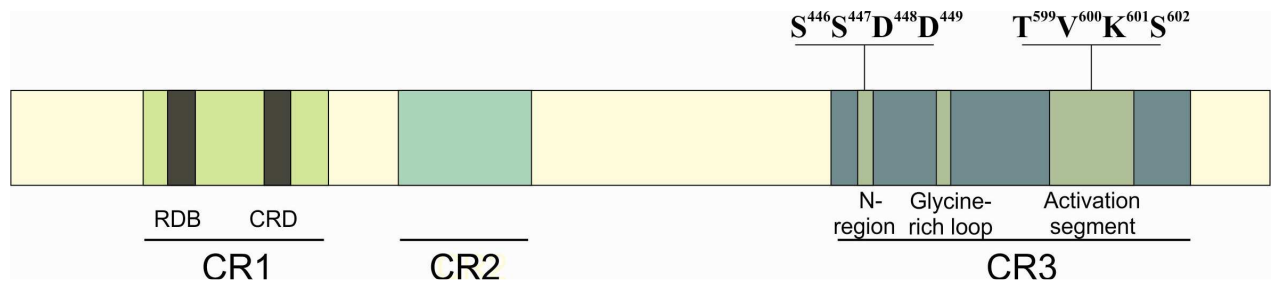
Fig. 4. Schematic representation of the human BRAF protein domains. Indicated amino acids represent important sites for BRAF activation, regulation and function. CR1, CR2 and CR3 = Conserved region 1, 2 and 3, respectively; RDB = Ras binding domain; CRD = cysteine rich domain

RAF proteins carry out non-redundant functions in development as knockout mice for either ARAF (Pritchard *et al*, 1996), BRAF (Wojnowski *et al*, 1997) and CRAF (Mikula *et al*., 2001) die during embryonic development or shortly after birth. However, these knockout studies revealed both overlapping and unique function for RAF isoforms. For example, in CRAF knockout mice, BRAF can compensate CRAF loss in the activation of the MAPK pathway (Mikula *et al*., 2001). Besides that, biochemical differences were also found in RAF isoforms. ARAF is a much weaker activator of MAPK than the other members of the RAF family. Also, ARAF can only activate MEK1, while BRAF and CRAF can activate MEK1 and MEK2 (Wu *et al*, 1996).

1.3.2 Regulation of BRAF kinase activity

Binding of extracellular ligands such as growth factors, cytokines and hormones to the corresponding cell surface receptor may lead to activation of RAS and subsequent initiation of BRAF activation. RAS proteins are small GTPases that mediate signalling by binding and hydrolyzing GTP and subsequent phosphorylation of downstream signalling factors (reviewed in Wellbrock *et al*., 2004). The active, GTP-bound form of RAS binds to BRAF through its RAS binding domain (RBD) and cysteine rich domain (CRD) present on CR1, leading to BRAF recruitment to the membrane characterizing the initial event in BRAF activation (Chong *et al*., 2003). Once activated, BRAF protein phosphorylates and activates MEK1 and 2, which in turn phosphorylate ERK1 and 2 (MAPKs, Wellbrock *et al*, 2004). Other substrates have been proposed for CRAF and ARAF, but only MEK1 and MEK2 have been identified as substrates for BRAF (Kolch, 2000).

Phosphorylation is an important mechanism by which BRAF activity is regulated. Activation of BRAF by RAS requires phosphorylation of T599 and S602 (Michaloglou, 2008). Also, another serine, S446, which is necessary for the activation of other RAF members, is constitutively phosphorylated in BRAF, while the corresponding serine in ARAF and CRAF is not. Besides that, the S446 is located adjacent to two aspartic acids (D448, D449) instead of two tyrosines which are present in ARAF and CRAF (Mason *et al*., 1999). These aspartic acids mimic phosphorylated tyrosines. As a result, BRAF has a stronger basal activity and requires fewer phosphorylation steps to be active.

1.3.3 BRAF mutations in melanoma

BRAF is the only RAF protein to be frequently mutated in cancer. Among human cancers, BRAF mutations are most common in melanoma (Michaloglou, 2008). Also, mutations in BRAF are found in thyroid cancer in about 45% of sporadic papillary thyroid cancers (Xing, 2005) and in colorectal cancer (Sharma and Gulley, 2010). So far, no ARAF mutations have been related to cancer (Lee *et al*., 2005). CRAF mutations are rarely found in human cancers (Emuss *et al*, 2005).

The highest incidence of BRAF mutations is detected in approximately 66% of all malignant melanoma (Davies *et al*., 2002). The prevalence of BRAF mutations is variable among different types of melanoma. They are most common in cutaneous melanoma, are rare in mucosal, acral, conjunctival melanoma and are not present in uveal melanoma (reviewed in Michaloglou, 2008).

Also, BRAF mutations were identified in papillary thyroid cancer (Fukushima *et al*., 2003), colorectal cancer (Sharma and Gulley, 2010) and ovarian cancer (Estep *et al*, 2007) in lower frequencies (reviewed in Garnett and Marais, 2004). Over 40 different missense mutations in BRAF, involving 24 different sites, have been identified (COSMIC web site: www.sanger.ac.uk/genetics/CGP/cosmic/). However, a thymidine to adenosine transversion at nucleotide 1796, leading to a valine to glutamic acid conversion (BRAF V600E), predominates in most cancer lesions (Davies *et al*., 2002). This specific mutation accounts for over 90% of BRAF mutations in melanoma (Thomas, 2006) and thyroid cancer (Fukushima *et al*., 2003). In addition, clinical data of a specific BRAF V600E inhibitor indicated a significant effect of BRAF function on melanoma progression (Bollag *et al*, 2010). These patients show regressing melanoma after BRAF V600E inhibition, but melanomas acquire resistance by RTK or NRAS upregulation (Nazarian *et al*, 2010).

The mutant amino acid V600 is situated between T599 and S602, whose phosphorylation is responsible and sufficient for BRAF activity. The V600E mutation is thought to mimic the phosphorylation in these sites, giving to BRAF a constitutive activity (Michaloglou, 2008). BRAF V600E activity is independent of the presence of a negative charge in the N-region (S446) normally required for wild type BRAF activation (Brummer *et al*., 2006). Besides that, cell lines expressing BRAF V600E are capable to signal independent of RAS activation (Davies *et al*., 2002).

1.3.4 BRAF V600E model organisms

Several BRAF V600E mouse models have been generated. Mutated BRAF under the control of a thyroid follicular cell specific promoter (thyroglobulin promoter) develops papillary thyroid carcinoma (PTC) (Knauf *et al*., 2005). Also, a knock in mutant mouse expressing BRAF V600E only after Cre-mediated recombination during development resulted in embryonic lethality (Mercer *et al*., 2005). Additionally, expression of this mutant BRAF in somatic tissues only induced proliferation in liver and spleen. Furthermore, these mice developed non-lymphoid neoplasia and died after 4 weeks due to bone marrow failure. In a second Cre-recombinase knock

in mouse, in which the expression of cre recombinase was driven exclusively in the lung epithelium, BRAF V600E mice developed multiple lung adenomas (Dankort *et al*., 2007). A melanoma mouse model was generated with the induction of BRAF V600E combined with the PTEN tumour suppressor silencing (Dankort, 2009). In addition, the inducible expression of BRAF in mouse melanocytes led to skin hyperpigmentation, appearance of nevi harbouring senescent melanocyte and melanoma development (Dhomen *et al*, 2009).

Fishes have also been used to study the role of BRAF V600E in living organisms. Zebrafish expressing mutated human BRAF under the control of the zebrafish mitfa promoter developed focal sites of melanocytes hyper proliferation, which did not progress to malignancy (Patton *et al*, 2005). However, in a p53 negative background, BRAF V600E fishes developed malignant melanoma (Patton *et al*, 2005). These transgenic zebrafish embryos for human BRAF V600 under the control of the mitfa promoter and lacking p53 have been used in another study to identify the initiating transcriptional events that occur on activation of human BRAF V600E in the neural crest lineage by performing a chemical genetic screen to identify small molecules suppressors of the neural crest lineage. (White *et al*, 2011) One class of compound, DHODH, led to almost complete abrogation of neural crest development. When used alone or in combination with a specific inhibitor of the BRAF V600E, DHODH led to decrease in melanoma growth *in vivo* as well as in mouse xenograft studies (White *et al*, 2011). The same zebrafish model has been used to test the ability of genes to cooperate with BRAF V600E to accelerate melanoma (Ceol *et al*, 2011). In this study, SETDB1, an enzyme that methylates histone H3 on lysine 9 (H3K9), was found to accelerate melanoma formation significantly in zebrafish. So far, no fish utilizing a fish specific braf or a medaka model bearing BRAF V600E mutation have been generated.

1.4 Stat5

1.4.1 Stat family

Signal transducers and activators of transcription (Stats), as the name indicates, comprise a family of genes that play a role as cytoplasmatic signalling proteins and as nuclear transcription factors, that activate a diverse set of genes, including some implied in cancer progression (Lim and Cao, 2006). Seven members of the Stat family have been identified in mammals: Stat1, Stat2, Stat3, Stat4, Stat5a, Stat5b and Stat6 (Santos and Costa-Pereira, 2011).

In general, Stats proteins contain between 750 and 850 amino acids and share 6 structurally and functionally divergent domains (Fig. 5, reviewed in Paukku and Silvennoinen, 2004). The N-terminal domain (N-term) is important for dimerization or tetramerization of Stat monomers as well as for nuclear translocation and protein-protein interactions. The coiled-coil domain is involved in the interaction with other proteins, like the silencing mediator for retinoic acid receptor and thyroid hormone receptor, leading to down regulation of Stat5 activity (Nakajima *et al*, 2001). Also present is a DNA binding domain (DBD), which is able to bind DNA in an activated STAT dimer and is involved in nuclear translocation. In close proximity to the DBD lies the linker domain (LD), which is involved in transcriptional activation. The most well conserved

domain in the structure of Stats is the SH2 domain, which is necessary for receptor association and tyrosine phosphodimer formation. The C-terminus incorporates the transactivation domain (TAD), which is poorly conserved among Stats and regulates unique transcriptional responses (Lim and Cao, 2006).
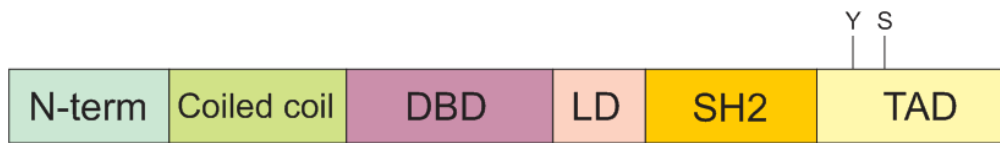
Fig. 5. Schematic representation of the human *Stat5* protein domains. Marked tyrosine (Y) and serine (S) residues represent the two amino acids important for Stat5 activation. In human Stat5a and Stat5b the position of this tyrosine is 694 and 699 respectively. The serine important for Stat5 activation lays on position 726 in human Stat5a and 731 in Stat5b. N-term = N-terminal domain; DBD = DNA binding domain; LD = linker domain; SH2 = SH2 domain; TAD = transactivation domain.

Stat proteins have central roles in cell differentiation and cell growth (Paukku and Silvennoinen, 2004). In addition to their central role in normal cell signalling, recent studies have demonstrated that diverse oncoproteins can activate specific Stats (specially Stat3 and Stat5) and that constitutively activated Stat signalling directly contributes to oncogenesis (Bowman *et al*, 2000). TGF-ß and PI3K/PTEN are controlled by Stat5 action (Ferbeyre and Moriggl, 2011).

The two Stat5 genes present in mammals, Stat5a and Stat5b, are very closely related. They share over 90% identity and diverge only at their C-terminus (Paukku and Silvennoinen, 2004). Stat5 (Stat5a) was first identified as a prolactin-induced mammary gland factor (Gouilleux *et al*, 1994). Soon after, another closely related gene (Stat5b) was identified in mice (Liu *et al*, 1995). Stat5a is the predominant form in mammary gland, while Stat5b is more prominently expressed in liver (Paukku and Silvennoinen, 2004). Stat5a knockout mice fail to develop mammary glands due to loss of prolactin responsiveness (Liu *et al*., 1997). By contrast, Stat5b knockout mice have sexually dimorphic growth retardation (Udy *et al*., 1997).

Two Stat5 homologues have been identified in zebrafish by Lewis and Ward in 2004, named Stat5.1 and Stat5.2. These authors suggest that the ancestral Stat5 gene has undergone two independent gene duplication events to generate a Stat5.2 paralogue in zebrafish and a Stat5a paralogue in mammals. However, no functional analysis was done in this work and no study focusing on medaka Stat5 genes has been performed so far.

1.4.2 Stat5 activation

Stat5 proteins, like all Stat members, are activated by different cytokines, including interferon and interleukin, as well as growth factors and hormones (Bromberg, 2001). Binding of growth factors and cytokines to their receptors results in the activation of intrinsic receptor-tyrosine-kinases or of receptor-associated kinases, such as the Janus kinase (JAK) or the SRC tyrosine kinase. These kinases subsequently phosphorylate the cytoplasmic part of the receptor, which recruits monomeric Stat proteins to the receptor. Recruited Stats themselves become subsequently activated by phosphorylation, dimerize and translocate to the nucleus, where they can directly regulate gene expression (Yu and Jove, 2004).

Two constitutively activated versions of mouse Stat5 have been identified. The first mutation identified was a Stat5a version bearing two amino acid substitutions: H299R located in the DNA binding domain and S711F present in the transactivation domain (Onishi *et al*, 1998). This mutant protein is constitutively phosphorylated at its tyrosine residues and is transcriptionally active even in the absence of stimulation. The same mutations in Stat5b have similar effects (Onishi *et al*, 1998). In addition, a single point mutation in the SH2 domain, N642H, gives rise to a constitutively active Stat5a and Stat5b (Ariyoshi *et al*., 2000). On the contrary, a deletion of the carboxyl-terminal transactivation domain of mouse Stat5a confers the gene a dominant negative phenotype (Moriggl *et al*., 1996). These protein versions sustain the DNA binding activity but fail in activation, thus leading to a dominant negative phenotype. In zebrafish, a constitutively active form of Stat5.1 was generated based on these previously identified murine Stat5. Expression of zebrafish Stat5.1 N646H and H298R/N714F mutants led to haematological perturbations (Lewis *et al*, 2006). So far, no animal model has been generated bearing any Stat5 constitutive active version.

1.4.3 Stat5 in cancer

Whereas Stat5 activation is tightly regulated in normal cells, the constitutive activation of tyrosine kinases in cancer causes continuous activation of Stat5, leading to permanent changes in the expression of genes that control fundamental cellular processes (Yu and Jove, 2004). It is conceivable that multiples factors, such as epigenetic changes, regulation by miRNA, altered proteolytic pathways, gene amplification and aberrant growth factor signalling contribute to activation of Stat5 proteins in human cancers (Ferbeyr and Moriggl, 2011). Stat5 activation has been correlated with initiation and/or progression of breast cancer (Wagner and Rui, 2008) and prostate cancer (Tan and Nevalainen, 2008). Also, Stat5 pathway is frequently activated in lung, head and neck cancers (Lai and Johnson, 2010).

Correlations of Stat5 with melanoma have been observed in the fish *Xiphophorus,* where the signalling of oncogenic receptor tyrosine kinase, *Xmrk*, leads to activation of Stat5 (Wellbrock *et al*, 1998). Also, Stat5 phosphorylation in malignant melanoma is important for survival (Mirmohammadsadegh *et al*., 2006) and contributes to anti-apoptosis in melanoma (Hassel *et al*, 2008). Besides that, in almost all melanoma cell lines, an abundant level of activated Stat5 protein was found (Morcinek *et al*., 2002). A dominant-negative form of Stat5 leads to apoptosis and inhibits melanoma cell growth *in vitro* (Hassel *et al*., 2005).

1.5 C-myc

1.5.1 Myc family

The human *myc* gene family, comprising *c-myc*, *mycN* and *mycL*, contains a   basic   helix-loop-helix leucine zipper (BHLH/LZ) domain (Fig. 6). Myc protein through its BHLH domain can bind to DNA while the LZ allows the dimerization with its partner Max, another BHLH transcription factor (Eilers and Eisenman, 2008). The basic region motif is the region involved in

determining sequence-specific DNA binding (Ryan and Birnie, 1996). Sub cellular localization to the nucleus is encoded primarily by the nuclear localization region (Meyer and Penn, 2008). The transactivation domain acts as a transcription activator (Ryan and Birnie, 1996).

Transactivation domain		Nuclear Localization		Basic Region	Helix-Loop-Helix	Leucine Ziper
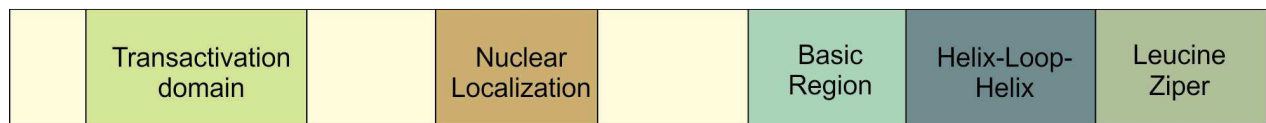
Fig. 6. representation of the human *C*-myc protein domains.

Genes of the *myc* family are considered to be proto-oncogenes due to raised activity in a variety of human cancers following alterations in their structure or changes in expression. One example is Burkitt lymphoma, where the t(8;14)(q24;32) translocation places *myc* in juxtaposition with regulatory elements of the immunoglobulin heavy or light chain genes (Klapproth and Wirth, 2010). Deregulated expression of *c-myc* has also been detected in a large variety of other human cancers, like breast and colon cancer, small cell lung carcinoma and neuroblastoma (reviewed in Nesbit *et al*, 1999). *c-myc* overexpression (Ross and Wilson, 1998) and increased copy number (Kraehn *et al*., 2001) have been also described in human melanomas indicating that C-myc plays a role in this disease.

1.5.2 c-myc regulation

c-myc expression is strictly controlled, at transcriptional and also at translational level (Meyer and Penn, 2008). In non tumorigenic cells, *c-myc* levels are low and dependent on mitogen signalling (Grandori *et al*, 2000). In most solid human tumours, c-*myc* expression is deregulated and is thought to promote tumour progression (Yokota *et al*, 1986). C-myc deregulation can be caused either by retrovirus integration, insertional mutagenesis, chromosomal translocation, gene amplification, increase in *c-myc* mRNA levels or decrease of C-myc protein stability (for review see Meyer and Penn, 2008). Although oncogenic activation of *c-myc* alone causes uncontrolled cell proliferation *in vitro*, cellular transformation requires additional oncogenic lesions, like Ras activation (Jacobs *et al*., 1999), interaction with the anti-apoptotic activity of Bcl2 and Bcl-x (Strasser *et al*, 1990) or loss of the tumour suppressor p53 (Blyth *et al*, 1995).

C-myc stability is linked to its phosphorylation status. Ras controls C-myc stability by phosphorylating two myc residues, T58 and S62 (Sears *et al*., 2000). Also, C-myc is phosphorylated at S71 by a Rho-dependent kinase (Watnik *et at*, 2003). Besides that, Myc function is controlled post translationally by six lysine residues that are direct substrates for p300-mediated acetylation (Zhang *et al*, 2005) and by ubiquitination stimulating proteosomal degradation of the protein (Sears, 2004).

1.5.3 C-myc function

The general function of C-myc is to act as a global transcriptional regulator controlling normal cell proliferation, growth, survival and differentiation (Meyer and Penn, 2008). Its main function

is the activation of gene transcription, which happens through the formation of a heterodimeric complex with Max through its C-terminal region where a basic helix-loop-helix and a leucine-zipper are present (Lüscher and Larsson, 1999). Myc-Max heterodimers bind to genomic E-box sequences (CACGTG) with high affinity (Blackwood and Eisenman, 1991). This heterodimerization is essential for Myc transformation (Amati *et al*., 1993). After forming a complex with Max, C-myc also recruits cofactors and promotes cell cycle progression (Lüscher, 2001). Transactivation by C-myc is antagonized by Mad proteins, which heterodimerize with Max and bind to the same DNA complexes but recruit repressor complexes to the promoter (Wanzel *et al*, 2003).

Also, C-myc/Max complexes regulate gene activation through chromatin remodelling (Amati *et al*, 2001). C-myc associates with the co-activator TRRAP, a component that bears acetyltrasferases (McMahon *et al*, 1998). After binding to cyclin D2 (CCND2), C-myc recruits TRRAP and induces the acetylation of histone H4, which alters the chromatin structure, allowing the access and binding of the C-myc/Max complex to target DNA sequences (Bouchard *et al*., 2001). Besides that, the induction of gene expression of several other C-myc target genes has been correlated with histone H4 acetylation (Frank *et al*, 2001).

In contrast to its activational role, Myc can also repress gene transcription by different mechanisms. First, C-myc is able to repress transcription indirectly by activating the synthesis of transcriptional repressor proteins (Wanzel *et al*, 2003). Also, Myc-Max complex is recruited to core promoters through protein-protein interactions with transcription activators that are bound directly to DNA, including the nuclear factor Y, NFY (Izumi *et al*., 2001), SP1 (Gartel *et al*., 2001) and the Myc-interacting zinc finger 1, MIZ1 (Peukert *et al*., 1997). These protein complexes are thought to displace co-activators and recruit co-repressors (Wanzel *et al*, 2003).

1.5.3.1 C-myc promotes cell proliferation

In quiescent cells *in vitro, c-myc* expression is virtually undetectable, but after mitogenic or serum stimulation its mRNA expression and protein production are rapidly induced, and cells enter G1 phase of the cell cycle (Pelengaris *et al*, 2002). Myc promotes cell division by activation or repression of genes that are involved in cell cycle progression. C-myc induces cyclin-E-CDK2 activity early in the G1 phase of the cell cycle (Steiner *et al*., 1995) by activating CCND2 (Bouchard *et al*., 1999) and CDK4 (Hermeking *et al*., 2000) and repressing genes which are involved in cell cycle arrest like p15 (Staller *et al*., 2001) and p21 (Perez-Roger *et al*, 1999). Myc is thought to contribute to tumorigenesis through unrestrained cellular growth and proliferation (reviewed in Arvanitis and Felsher, 2006).

1.5.3.2 C-myc induces apoptosis

 Two major pathways by which C-myc induces apoptosis have been uncovered. First, C-myc induces expression of the tumour suppressor protein p19 Arf, which activates p53, which in turn

activates proapoptotic genes including *bax* and *puma* as well as mediators of cell cycle arrest such as *p21CIP1* (Larsson and Henriksson, 2010). Also, C-myc represses expression of anti-apoptotic members of the *bcl-2* family including *bcl-x* and *bcl-2* (Eischen *et al*, 2001). Apoptosis is an important cellular mechanism against cancer formation. Thus, the loss of pro-apoptotic genes, such as *p53*, *Arf* and *Bax,* or overexpression of anti-apoptotic genes, such as *bcl-2* and *bcl-x,* cooperate with *c-myc* to accelerate tumorigenesis (Eischen, *et al*, 1999 and 2001).

1.5.4 c-myc model organisms

To better understand C-myc function, model organisms, like transgenic mice, were generated. *C-myc* null mice fail to develop normally and die at embryonic day 9.5 – 10.5 with abnormalities of the heart, neural tube and pericardium, thereby showing the crucial requirement of C-myc for embryonic survival and its role in organ development (Davis *et al*, 1993). A conditional c-*myc* knockout mouse, using the Cre-*loxP* technology, provided extra knowledge about *c-myc* role during cell cycle control, organ and body size control (Trumpp *et al*., 2001).

Different mouse models that enable temporal control of C-myc activation after tamoxifen treatment were developed by fusing the *c-myc* gene to a mutated form of the ligand binding domain of the estrogen receptor (ER, Eilers *et al*, 1989). This mutated ER does not bind to beta estradiol, its natural ligand, but instead binds to tamoxifen (Feil *et al*., 1996). In the absence of tamoxifen, the protein fused to ER is bound to the heat shock protein 90 (Hsp90, Tian *et al*., 2006) and is located at the cytoplasm, hence inactive. On administration of tamoxifen, Hsp90 is displaced leaving the transcription factor free to translocate to the nucleus and activate target genes.

C-mycER activation in the suprabasal epidermis under the control of the involucrin promoter is sufficient to induce cell cycle entry of post-mitotic keratinocytes and to block differentiation (Pelengaris *et al*, 1999). In this study, sustained C-myc activation for 21 days resulted in epidermal hyperplasia and induction of angiogenesis, but no C-myc induced apoptosis was observed. Interestingly, C-mycER activation in pancreatic islet ß-cells under the insulin promoter results predominantly in apoptosis (Pelengaris *et al*, 2002). Another ER model was used to investigate the effect of timed C-myc activation in the basal layer of the epidermis under the keratin 14 promoter (Arnold and Watt, 2001). In this model, C-myc forces cells out of the stem cell niches stimulating epidermal proliferation.

In addition to genetically engineered myc mouse models, zebrafish C-myc models have been generated. A T-cell acute lymphoblastic leukemia (T-ALL) model was generated using a human C-myc version under the control of the lymphoid cell specific *rag2* promoter (Langenau *et al*., 2003). This model was later improved by conditioning *c-myc* expression using Cre/lox (Langenau *et al*, 2005) and heat shock promoter systems (Feng *et al*, 2007). Recently this zebrafish T-ALL model has been extended for a tamoxifen inducible version of myc under the control of the *rag2* promoter (Gutierrez *et al*, 2011). Although very important for understanding C-myc function *in vivo*, these zebrafish models have been generated using the mouse or human gene instead of

utilizing the species-specific orthologue, therefore ignoring possible species-specific functions of C-myc. So far, no investigation of medaka *c-myc* genes has been performed and facilitate the possibilities to investigate evolutionary and general functional aspects of Myc.

1.6 Aims

As discussed above, melanoma is one of the most dangerous forms of cancer. Consequently, it is essential to investigate the function of genetic factors known to be involved in this malignancy in more detail. The first aim of this work was to investigate known downstream signals of Xmrk contributing to the tumour phenotype *in vivo* in the medaka system. To accomplish this, I identified, cloned and produced different medaka transgenic lines expressing oncogenic factors in pigment cells under the control of the *mitf* promoter.

The first target was to identify the complete medaka BRAF gene and to clone it. Subsequent sequence modifications should result in a constantly activated BRAF version, similar to BRAF V600E in humans. BRAF is found mutated in high incidence in human tumours like malignant melanoma and thyroid cancer (Davies *et al*., 2002). I also wanted to produce transgenic lines, bearing both medaka BRAF versions under the control of the MITF promoter. These lines should bring new insights on how BRAF functions modulate pigment cells *in vivo,* since for the first time a fish BRAF would be analysed.

A second target for investigation was medaka Stat5a and Stat5b. Stat5 is essential for Xmrk induced invasive progression of melanoma (Schartl *et al*., 2010). Identification, cloning and production of transgenic medaka lines utilizing both medaka orthologues of these two genes should be helpful to understand how Stat5 functions are correlated to melanoma invasiveness *in vivo* and how both versions diverge between each other. Besides that, for the first time a living organism carrying constitutive active and dominant negative versions of these genes would be produced. These lines will additionally help to bring new insights on how activation or lack of Stat5 affects the physiology of a living organism. For example, these fish would allow investigation of angiogenesis processes in cancer which are not possible in cell culture.

The integration of medaka genetics with the large tools available to study cancer will provide a wider understanding on cancer formation in general. For example, medaka fishes are suitable for high-throughput chemical screens. In addition, the lines generated here will constitute promising models to test new genes as a cancer therapy agent, since medaka fishes can be easily crossed with cancer developing lines, like the melanoma developing *Xmrk* fishes. Also, medaka fishes can be used in genetic screens to detect new tumour suppressors or genetic modifiers in melanoma development.

A third aim of this work was to investigate *in vivo* c-myc, a well known regulator of cell cycle progression and potential oncogene. C-myc expression is induced by activation of Xmrk *in vitro* (Svenja Meierjohann, personal communication) and may link Xmrk induced melanoma progression and cell cycle regulation. Due to its known harmful developmental effects *in vivo*

after activation, I wanted to create a medaka model utilizing a genetically modified species specific C-myc version with strictly controllable activation. Detailed analyses on proliferation and apoptosis potentials in individuals of these lines will result in insights into cell fate decisions and potential tumour initiation after C-myc deregulation.

2. MATERIALS

2.1 Chemicals and reagents

Basic chemicals were purchased from MERCK, Sigma-Aldrich and Roth. Specific chemicals are listed in the table above.

Compound	Supplier
1 kb DNA ladder	Fermentas
100 bp DNA ladder	Fermentas
4-OHT (4-Hydroxytamoxifen)	Sigma-Aldrich
Agarose	Roth
Albumin bovine serum	PAA
Aprotinin	Sigma-Aldrich
Bacto® agar	A. Hatenstein
Bacto® tryptone	A. Hatenstein
Bacto® yeast extract	A. Hatenstein
Bradford reagent	Sigma-Aldrich
BrdU (5-bromo-2`-deoxyuridine)	Sigma-Aldrich
Chelex	Bio-Rad
Chloroform	Roth
Choleratoxin	Sigma-Aldrich
deoxycholate	Sigma-Aldrich
DIG RNA labeling mix	Roche
DMEM	Invitrogen
DMSO	Roth
DNA oligonucleotides	Sigma-Aldrich
DNTPs (Deoxynucleotides triphosphate)	Fermentas
Ethidium bromide	Roth
EtOH	Sigma-Aldrich
FCS	PAA
FCS gold	PAA
Fetal bovine serum	PAA
Fitc-dextran	Sigma-Aldrich
FLU RNA labeling mix	Roche
FuGENE HD transfection Reagent	Roche
Gel Loading Buffer II"	Ambion
Glutamine	PAA
Heparin	Sigma-Aldrich
Hoechst	Invitrogen
IPTG (isopropyl-ß-thiogalactopyranosid)	Roth
Leibovitz 15 medium	Gibco
Leupeptin	Sigma-Aldrich
Na_3VO_4	Sigma-Aldrich
NaOAC (3M)	Roth
PageRuler™ prestained protein ladder	Fermentas
peqGOLD TriFast	Peqlab
Phenol	Roth
Phenol red	Sigma-Aldrich
Roti® Histo kit II	Roth
Roti® Histokit II	Roth
Rotiphorese® Gel 40 (37.5:1)	Roth
RPM1 medium	Gibco
Sheep serum	Sigma-Aldrich

Torula-RNA	Sigma-Aldrich
TPA	PAA
Tricaine	Sigma-Aldrich
Triton X-100	Roth
Tween® 20	Roth
X-gal (5-bromo-4-chloro-3-indolyl-beta-D-galactopyranoside)	Sigma-Aldrich
Xylene	Roth

2.2 Antibiotics

Antibiotic	Supplier
Ampicillin	Roth
Kanamycin	Roth
Streptomycin	Invitrogen
Penicillin	Invitrogen

2.3 Enzymes

Enzyme	Supplier
Ligase	Fermentas
Meganuclease	Fermentas
Pfu DNA polymerase	Fermentas
Proteinase K	Roth
ReproFast polymerase	Genaxxon
Restriction endonuclease	Invitrogem, NEB, Fermentas
Sp6 Polymerase	Roche
T7 Polymerase	Roche

2.4 Antibodies

2.4.1 Primary antibodies for western blot (WB) and immunofluorescence (IF)

Antibody anti-	Species/isotype	Dilution for WB	Dilution for IF	Supplier
ER IgG	Rabbit	-	1:500	Santa Cruz
ß-actin IgG	Mouse	1:10000	1:10000	Santa Cruz
BrdU IgG	Rat	-	1:250	Serotec
phospho MAP IgG	Rabbit	1:5000	-	Cell signalling

2.4.2 Primary antibodies for *in situ* hybridization

Antibody anti-	Species/isotype	Dilution	Supplier
fluorescein	Sheep	1:2000	Roche
digoxigenin	Sheep	1:2000	Roche

2.4.3 Secondary antibodies

Antibody anti-	Properties	Dilution for WB	Dilution for IF	Supplier
Mouse IgG	Peroxidase-coupled	1:3000	-	Thermo Scientific
Rabbit IgG	Peroxidase-coupled	1:10000	-	Bio-Rad
Rat IgG	Alexa 568-coupled	-	1:250	Serotec
Rabbit	Alexa 488-coupled	-	1:3000	Invitrogen

2.5 Disposables and kits

Products	Supplier
TOPO TA cloning Kit	Invitrogen
GenElute™ Gel Extraction Kit	Sigma-Aldrich
GenElute™ HP Plasmid Miniprep Kit	Sigma-Aldrich
GenElute™ PCR Clean-Up Kit	Sigma-Aldrich
GenElute™ HP Plasmid Miniprep Kit RevertAid ™	Fermentas
First Strand cDNA Synthesis Kit	Fermentas
ApopTag Red *In Situ* Apoptosis Detection Kit	Milipore
NucleoSpin RNA Clean up Kit	QIAGEN

2.6 Laboratory equipments

Device	Model/ Supplier
Microinjection	
Microinjector	FemtoJet and Microinjector 5242, Eppendorf
Micromanipulator	Leitz
Stereo microscope	Stemi SV6 and SV11, Zeiss
Capillary puller	Kopf vertical pipette puller model 720, Bachhofer
Glass capillaries	GC100F-10; Harvard Apparatus
Documentation	
Microscope	Axiophot POL, Zeiss
	Fujix hc-2000, Fujifilm
	Leica CTR 6000
Stereo microscope	SMZ1000, Nikon
	CC-12 FW Soft imaging system, Olympus
Confocal microscope	Nikon eclipse Ti, Nikon
PCR and Gel electrophoresis	
TGradient PCR machine	Biometra
MyiQ™ Single-color Real-time PCR Detection system	Bio-Rad
Gel chambers	Department's workshop
Power supply	EPS 301, Amersham-Pharmacia biotech
Thermocycler	TGradient, Biometra (Goettingen) and DNA Engine Dyad thermal cycler, Biorad (Hercules, CA)
Centrifuges	
Tabletop	Centrifuge 5415D and Centrifuge 5415R with rotor

	F45-24-11, Eppendorf
High-speed	Sorvall RC-5B with rotor GSA and SLA-1500 rotor, DuPont (Bad Homburg) and MinifugeRF, Heraeus

Lab equipment

Incubator	B5050E, Heraeus
Water bath	Model 1083, GFL
pH meter	pH523, WTW
Balance	BP, Kern and Sohn
Shaker	Reax3, Heidolph
Spectrophotometer	BioPhotometer, Eppendorf
	UV-visible- Spectrophotometer, Varian
Thermal block	Thermomixer compact, Eppendorf
UV-sterilizer	GS GeneLinker, Biorad
Vortex	Vortex genie, Scientific industries INC.
Pipettes	Pipetman, Gilson
Ultra turrax T5 Fu	IKA

2.7 Olinonucleotides

Oligonucleotides were synthesized and purchased from Sigma-Aldrich in HPLC quality.

2.7.1 Olinonucleotides for cloning and screening

Primer	Sequence (5`-3`)
Ory_BRAF_ATG_fish_FOR	GCTCGAGATGGCGGCGTTGAGC
BRAF_mdka_R1	TTGACACGAGCAACAAATCC
BRAF_mdka_F2	TGATGAGGGGACTCATACCC
BRAF_mdka_R2	GGTGACGTTCAGCATCTTCA
BRAF_mdka_F3	CAACGTCAAAGTCCCACAGA
BRAF_v1_mdka_R	CCCAAGCTTCTTAAATGCAGAAAACTCCCC
BrafHindIIIHAFLAGSpeIFOR	AGCTTTCACTTGTCATCGTCGTCCTTGTAGTCAGCGTAATCTGGAACATCGTATGGGTAG
BrafHindIIIHAFLAGSpeiREV	AGCTCTACCCATACGATGTTCCAGATTACGCTGACTACAAGGACGACGATGACAAGTGAA
BRAFV614Efor	GGAGACTTTGGCCTGGCGACCGAAAAGAGCCGCTGGAGTGGCTCC
BRAFV614Erev	GGAGCCACTCCAGCGGCTCTTTTCGGTCGCCAGGCCAAAGTCTCC
Stat5ab/a_mdka_left	GCTCGAGATGGCCGTGTGGATCCA
Stat5ab/aR1	TGACCAATGCCGAGATGATA
Stat5ab/aF1	AAACGATTTGGCAAAACAGG
Stat5ab/aR2	TGCGGCTTTAGATGCTTTTT
Stat5ab/aF2	GCCTTTCCTTGTGCCAGATA
Stat5ab/a_mdka_right	GGAATTCGGGACTGCTGGCCCCC
Stat5ab/b_mdka_left	GCTCGAGATGTCCCTGTGGATCCAGG
Stat5ab/bR1	CTCACACCAGGACTGCAGAA
Stat5ab/bF1	CTTACCAGAGAGGCCAGCAC
Stat5ab/bR2	GCGGCTTCAGATGTTTCTTC
Stat5ab/bF2	AGTTGGGTTTCCACGTCAAG
Stat5ab/b_mdka_right	GGAATTCGTTGCTGGCTGCTCCACT

Full length medaka c-myc17 for	ATTGCTAAGCTTATGCCACCTGTGTTATC
Full length medaka c-myc17 rev	TTCGTG GATCCCCATGTAAAGTCCTGAGCTGCT
MF_ef1a1-f02	GCAAGGGCTCCTTCAAGTACGC
MF_ef1a1-r02	CAGCAGCGACAATCAGCACAG
Full length medaka c-myc for	ATTGCTAAGCTTATGCCACCTGTGTTATC
Full length medaka c-myc rev	TTCGTGGATCCCCATGTAAAGTCCTGAGCTGCT
Haflag for	ATGTACCCATACGATGTTCCAGA
Stat5ab/a sibling screen rev	ACCTCGATGGGAAAATGTTG
Stat5ab/b sibling screen rev	ATAATGCCGCACCTCTATGG
BRAF sibling screen for	TACCACCACCTGCACATCAT
BRAF sibling screen rev	TGGGTAGAGCTTCTTAAATGCAG
c-myc sibling screen for	ATCCTGAGAAAGGCGACAGA
c-myc sibling screen rev	AAGGACAAGGCAGGGCTATT
MITF_screen_FOR	AGGGGAAGCCTGATGTCTTT
Stat5ab/a_N646H_For	GCAGGTGAGCGAATGGTCTGGCATTTAATGCCATACACA ACCAAA
Stat5ab/a_N646H_Rev	TTTGGTTGTGTATGGCATTAAATGCCAGACCATTCGCTCA CCTGC
Stat5ab/b_N647H_For	CAAGGGGAAAGACTGGTATGGCACTTATTACCGTACACC ACCAAA
Stat5ab/b_N647H_Rev	TTTGGTGGTGTACGGTAATAAGTGCCATACCAGTCTTTCC CCTTG
Stat5ab/a_neg_Rev	TCATGAGGCGCCTTGATCCA
Stat5ab/b_neg_Rev	TCACAGGATGTTGTCACCGACC
mdk_cmyc20_gap_for	CCAAGCTGAAGAAGGTGGTC
mdk_cmyc20_gap_rev	TCCTCTTCCTCCTGGTCCTC

2.7.2 Oligonucleotides used for quantitative real-time PCR

Primer	Sequence (5`-3`)	ENSEMBL code
Stat5ab/a_rt_for	AGTGTCGGAAGCAACGAACT	ENSORLG00000003961
Stat5ab/a_rt_rev	CCGGTAGTCGTCAGGATTGT	
Stat5ab/b_rt_for	ACGGGAGTCAGGACAACAAC	ENSORLG00000014335
Stat5ab/b_rt_rev	GCGGCTTCAGATGTTTCTTC	
BRAF_rt_for	GCCTGGCAACAGTCAAATCT	ENSORLG00000009843
BRAF_rt_rev	ACAGTCAGCCATCAGCCTCT	
CDKN2_rt_for	ATGATGATGGGGAACTCCAA	Primer from Brigitta Wilde
CDKN2_rt_rev	GATGTTCACCGAAGCTCCAT	
ef1a1_rt_for	GCCCCTGGACACAGAGACTTCATCA	ENSORLG00000007614
ef1a1_rt_rev	AAGGGGGCTCGGTGGAGTCCAT	
ODC1_rt_for	TGACAATGCCAAACTGGTGT	ENSORLG00000017758
ODC1_rt_rev	CCAGCTCCTCACCCATATCA	
CBX3_rt_for	CGTCTCGTCAATGGGAAAGT	ENSORLG00000007692
CBX3_rt_rev	TGTCTCTGGCTCATCTGTGG	
CCT5_rt_for	GGTAAATCGGGCTGCAGATA	ENSORLG00000007700
CCT5_rt_rev	GCTTTTTGGCGATCAGAGTC	
EIF3S8_rt_for	GGAGAGGAACGCAGAACAAG	ENSORLG00000006318
EIF3S8_rt_rev	GTGATGGAACTGCTTGCTGA	
METTL1_rt_for	ACCCAGGGAGTTATGGGAAC	ENSORLG00000015181
METTL1_rt_rev	GTGTACACCAAACCCCCAAC	

2.8 Plasmids

2.8.1 Standard vectors

Vector	Properties	Promoter	Reference/Supplier
pCR® 2.1-TOPO®	Amp, Kan	T7, T3, Sp6, M13fwd, M13rev, Kan	Invitrogen
pI-SceI MITF		MITF	From Isabell Erhard
pCDNA3	Amp	CMV	Invitrogen
pCSKA	Estrogen receptor	unknown	From Manfred Gessler

2.8.2 Vectors generated in this work

Plasmid	Cloning strategy/reference
BRAF pCR2.1	Chapter 4.1.1.1
BRAF V614E pCR2.1	Chapter 4.1.1.2
BRAF pI-SceI	Chapter 4.1.1.3
BRAF V614E pI-SceI	Chapter 4.1.1.3
BRAF pCDNA3	Chapter 4.1.1.3
BRAF V614E pCDNA3	Chapter 4.1.1.3
Stat5ab/a pCR2.1	Chapter 4.2.1.1
Stat5ab/a N646H pCR2.1	Chapter 4.2.1.3
Stat5ab/a DN pCR2.1	Chapter 4.2.1.3
Stat5ab/a pI-SceI	Chapter 4.2.1.4
Stat5ab/a N646H pI-SceI	Chapter 4.2.1.4
Stat5ab/a DN pI-SceI	Chapter 4.2.1.4
Stat5ab/b pCR2.1	Chapter 4.2.1.2
Stat5ab/b N647H pCR2.1	Chapter 4.2.1.3
Stat5ab/b DN pCR2.1	Chapter 4.2.1.3
Stat5ab/b pI-SceI	Chapter 4.2.1.4
Stat5ab/b N647H pI-SceI	Chapter 4.2.1.4
Stat5ab/b DN pI-SceI	Chapter 4.2.1.4
c-myc17-ER pCSKA	From Cornelia Schmidt
c-myc17-ER pI-SceI	Chapter 4.3.1

2.9 Bacteria strains

Strain	Properties	Supplier
XL1-blue	recA1, lac-, endA1, gyrA96, thi, hsdR17 (rk-, mk+), supE44, relA1, λ-, [F',proAB, lacIqZ, ΔM15, Tn10 (tetr)]	NEB
DH5α	*sup*E44 Δ*lac*U169 (φ80laxZΔM15) *hsd*R17 *rec*A1 *end*A1 *gyr*A96 *thi*-1 *rel*A1	NEB

2.10 Eukaryotic cell lines

Strain	Souce/Reference
Melan A	Bennett *et al*, 1987

2.11 Hardware

Microsoft system

2.12 Softwares

Word-processing	Microsoft Word 2007 (Microsoft)
	Ultraedit-32 (IDM Computer Solutions)
Graphics	CorelDRAW X4 (Corel)
	ImageJ (NCBI)
	NIS elements imaging software
Statistics	Microsoft Excel 2007 (Microsoft)
Vector database	Vector NTI advance 10 (Invitrogen)
Sequence alignment	BioEdit and ClustalW
Phylogenetic analysis	Mega 5.0
Bibliography	Mendeley Desktop (Mendeley Ltd.)

2.13 Internet resources

ENSEMBL	http://www.ensembl.org/index.html
NBRP medaka	http://www.shigen.nig.ac.jp/medaka/

3. METHODS

3.1 Animal maintenance

Wild type medaka embryos (*Oryzias latipes*) of the *carbio* strain (WLC# 2674) were raised as described by Kirchen and West (1976) under standard laboratory conditions at 26°C. Embryos were staged by morphological characteristics according to Iwamatsu (2004). All procedures involving experimental animals were performed in compliance with local animal welfare laws, guidelines and policies.

3.2 Microbiological methods

3.2.1 Sterilization

Solution, media and buffers were sterilized by autoclaving at 121 °C and 138 kPa for 80 min.

3.2.2 Bacterial cultivation and long time storage

For bacteria cultivation, Luria-Bertani (LB) medium was used containing appropriate concentrations of antibiotics (60µg/ml ampicillin or 50 µg/ml kanamycin) for colony selection according to vector requirements. Cultivation was performed over night at 37°C with permanent shaking.

> **Luria-Bertani-medium (LB)**
> 10g/l bacto-tryptone
> 5g/l bacto-yeast extract
> 10g/l NaCl
> After dilution in dH_2O, a pH 7.4 was adjusted and the solution was autoclaved

For long term storage of bacteria, 800µl of a freshly prepared bacteria suspension were mixed with 200µl sterile glycerol in a safe lock vial, frozen in liquid nitrogen and stored at -80°C.

3.2.3 Preparation of competent *E.coli* cells

For production of chemically competent bacteria, a single colony from XL1-Blue or DH5α grew overnight in 1ml LB medium. The next day, this 1ml culture was added into 100 mL of LB medium and incubated under constant shaking at 37°C until optical density (OD600) reached a value between 0.3 and 0.5. After 15 min incubation on ice, the solution was centrifuged for 10 min at 4°C 600 rpm. The supernatant was discarded and the pellet was resuspended in 20 ml ice-cold 0.1 M calcium chloride solution. After 30 min incubation on ice, the bacteria solution was centrifuged for 10 min at 4°C 600 rpm. Then, the supernatant was discarded again and the bacteria pellet was resuspended in 10 ml of ice-cold 0.1 M calcium chloride/20% glycerol solution. The competent bacteria were divided into 250 µl aliquots and stored at -80°C.

3.2.4 Transformation of competent bacteria

For plasmid transformation into chemically competent bacteria cells, 100 µl competent bacteria thawed on ice and 1-10 ng of DNA plasmid were added to it. After 30 min of incubation on ice, a heat-shock was performed at 42°C for 90 seconds, followed by another step on ice, this time for 2 min. Subsequently, 1 ml LB-medium was added and the bacteria were incubated for 1h at 37°C under constant shaking. For selection, this solution was platted on LB-agar plate containing the appropriate antibiotic (60µg/ml ampicillin or 50 µg/ml kanamycin). For blue-white selection, 40 µl of 40 mg/ml IPTG and 40 µl 20mg/ml of X-gal were spread 20 min before use on top of the plates. Agar plates were incubated ON at 37°C. Plasmid DNA was isolated using gen Elute plasmid mini-prep kit (Sigma-Aldrich).

LB agar

15g/liter bacto-agar dissolved in LB medium

After autoclaving and LB agar medium cooled down to 40°C, I added desired antibiotics (60µg/ml ampicillin or 50 µg/ml kanamycin). Subsequently liquid LB agar was poured into petri dishes and cooled down to RT to polymerize.

3.3 Cloning

Cloning of full length medaka BRAF, Stat5ab/a and Stat5ab/b coding sequence (CDS) were performed with Pfu DNA polymerase (5U/µl, Fermentas) using cDNA pool from different medaka organs. Before the last amplification step, 0.3µl of dream Taq (5U/µl, Fermentas) was added to the reaction to add an adenine overhang for cloning purpose. Each gene was cloned in three parts into the plasmid pCR 2.1-TOPO (invitrogen).

Full length CDS medaka *c-myc,* of the gene copy present on chromosome 17, was PCR amplified and further sub-cloned into the vector pCSKA containing the mouse estrogen receptor. This work was done by Cornelia Schmidt from Manfred Schartl's laboratory, who kindly provided me the vector to work with.

3.3.1 Sequencing

Each cloned fragment, as well as full length sequences from all genes cloned in this work, was confirmed by DNA sequencing carried out by GATC biotech.

3.3.2 Ligation

For ligation reaction, 2 to 5U of T4 DNA Ligase (Fermentas) were incubated with corresponding buffer either at RT for 2 hours or ON at 16°C.

3.3.3 Enzymatic DNA digestion

For enzymatic digestion of DNA fragments or plasmids, 2 to 5U of restriction enzymes from different companies for 1 μg of DNA were incubated with corresponding buffers at optimal temperatures according to manufacturer's standards for 1 to 10 hours.

3.3.4 Oligo cloning to include HA and Flag tags

Oligos were designed with respective 5' prime overhang for desired restrictions enzymes. Primers were annealed as follows: 5μl of each primer (100μM in ddH$_2$O) were heated up to 95°C for 300 sec, and then temperature was slowly decreased until 20°C (minus 5°C each 30 sec). Plasmids were cut with corresponding restriction enzymes and precipitated as follows:

> 15µl of cut plasmid (~1µg)
> 1.5µl 3M NaOAC
> 45µl 100% EtOH

This solution was incubated for 1 hour on ice. After 30 min 14000 rpm (in Centrifuge 5415R with rotor F45-24-11, Eppendorf) centrifugation, the supernatant was discarded. The next step was to wash with 70% EtOH, centrifuge 15 min 14000 rpm and discard supernatant. The DNA pellet was air dried and dissolved in annealed oligonucleotides. After that, 5U of ligase (Fermentas) and 1.2 µl of corresponding ligase buffer were added. The solution was left ON at RT. On the next day, 2µl or 5 µl of this ligation were transformed into competent bacteria and plated for screening.

3.3.5 Site directed mutagenesis

To be mutagenized, genes were amplified in two PCR reactions, one amplifying from the ATG Start codon until 21 nucleotides downstream the codon to be mutated, which introduces a mutation during the first cycle of the reaction by an engineered mis-match. The second PCR was performed using primers binding 21 nucleotides upstream the codon to be mutated until the stop codon, also introducing the desired mutation. Because PCR employs exponential growth, after a sufficient number of cycles the mutated fragment will be amplified sufficiently to jut from the original. Both PCR fragments were purified from a TAE gel using GenElute™ Gel Extraction Kit (Sigma-Aldrich). Both purified PCR fragments containing the desired mutation were used as template for a new PCR reaction to amplify full length gene containing the desired mutation that leads to specific amino acid change.

An example of the first PCR reactions, where the whole gene is amplified in two different fragments to add the mutated nucleotide is listed above:

16.875µl	H_2O
2.5µl	Buffer (Pfu buffer, Fermentas)
1µl	$MgSO_4$ (25mM)
1µl	DNTP (2.5mM)
1µl	Primer forward (10pMOL)
1µl	Primer reverse (10pMOL)
1µl	cDNA (1µg/20µl)
0,5µl	DMSO
0.125µl	Pfu Polymerase (5U/µl)

An example of the second PCR reaction, where the purified PCR products are used as a template to amplify the whole gene bearing the mutated nucleotide is listed above.

23.75µl	H_2O
5µl	Buffer (Pfu buffer, Fermentas)
4µl	$MgSO_4$ (25mM)
5µl	Purified PCR product from ATG to mutagenizing primer
5µl	Purified PCR product from mutagenizing primer to stop codon
2µl	Primer forward (10pMol)
2µl	Primer reverse (10pMol)
2µl	DNTP (2.5mM)
1µl	DMSO
0.25µl	Pfu Polymerase (5U/µl)

A standard program for the PCR thermo cycler for both reactions was:

reaction step	temperature	time	
pre-heating	95°C	5`	
denaturation	95°C	30s	
primer anealing	50-62°C	30s	40x
elongation	72°C	180s	
final elongation	72°C	5`	

Oligonucleotides were engineered for mutagenesis as follows. Each primer was comprised of 45 nucleotides corresponding to the codon to be mutated and nucleotides corresponding to 7 codons downstream and 7 codons upstream of the targeted amino acid to be mutated. The nucleotides corresponding to the 5 first and the 5 last amino acids were 100% conserved to the template. The nucleotides corresponding to the 5 amino acids in the middle of the primer should be as different as possible without changing the codon sequence, except for the amino acid to be mutated. The reason for this is to avoid hybridization of the original sequence (without the mutation) in the second round of PCR to amplify the full length sequence.

3.4 Molecular biology standard methods

3.4.1 Plasmid DNA amplification and isolation

For plasmid DNA amplification, a single colony was selected from agar plates. Overnight bacterial cultures were set up for mini-preparation using GenElute™ HP Plasmid Miniprep Kit from Sigma-Aldrich according to manufacturer's protocol. Purified DNA was dissolved in 50µl of deionized water.

3.4.2 DNA purification

For purification from PCR reactions and cleaning of DNA from solution containing proteins, ion and other impurities GenElute™ PCR Clean-Up Kit (Sigma-Aldrich) was used according to manufacturer's protocol.

3.4.3 DNA extraction

For genomic DNA extraction from 30-50 medaka embryos of a desired age were collected into eppendorf tubes and homogenized in 150µl homogenizing buffer using micropestils. After solution was looking homogenous, 350µl of lysis buffer was added and solution was incubated at 65° for 15 min. After incubation, 250µl of Phenol and 250µl of Chloroform was added and solution was left under constant rocking for 10 min. Solution was centrifuged for 10 min at 4000 RPM in a table top centrifuge and the supernatant was transferred to a new tube. For precipitation, 350µl of Isopropanol was added and solution was kept for 2 hours on ice. Centrifugation at 4000 rpm at 4°C for 10 min followed by 45 minutes at 13000 rpm was conducted for gDNA precipitation. DNA was washed once with 70% EtOH (in H_2O). After the DNA pellet was dry, DNA was resuspended in 50µl of dd H_2O.

3.4.4 RNA extraction

For RNA extraction from medaka embryos 30-50 eggs of desired age were collected into eppendorf tubes and homogenized with solution D using micropestils. 20 µl of 2M sodium acetate (pH 4.0) and 200 µl of water saturated phenol and 100 µl Chloroform were added and samples were vortexed. Samples were incubated on ice for 20 min and centrifuged at maximum speed (in Centrifuge 5415R with rotor F45-24-11, Eppendorf) for 10 min. Supernatant was taken to another eppendorf reaction tube, washed with ethanol and ressuspended in 25 µl DEPC H_2O. About 1µg of RNA was added in DNAse master mix for treatment with DNAse for 30 min at 37°C.

Solution D	23.4g	quanidine thiocyanate
	1.67ml	750 mM sodium citrate
	2.5ml	10% sarkosyl
	27.8ml	ddH2O
		add 7.2µl/ml Beta-mercaptoethanol just prior to use

DNAse Master-Mix	10µl	DNAse buffer (Fermentas)
	5µl	DNAse (1 U/µl, Fermentas)
	2.5 µl	RNAse inhibitor (Fermentas)
		add ddH2O to 100µl

For RNA extraction from different tissues, medaka fishes were anesthetized with tricaine (100mg/L, MS-222, Sigma) and subsequently killed. Selected organs were homogenized in 100µl peqGOLD trifast with the Ultra-Turrax and centrifuged 10 min 12000 rpm at 4°C. Supernatant was removed to a new eppendorf tube and 200 µl of chloroform were added. After 30 sec of shaking, samples were incubated on ice for 3 minutes followed by 15 min centrifugation 12000 rpm at 4°C. Supernatant was removed to a new eppendorf tube, precipitated with 500µl isopropanol and ressuspended in DEPC H$_2$O.

3.4.5 DNA and RNA concentration determination

The concentration of nucleic acids was determined by measuring the absorption of an aqueous solution at a wavelength of 260 nm using a spectrophotometer. The absorption spectrum was measured at the range of 240 to 320 nm after having calibrated the photometer with pure water. The concentration (c) of the original solution was calculated by the following formula:

DNA c = 50 x A$_{260nm}$ x dilution factor [µg/ml]
RNA c = 40 x A$_{260nm}$ x dilution factor [µg/ml]

3.4.6 Polimerase chain reaction (PCR)

3.4.6.1 Standard PCR procedure

PCR was used for amplification of cDNA, plasmid or genomic DNA templates. PCR reactions were performed using either Dream Taq polymerase (Fermentas), PFU polymerase (Fermentas) or ReproFast polymerase (Genaxxon). Primers used for PCR reaction are listed in the section 2.7.1 in materials.

2.5µl	buffer (Fermentas)
0.5-1.5µl	ethylene glycol or DMSO
0.5-1µl	DNTP (each nucleotide at 2.5mM)
0.5-1.5µl	MgCl$_2$ (50mM)
0.75-1µl	primer forward (10pMol)
0.75-1µl	primer reverse (10pMol)
0.25-1µl	cDNA/gDNA
To 25µl	H$_2$O

A standard program for the PCR thermo cycler was:

reaction step	temperature	time
pre-heating	95°C	5`
denaturation	95°C	30s
primer anealing	50-62°C	30s
elongation	72°C	25-300s
final elongation	72°C	5`

30-40x

A template for PCR reaction is listed above. The amount of ethylene glycol, DMSO, $MgCl_2$, primers and DNA used as well as the temperature were optimized for each PCR reaction.

3.4.6.2 Agarose gel electrophoresis

Electrophoretic separation of RNA and DNA was performed in 1% up to 2% (w/v) agarose gels. Samples containing DNA were mixed with 10 x DNA sample buffer and loaded into the gel. Gel run was carried out at 80 to 200 V in an electrophoresis chamber containing 1x TAE-buffer. RNA samples were mixed with "Gel Loading Buffer II" (Ambion) and denatured at 70°C for 10 min before loading to gel. After separation, DNA and RNA were bathed for 5 to 15 min in EtBr for visualization on an UV-transilluminator at a wavelength of 254 nm.

(10x) DNA loading buffer	25mg	bromphenol blue
	25mg	xylene cyanol
	3ml	glycerol
	2ml	0,5M EDTA
	1ml	10% SDS
		Add ddH_2O to achieve final concentration of 10ml

(50x) TAE buffer	242g	tris base
	57.1ml	acetic acid
	100ml	0,5M EDTA
		Add ddH_2O to achieve final concentration of 1 litre

3.4.6.3 Gel extraction of DNA fragments

To purify DNA fragments separated by gel electrophoresis, the desired band was cut out of the gel and extracted with GenElute™ Gel Extraction Kit (Sigma-Aldrich). Purified DNA was dissolved in 10 to 20 µl ddH_2O.

3.4.6.4 cDNA synthesis

Single stranded cDNA was synthesized using 1µg of RNA using RevertAid ™ First Strand cDNA Synthesis Kit (Fermentas) using oligo dT primers according to supplier's protocol.

3.4.6.5 Quantitative Real Time PCR (qPCR)

For qPCR detection primers were developed flanking the fusion point of exon/intron boundaries. cT values were relatively calculated to the house keeping gene *ef1a1* (ENSORLG00000007614). All qPCR experiments were performed in MyiQ^{TM} Single-color Real-time PCR Detection system (Bio-Rad). Primers used in qPCRs are listed in the section 2.7.2 in materials.

A standard qPCR mix consisted of:

17,75µl	H2O
1 µl	MgCl2 (50mM)
0,7 µl	DNTPs (10mM each)
0,75 µl	SYBR green (1:2000 in DMSO)
0,25 µl	Fitc (1:2000 in DMSO)
2.5 µl	10X PCR buffer (Fermentas)
0,3 µl	Dream Taq-Polymerase (Fermentas)
0,75 µl	Primer fwd
0,75 µl	Primer rev
0,25 µl	Template

A standard program for the qPCR thermo cycler was:

95°C	3 min	
95°C	10s	⎤ 40
60°C	30s	⎦ cycles

with subsequent melting curve analyses

The different amount of target, normalized to the endogenous reference (*ef1a1*) and relative to a calibrator, is given by: $2^{-\Delta\Delta Ct}$. Where: $\Delta\Delta Ct = \Delta Ct_{sample} - \Delta Ct_{reference\ control}$.

3.4.6.6 Genotyping from fin biopsies

To genotype adult fishes, gDNA was extracted from sectioned tail fin tissue. Therefore, fishes were anesthetized with tricaine (100mg/L, MS-222, Sigma -Aldrich) and the posterior part of the pectoral fin was cut using scissors. Tissue was digested in digestion solution (5% chelex (w/v; Bio-Rad) in H$_2$O; just before use, 10µg/µl proteinase K was added). Fins were kept for 1h at 55°C, followed by 10 min at 95°C. For PCR reaction 1µl supernatant of this digested solution was used as DNA template.

A standard mix for PCR for genotyping consisted of:

2.5µl	buffer (Fermentas)
0.5-1.5µl	ethylene glycol or DMSO
0.5-1µl	DNTP (each nucleotide at 2.5mM)
0.5-1.5µl	MgCl$_2$ (50mM)
0.75-1µl	primer forward (10pMol)
0.75-1µl	primer reverse (10pMol)
0.25-1µl	cDNA/gDNA
To 25µl	H$_2$O

3.4.7 Synthesis of labelled RNA probes for *in situ hybridization*

Plasmids containing the 600 to 900 base pairs of genes of interest were linerized for antisense probes at 5`end and for control sense probes at the 3`end. After checking of digestion efficiency on agarose gel, linerized plasmids were extracted by phenol-chloroform. DNA was precipitated with 3M NaOAc and again checked on agarose gel. Reverse transcription was performed as follows:

2µg	template
2µl	Dig/Flu RNA labeling mix (Roche)
0.5µl	RNAse Inhibitor (Roche)
2µl	10x transcription buffer (Roche)
1µl	T7/Sp6 polymerase (5U/µl, Roche)
To 20µl	H$_2$O

After 2h at 37°C 1µl of DNAse was added and the solution was kept for 30 min at 37°C. Ripobrobes were purified with the NucleoSpin RNA clean up kit and eluted in 50µl H$_2$O. After checking correct RNA synthesis on an agarose gel, riboprobes were filled up to 100µl with Hybmix and stored at -20°C.

Hybmix	50% (w/v)	formamid
	5% (w/v)	1x SSC
	0,1% (w/v)	Tween 20
	5mg/ml	Heparin
	150µg/ml	Torula-RNA

3.4.8 Whole mount *in situ hybridization* (ISH)

One color RNA *in situ* hybridization was performed according to protocol described by Hauptmann and Gerster (1994) with RNA probes digoxigenin-UTP (DIG-UTP) or fluorerscein-UTP (FLU-UTP) to visualize gene expression. Embryos were fixed at desired time point of development with 4% paraformaldehyde (PFA) in phosphate buffered saline (PBS) solution at 4°C over night. Chorions were removed and PFA was replaced by MetOH for long time storage. Embryos were rehydrated and were digested with proteinase K at RT. Hybridization was performed ON at 65°C. In the next day, washes in 50% Formamid in 2x SSCT, 2x SSCT and 0,2x SSCT were performed also at 65°C.

Embryos were incubated 1h in blocking solution, and afterwards, with first AB (sheep anti-fluorescein or anti-digoxigenin, dilution 1:2000, Roche) at 4°C ON. Then, embryos were washed six times in PBST for 20 min each and two times in staining buffer. For staining, embryos were incubated in the dark with staining solution up to 48 hours.

10x PBS (1 liter)	1M NaCl (58.44g)
	19.5mM KCl (1.45g)
	59mM Na$_2$HPO$_4$ (10.5g)

20x SSC (1 liter)	175.3g NaCl
	88.2g sodium citrate
1x SSCT	10ml 20x SSC
	190ml ddH$_2$O
	0,1% (w/v) tween 20
1x PBST (1 liter)	100ml 10x PBS
	5mL 20% Tween20

75%, 50%, 25% Methanol in PBST

50% Formamid in 2x SSCT (100mL)	10ml 20x SSCT
	500µl 20% Tween 20
Proteinase K	5µl Proteinase K (10mg/mL) in 1 ml 1x PBST
4% PFA	3ml 16% PFA (80g to 500mL H$_2$O) in 9ml PBST
1x glycine	1M glycine in PBST
blocking solution	1:20 dilution of sheep serum (Sigma-Aldrich) in PBST
staining buffer	1ml 5M sodium chloride
	2,5ml 1M Magnesium chloride
	5ml 1M Tris-Cl pH 9.5
	0,1% Tween 20
	Add H$_2$O to 50ml
staining solution	20µl NBT/BCIP (Roche) in 1mL staining buffer

3.4.9 Cell culture

3.4.9.1 Primary cell culture

Anal medaka fins were cut from anesthetized fishes from both *c-myc17* lines and wild type and immersed in PBS containing 0.4% Sodium hypochlorite for 30 seconds. Tissues were rinsed three times in PBS and minced into small fragments. PBS was replaced by Leibovitz L-15 medium (Invitrogen). Tissues fragments were cultivated in a gelatin-coated µ-slide 8 well (IBIDI) containing 300µL of the culture medium. The culture was incubated at 28°C for five days and fixed with 2% Formaldehyde.

Leibovitz L-15 medium To 200mL
     176mL L-15 medium
      2mL glutamin
      2mL Pen-Strep (100u/mL-100µg/mL, Invitrogen)
     20mL FCS gold (20%, PAA)

3.4.9.2 Mouse melanocyte cell culture

Melan A cells were originally derived from C57BL/6 J (black a/a) mice, originating from Prof. Dorothy C. Bennett lab (St, George`s Hospital, London, UK). Melan A cells were cultivated in DMEM medium. To passage Melan A cell line, cells were washed with PBS, treated with trypsin-EDTA for 3-5 min and splited. Cultures were kept in an incubator at 37°C in a humidified atmosphere with 5% CO_2. Prior to cell harvesting to check constitutively activity of BRAF V614E cells were cultivated in starving medium for 2 hours.

DMEM medium   To 500 ml
           440,5ml DMEM
            50ml FCS (10%)
             5 ml 10x Pen/Strep (1x)
           2,5 ml TPA from 40 µM stock solution (200nM)
           2,0 ml Choleratoxin from 25 µg/ml stock solution (0,1 µg/ml)

Starving medium   DMEM
           2,5% dialysed FCS

3.4.9.3 Mouse melanocyte cell transfection

Plasmids BRAF pCDNA3 and BRAF V614E pCDNA3 (2µg of each) were transfected to Melan A cells using FuGENE HD transfection reagent (Roche) in 6 well plates containing $1x10^5$ cells according to supplier`s protocol.

3.4.10 Western Blot

Total protein was prepared from hatched medaka embryos or from cell pellets. Embryos were kept for 2 hours in lysis buffer in ice for lysis. Protein concentration was measured by adding 1µl of protein lysate in ml of Brafford reagent (Sigma) and measured at the spectrophotomer. Before loading protein samples were kept with 1x Laemmli buffer at 95°C for 10 minutes. A total of 50µg of protein lysate was separated by 10% SDS/PAGE gel for 3 to 4 hours at 25mA. After the run proteins were transferred to a nitrocellulose membrane according to standard western blotting protocols (Sambrook *et al*, 1989). For testing constitutively activity of BRAF V614E anti-phospho MAP kinase was used. For checking if *c-myc* transgenic lines are producing the fused protein an anti-ER antibody (1:500, santa cruz) was used. For both experiments, anti-beta-Actin (1:10000, Santa Cruz) was used as positive control. Peroxidase-coupled anti-mouse (1:3000, Thermo Scientific) and anti-rabbit (1:10000, Bio-Rad) were used as secondary antibodies.

Nonidet-P40 (NP40)   20mM   HEPES pH 7.9
                           500mM   NaCl
                           5mM $MgCl_2$
                           5mM   KCl
                           1%   Nonidet-P40

Lysis buffer	0,5%	(NP40)
	0.1%	deoxycholate
	10μg/ml	Aprotinin
	10μg/ml	Leupeptin
	200μM	Na_3VO_4
	1mM	PMSF
	100mM	NaF

| 10x TBS | 100mM | Tris pH 7.9 |
| | 1,5M | NaCl |

10% polyacrylamide gel	4152μl	H_2O
	2125μl	1,5M TrisHCl pH 8.8
	2138μl	Acrylamid 40 (37,5:1)
	85μl	10% SDS
	42,5μl	10% APS
	8,5 μl	TEMED

4% Stacking gel	1408μl	H_2O
	550μl	0,5M TrisHCl pH 6.8
	220μl	Acrylamid 40% (37,5:1)
	22μl	10% SDS
	11μl	10% APS
	2,2μl	TEMED

SDS gel loading buffer (2x)	100mM	Tris-Cl (pH 6.8)
	200mM	Dithiothereitol
	4%	SDS
	0,2%	Bromophenol blue
	20%	glycerol

| 5x Blotting buffer | 125mM | Tris |
| | 960mM | Glycine |

5x SDS running buffer	250mM	Tris
	192mM	Glycine
	0,5%	SDS

Transfer buffer	39mM	Glycine
	48mM	Tris base
	0,037%	SDS
	20%	methanol

5x Laemmli buffer	312,5mM	Tris pH 6.8
	50%	Glycerin
	10%	SDS
	0.005%	bromophenol blue
	Add H_2O to 75ml	
	25%	ß-mercapthoethanol

3.4.11 4-OHT treatment for C-myc induction

4-Hydroxytamoxifen (4-OHT; H7904; Sigma-Aldrich) was dissolved in ethanol at a final stock concentration of 10mM and kept in dark at 4°C. To induce the estrogen receptor coupled C-myc17 activity, transgenic adult fishes were kept continuously in tap water (pH 7) containing 1μM of 4-OHT in the dark for forty eight hours. To validate the effect of long C-myc17 activation, fishes were kept for four weeks in water containing 1μM of 4-OHT, with medium changes after 3 days. To induce *c-myc17* activity in primary cell culture, L-15 medium was mixed with 1μM of 4-OHT for twenty four hours.

3.4.12 Paraffin embedding

Adult fishes were anesthetized, killed and fixed ON in 4% PFA. Fixed fishes were kept in decalcification solution (10% Formic acid, 10% Formalin, 80% H_2O) for 24 hours followed by 2 times 10 minutes washes with PBS and 1 time 10 minutes at 0,9% NaCl in room temperature. For dehydration fishes were transferred every 2 hours in solutions containing different proportions of isopropanol (30%, 50%, 70%, 85%, 95% and 100% of isopropanol in H_2O, respectively, 2 hours each) in room temperature. Dehydrated fishes were transferred to a 1:1 (v/v) isopropanol/chloroform solution followed by chloroform for 2 hours each in room temperature. The next step was to transfer the fishes to a 1:1 (v/v) chloroform/paraffin solution at 60°C. The last step was to transfer fishes to paraffin and let it cool until room temperature. Paraffin embedded fishes were kept in 4°C until myotome sectioning, where 6μm thick sections were produced.

3.4.13 Hematoxylin and eosin (HE) staining

For histological analysis of paraffin sections, fishes were stained with haematoxylin and eosin (HE). Slides were kept for 30 min at 68°C to melt the paraffin. After 2 times 5 min bath in xylene, slides were transferred to a glass coplin jar containing 100%, 95%, 80% EtOH in H_2O for 2 min each, respectively. Slides were stained in haematoxylin for 2 to 5 min and bathed in warm water for 10 min. After that, slides were stained with eosin for 3 to 5 min and dehydrated with a fast rinse in H_2O, 30%, 50%, 70%, 85%, 95% and 100% of EtOH in H_2O, respectively. Glass slides were mounted with Roti® Histokit II (Roth). Hematoxylin and eosin solutions were kindly prepared by Robin Wacker, Biozentrum, University of Würzburg.

Hematoxylin	50g	potassium
	1g	haematoxylin
	0.2g	sodium iodate
	1g	citric acid
	To 1000	ddH$_2$O
Eosin	10g	Eosin y
	200ml	ddH$_2$O
	800ml	95% EtOH in H$_2$O

3.4.14 Proliferation and apoptosis assays

For the *in vivo* analysis of BrdU incorporation and apoptosis detection liver and gills from adult fishes were fixed for two hours in 10% neutral buffered formalin (RT or 4°C). For *in vivo* and primary cell apoptosis detection TUNEL assay was performed using ApopTag Red *In Situ* Apoptosis Detection Kit (Milipore) according to manufacturer's protocol. For detection of proliferating cells, adult fishes were bathed in a solution of 1g/L BrdU (Sigma-Aldrich) in aquarium water for five hours before dissection of organs. BrdU assays were performed using anti-BrdU antibody (1:250, serotec) and anti-rat 458 secondary antibody (1:250, serotec).

3.4.15 Nuclear translocation assay

Primary cell culture from medaka anal fins were cultured with 4-OHT (1mM, soluted in L-15 medium) for 2 hours and fixed with 2% formaldehyde. Nuclear translocation assays were performed using anti anti-ER antibody (Santa Cruz). Nuclei were counter-stained with Hoechst 33342 fluorescent stain (Invitrogen). Imaging was done with Nikon eclipse Ti confocal microscope and NIS elements imaging software. Translocation ratio was calculated by the following formula: $FI_{nucleus} - FI_{cytoplasm.}$ FI indicates fluorescence intensity.

3.5 Generation of transgenic lines

To obtain freshly fertilized eggs male and female fishes were separated in different tanks the evening before injection. At the next day, 2 males were put together in tanks containing 3 to 5 females. 30 to 45 min later each female laid eggs, which were kept attached to the belly of the females. Freshly laid eggs were transferred into Petri dishes with fresh 0,3x Danieau`s medium. The injection dish was freshly made from 2% agarose in 0,3x Danieau`s medium.

Medaka transgenics were generated using the Meganuclease (*I-SceI*) technology (Thermes *et al*, 2002). One-cell-stage eggs were injected with the following solution: 10 ng/µl of plasmid, 1x Tango buffer (Fermentas), 0.35 U/µl of *I-SceI* (Fermentas). Injection solution was incubated for 30 min at 37°C. Before injection 0.1% phenol red for visualization and 0.2% Fitc-dextran (Sigma-Aldrich) for screening of positive injected were added to the solution. Approximately 500pl of DNA solution was directly injected through the chorion into the cytoplasm of the first cell.

Injected embryos were transferred to a new Petri dish with fresh 0,3x Danieau`s medium and incubated at 28°C. After injection, embryos were controlled for positive injection, by fluorescence of Fitc-dextran. Positive injected embryos were sorted under the fluorescent microscope and raised for further investigations and breeding. Visual control of dead or mal-formed embryos was performed every day. Embryos were raised to sexual maturity followed by sibling screening for transgene integration by fin clipping as described in section 3.4.6.6.

1x Danieau`s	58 mM	sodium chloride
	0,7 mM	potassium chloride
	0,4 mM	magnesium sulfate
	0.6 mM	calcium nitrate
	0.5 mM	HEPES
	0,1%	methylen blue
0,3x Danieau`s	30%	Danieau`s in H_2O

3.6 Phylogenetic methods and alignments

Sequence alignments were generated applying BioEdit (Hall, 1999) and ClustalW (Thompson *et al*, 1994). Maximum likelihood analysis was performed using Mega 5.0 software according to a JTT model of amino acid substitutions. Confidence of each node was confirmed by 100 bootstrap replicates. Analysis of *c-myc* gene synteny was performed utilizing the ENSEMBL database and the synteny database (Catchen *et al*., 2009).

4. RESULTS

4.1 BRAF

BRAF is a serine threonine kinase found mutated in high incidence in human tumours like malignant melanoma and thyroid cancer (Garnett and Marais, 2004). A deeper understanding of BRAF biology will help to elucidate its function in cancer initiation and progression and will open up the possibility to further investigate BRAF as a possible target for cancer therapy. To gain new knowledge on BRAF function I have identified and cloned for the first time the medaka *braf* gene.

4.1.1 *braf* cloning and sequence analysis

4.1.1.1. Full length Medaka braf cloning

Initial investigations of published database sequence information showed that Medaka BRAF sequence in ENSENBL database (ENSORLG00000009843) is not complete. Based on comparison with orthologues of fugu (*Takifugus rubripes*), zebrafish (*Danio rerio*), tetraodon (*Tetradon nigroviridis*) and stickleback (*Gasterosteus aculeatus*), I noticed that the first 156 nucleotides are missing. As the first 20 nucleotides from these species are 100% conserved, I used a degenerated forward primer (OrybrafATGfish) for cloning full length medaka BRAF based on their sequences. The newly annotated sequence not present in the database is marked in purple in Figure 7. After cloning of the full length BRAF sequence, a tandem sequence for Ha (Field *et al*., 1988) and Flag tags (Thomas *et al*, 1988) were added to the C-terminal region of the protein and are marked in red and green, respectively, in Figure 7.
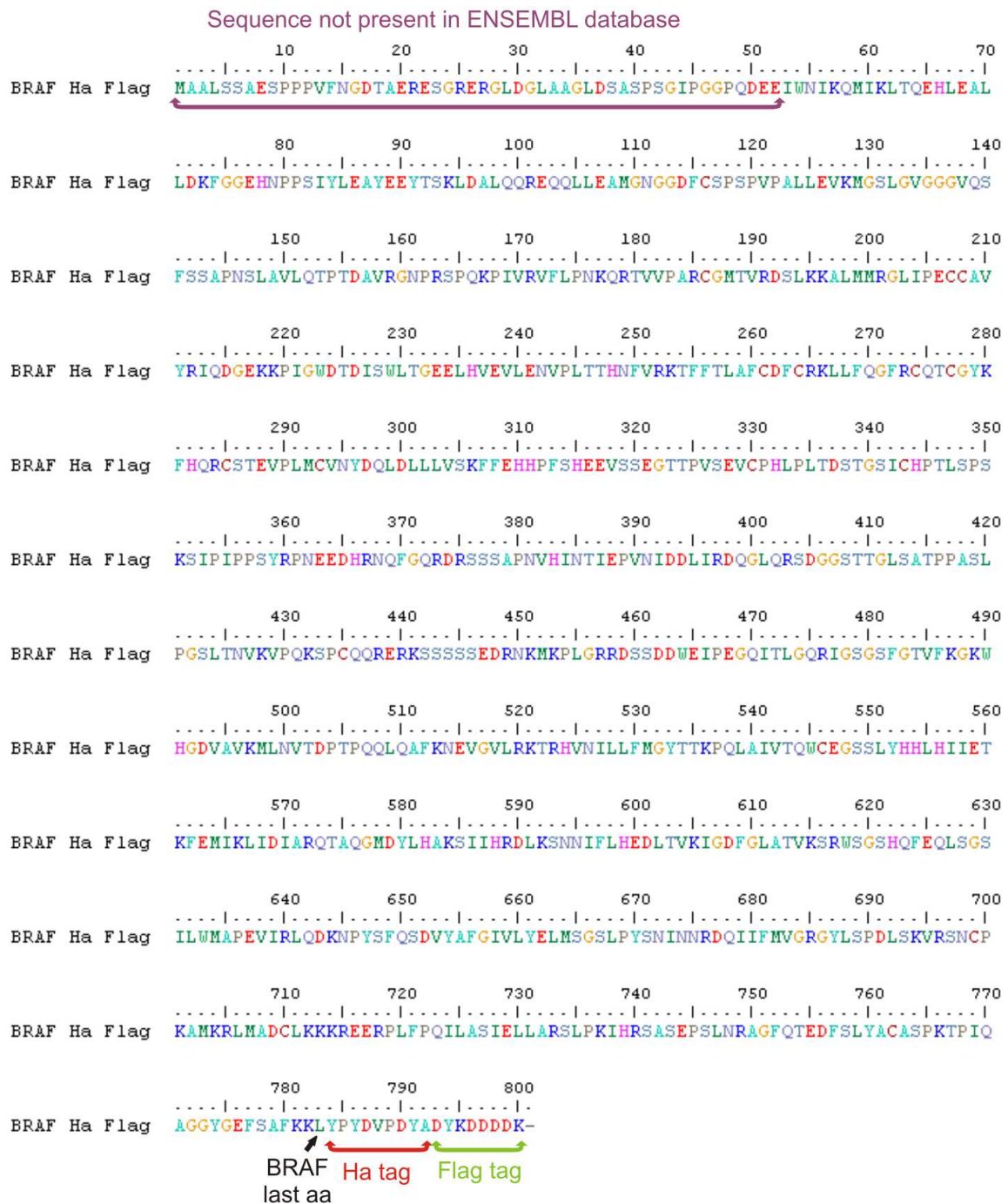
Fig 7. Protein sequence of the translated full length medaka BRAF coding sequence. Marked in purple is the sequence lacking in ENSEMBL database but cloned in this work based on homology to other fish sequences. Ha (marked in red) and Flag (marked in green) tags were added in the N-terminal region of the protein after the last BRAF amino acid before the stop codon.

The strategy used to clone BRAF was to amplify the full length gene in three, partly overlapping parts and clone these into the pCR2.1 vector (Invitrogen, Fig. 8). The first comprised from the first ATG until nucleotide 915 (using primers Ory BRAF ATG fish FOR and BRAF R1), the second from nucleotide 596 until 1506 (using primers BRAF F2 and BRAF R2) and the third part comprising nucleotide 1275 until the last nucleotide before the stop codon (2343, using primers

BRAF F3 and BRAF_v1_mdka_R). The next step was to combine each of the overlapping fragments together to obtain full length BRAF sequence.

Part one was cut from the vector using XbaI and AccI, and the vector was further digested in a way that after purification the only fragment with overlapping ends to the desired receiving vector was the BRAF segment (Fig. 8). This way, without the need of gel purification, I was able to fuse part one and part two, previously cut with the same enzymes. After control digestions to confirm the acquisition of the sequence corresponding to the beginning of BRAF in the vector containing the middle sequence, part one and two, now together in the same vector, were cut using XbaI and BsEI and added in vector containing the C-terminal part in a similar way as described for the first sub-cloning step. Ha and Flag tags were added at the full length gene by oligo cloning as described in section 3.3.4.
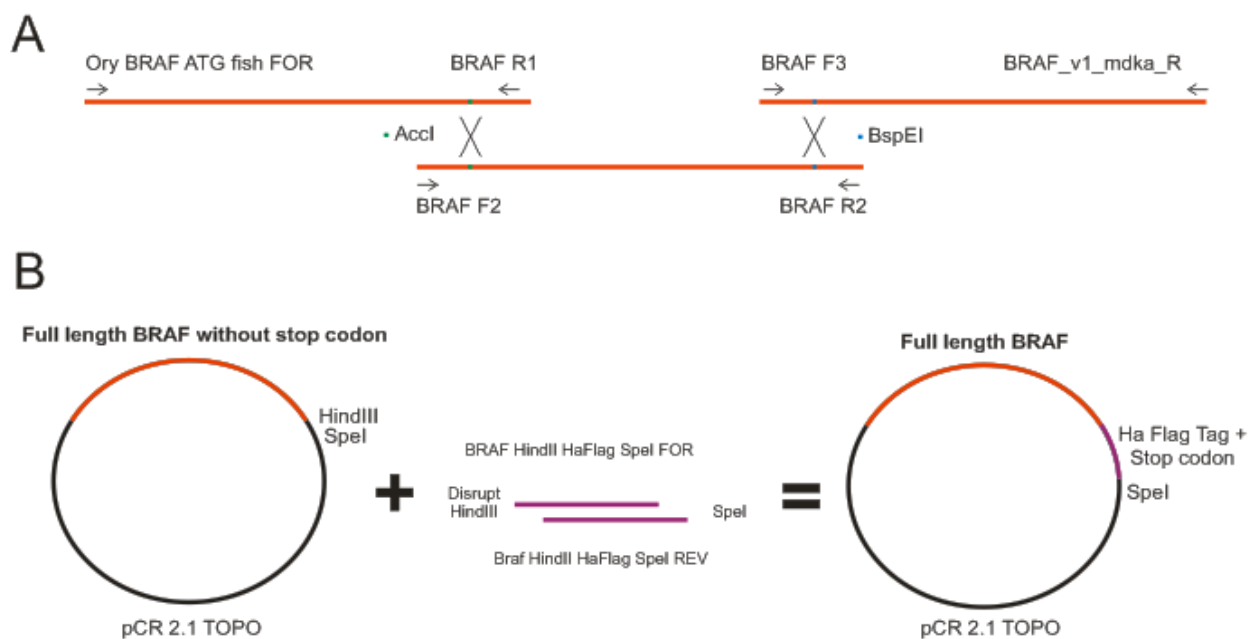
Fig. 8. Schematic representation of full length *braf* cloning strategy. (A) The *braf* coding sequence was cloned in three parts, each with overlapping sequences containing restriction endonuclease sites. Those restriction sites were used for sub-cloning all parts together in the same vector. (B) After full length *braf* sequence was generated, Ha and flag tags were added by oligo cloning.

4.1.1.2 Generation of constitutively activated BRAF

After production of full length BRAF containing the HA and FLAG tags, I developed a constitutive active version of BRAF by site directed mutagenesis as described in section 3.3.5. It is known that a single point mutation in *braf* sequence leading to a valine to glutamic acid substitution at the position 600 of the corresponding protein results in a constitutively active version in humans (Davies *et al*., 2002; Wellbrock and Hurlstone, 2010). Figure 9A shows the wild type amino acid (big letters) and nucleotide (small letters) sequence of the region flanking the corresponding valine in medaka. Figure 9B shows the amino acid (big letters) and nucleotide (small letters) sequence of the same region after mutagenesis. Figure 9C shows the alignment of human and medaka BRAF protein sequences confirming that the valine in position 600 in human

is conserved in medaka (present in position 614). After production of this mutation the region containing medaka valine 614 was sequenced to confirm success of mutagenesis (Figure 9D).
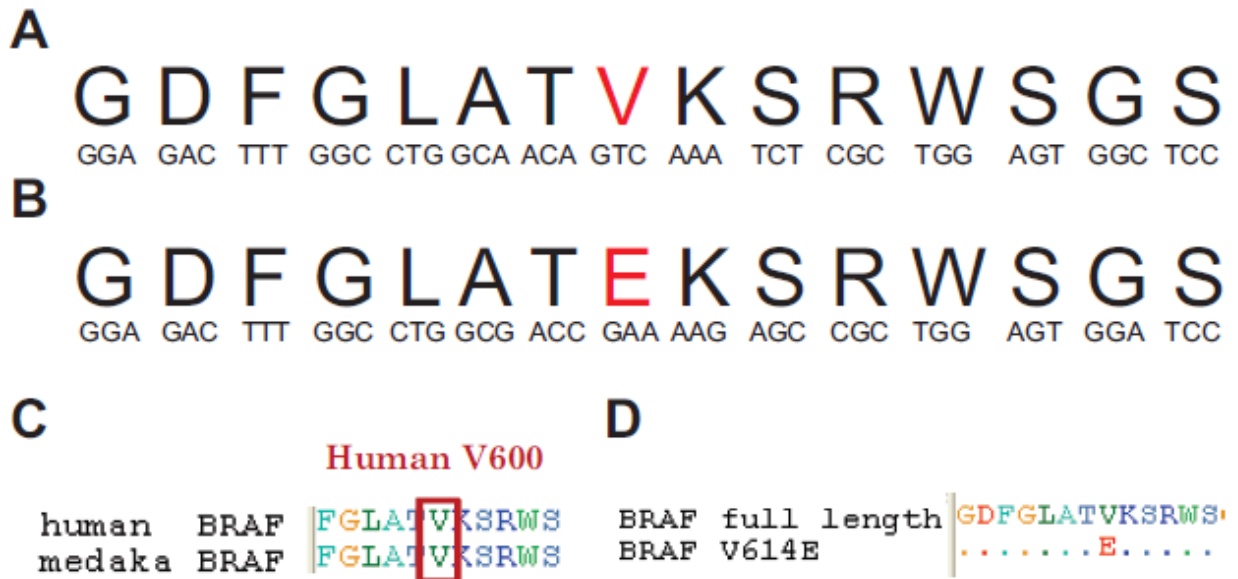
Fig. 9. Mutagenized BRAF sequence in medaka. (A) Wild type BRAF amino acid (big letters) and nucleotide (small letters) sequence. In red is the amino acid to be mutagenized. (B) Mutagenized BRAF amino acid (big letters) and nucleotide (small letters) sequence. In red is the amino acid that was mutagenized. (C) Alignment sequence of human and medaka BRAF showing conservation in both species of human V600. (D) Alignment of cloned medaka wild type and mutagenized BRAF sequences showing the successful mutagenesis of a valine to glutamic acid.

BRAF sequence was amplified in two parts with primers inserting desired mutation (Ory_BRAF_ATG_fish_FOR and mdkaV614Erev for the first PCR and mdkaV614Efor and BRAF_v1_mdka_R for the second PCR) as described in Figure 10A. After gel purification (Fig. 10B), both fragments were used as a template for a new PCR reaction to amplify the sequence containing the mutation (Fig. 10C).

A PCR amplification adding desired mutation

B Gel purification of amplified fragments containing the desired mutation
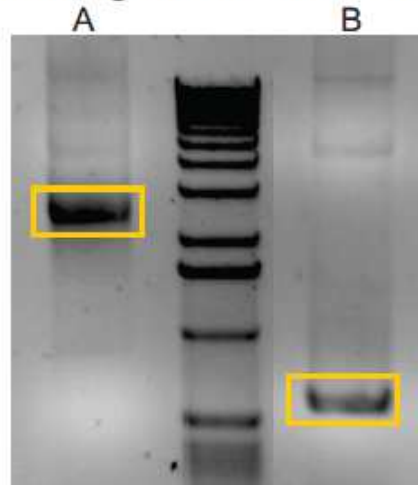
C PCR amplification of the full length sequence bearing desired mutation

Fig. 10. Schematic representation of site directed mutagenesis. (A) Medaka BRAF was PCR amplified in two parts using primers including desired mutation. (B) Both PCR products were gel purified (C) Purified PCR products were used as a template for a new PCR that amplified full length gene bearing the desired mutation.

4.1.1.3 Sub-cloning of BRAF gene sequences into expression plasmids

Full length BRAF and BRAF V600E bearing Ha and Flag tags in the C-terminal sequence, were sub-cloned into I-SceI MITF - polyA plasmid (received from Isabell Erhard) using XbaI and SpeI restriction enzymes. This plasmid contains the pigment cell specific medaka *mitf* promoter (Schartl *et al*., 2010), a SV40 poly A site and two meganuclease (I-SceI) sites flanking the construct. The plasmids containing the desired coding sequences were used for microinjection into one-cell stage medaka embryos to produce transgenic lines (Grabher and Wittbrodt, 2007).

Full length BRAF and BRAF V600E bearing Ha and Flag tags in the C-terminal sequence were also sub-cloned into the mammalian expression plasmid pCDNA3 (Invitrogen) using XbaI and HindIII restriction endonucleases. This plasmid contains the ubiquitously expressed ß-actin

promoter and a SV40 poly A site. This plasmid was used for transfecting Melan A cells (Bennett *et al*, 1987) to test BRAF constitutive activity (chapter 4.1.3). Correct construct assembly was controlled by restriction endonuclease digestion and sequencing.

4.1.2 BRAF evolution

By comparing the full length amino acid sequences of medaka, fugu, tetraodon, stickleback, zebrafish, xenopus (*Xenopus tropicalis*), mouse and human, I observed a high degree of similarity in the known BRAF domains CR1, which contains the Ras-binding domain (RBD) and the cystein-rich domain (CRD), CR2 and CR3, which is also known as the kinase domain (Fig. 11). The CR1 domain from medaka is 99% identical to human. The CR2 domain is 100% identical between these two species, while the kinase domain is 96% similar.

```
                     10        20        30        40        50        60        70
                     ....|....|....|....|....|....|....|....|....|....|....|....|....|....|
medaka BRAF      MAALSSAESPPPVFN---------------GDTAERESGRERGLD-GLAALDSASPSGIPG----GPQDEE
fugu BRAF        ....|....|....L---------------A...DP....E-E.DS.FN..CTTRV..----..A.N.
tetradon BRAF    .....................A...P....E-EPGS.FNT.YTTR..----..A.N.
stickleback BRAF ....|.TQ---------------..P..Q..E-E.GP---------------
danio BRAF       ...............MN.DPE.DP...E..EHC.GEAAIPECQQGIP.
xenopus BRAF     ------.T.G.SLLN---------------LL.S.T.GLG.AGEMC.S..........GYP.
mouse BRAF       ....GGGGSSSGGGGGGGGGGGGGGDGG.GAEQGQALFNGDMEPEAG..A-.AS.AADP-----AIP.
human BRAF       ....GGGG-----------------GAEPGQALFNGDMEPEAG..AGA.AS.AADP-----AIP.

                     80        90        100       110       120       130       140
medaka BRAF      IWNIKQMIKLTQEHLEALLDKFGGEHNPPSIYLEAYEEYTSKLDALQQREQQLLEAMGNGGDF-CSPSPV
fugu BRAF        .................T.........GS.W.....T.P.....M
tetradon BRAF    ...........................A.P.....M
stickleback BRAF ..................................G.A
danio BRAF       .T................................I..TE.CS.T--
xenopus BRAF     VRGPVRGGFGVSAY.IRWCLYL..LLYNCVPPIQ.......I....S...T.STSL..EL
mouse BRAF       V...................I.....................SL-----------
human BRAF       V...................I.....................SI..T..SVS.AS

                     150       160       170       180       190       200       210
medaka BRAF      PALLEVKMGSLGVGGGVQSFSSAPNSLAVLQTPTDAVRGNPRSPQKPIVRVFLPNKQRTVVPARCGMTVR
fugu BRAF        ...............GCVP.V.A----.........GS.W.................S.
tetradon BRAF    ...............GC.I...A----T.S.......I.GM.I.................S.
stickleback BRAF .............MS.GC..A..A.P..........G.A..............
danio BRAF       .T..D.-------..Q.I..APT...T.......T..............
xenopus BRAF     TLSSVPSN-----------L.L..SAL.SA.R..S..PS.I..R.............S..V..
mouse BRAF       ------------------------.........SN..K.........W.
human BRAF       MDTVTSS-------SSS.L.VL.S.S.F..VA.S..K.........
                                                                           RBD

                     220       230       240       250       260       270       280
medaka BRAF      DSLKKALMMRGLIPECCAVYRIQDGEKKPIGWDTDISWLTGEELHVEVLENVPLTTHNFVRKTFFTLAFC
fugu BRAF        .................I.................M...............
tetradon BRAF    .................I...............
stickleback BRAF ....................E...............
danio BRAF       ....................V...............
xenopus BRAF     ....................V.............I.............
mouse BRAF       .......................................
human BRAF       .......................................
          RBD                                            CRD

                     290       300       310       320       330       340       350
medaka BRAF      DFCRKLLFQGFRCQTCGYKFHQRCSTEVPLMCVNYDQLDLLLVSKFFEHHPFSHEEVSSEGTTRVSEVCF
fugu BRAF        ..............................TQ.....................
tetradon BRAF    ..............................TQ.....................
stickleback BRAF ..............................TQ...................DA.
danio BRAF       .......................A....LV..ITQ.........I..M..
xenopus BRAF     ...............S......F.....I.Q.APF.EVA.AA.SST
mouse BRAF       ...................VPQ...FPE.ALP.GSS-
human BRAF       ...................IPQ...LAE.ALT.GSS.
                          CRD                                         CR2

                     360       370       380       390       400       410       420
medaka BRAF      HLPLTDSTGSICHPTLSPSKSIPIPPSYRPNEEDHRNQFGQRDRSSSAPNVHINTIEPVNIDD------
fugu BRAF        S..PS....QS.V.........F.SS.
tetradon BRAF    S..PS...I....S.V.........F.SS.
stickleback BRAF S..PS.....M..T.........F..D
danio BRAF       S..PSE....L...V.........Q.F..G.
xenopus BRAF     PP..P.....PL.L.ST.......QPF..D
mouse BRAF       SA.PS.....PQILTSP.......QPF..AD.............EKFPEVEL
human BRAF       SA.PS.....PQILTSP.......QPF..AD
                                               CR2

                     430       440       450       460       470       480       490
medaka BRAF      ------LIRDQGLQRSDG.....................................GSTTGLSATPPAS
fugu BRAF        -----.M...F....APPTHPARCLRKHRTRTSSPLLYSYPNDIVFDFEPEPVFQ............
tetradon BRAF    -----.....F....APLTHPARCLRKHRTRTSSPLLYSYPNDIVFDFEPEPIFR............
stickleback BRAF -----.....F.....................................I.....
danio BRAF       -----.....F....................................
xenopus BRAF     -----...E.E...APSVQP-TCHRKYHSRDPSPLLHTLPSEIVFDFESDPVCR.....I......
mouse BRAF       QDQRD.....F-...APLNQLMRCLRKYQSRTPSPLLHSVPSEIVFDFEPGPVFR..........
human BRAF       -----.....F....................................
```
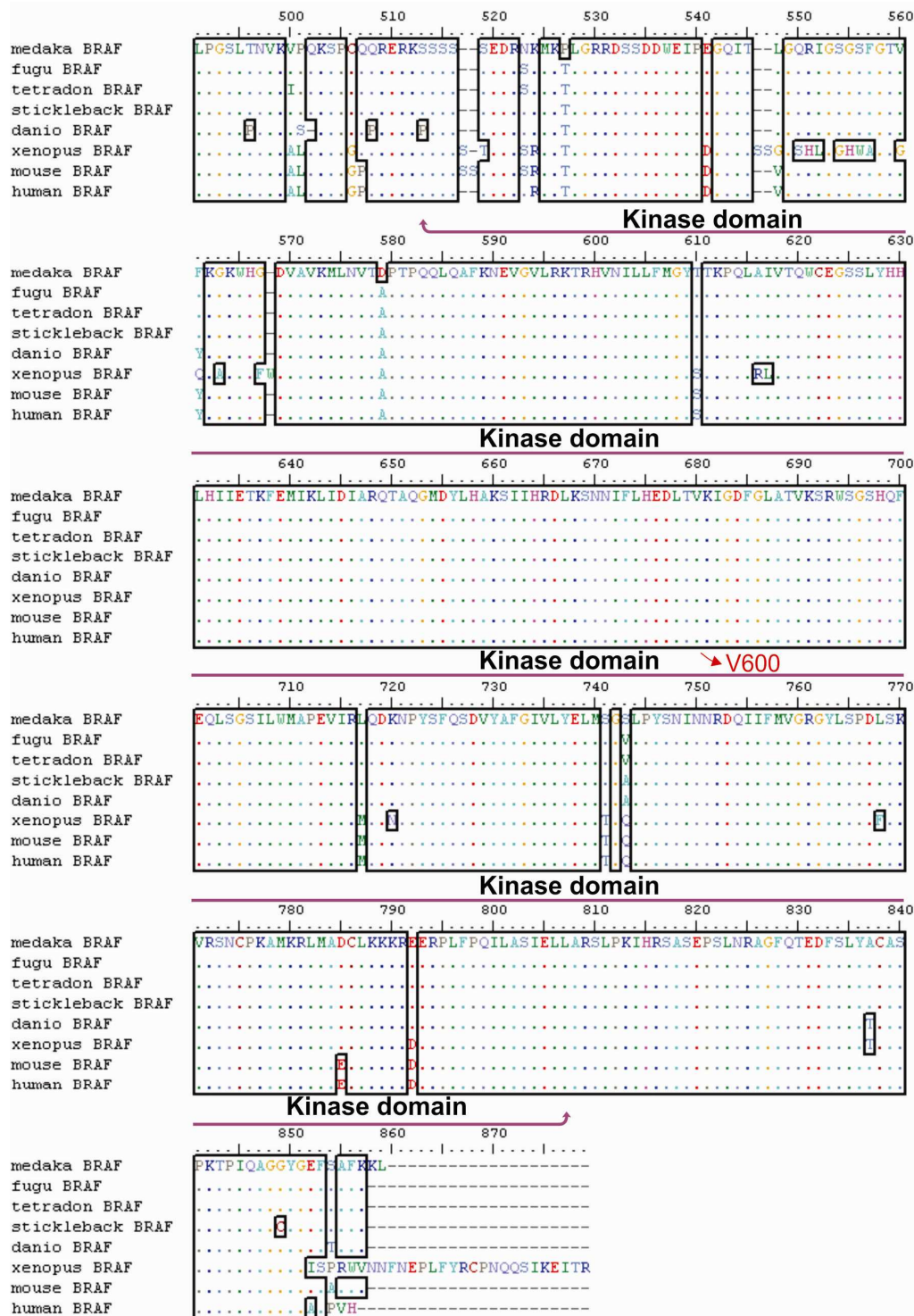
59

Fig 11. Protein alignment of full length BRAF from medaka, fugu, tetraodon, stickleback, zebrafish, xenopus, mouse and human. Conserved domains are marked in purple base on human sequence. RBD = Ras-binding domain; CRD = cystein-rich domain; RBD and CRD together constitute the conserved region 1, CR1; CR2 = conserved region 2; the kinase domain is the conserved region 3 (CR3).

Although human and medaka BRAF protein sequences are very conserved, synteny analysis comparing human BRAF locus on chromosome 7 and the corresponding medaka locus on chromosome 23 revealed no conservation between these species (Table 1).

Human BRAF up genes	Medaka BRAF up genes	Human BRAF down. genes	Medaka BRAF down. genes
C7orf5	PIK3CG	**BRAF**	**BRAF**
LUC7L2	HBP1 (2 of 2)	CCT4P1	LARGE
KLRG2	PTPRZ1 (1 of 3)	MRPS33	BICD1 (2 of 2)
CLEC2L	ARNTL2 (2 of 2)	AGK	TMPO (2 of 2)
HIPK2	STK38L	KIAA1147	STRAP
TBXAS1	MED21	WEE2	SLC25A3
PARP12	FGFR1OP2	SSBP1	LDHB (1 of 2)
JHDM1D	TM7SF3	TAS2R3	CNTN1 (2 of 2)
RAB19	GAS2L3	TAS2R4	CNTN1 (2 of 2)
SLC37A3	ARID2	TAS2R5	THAP5
MKRN1	SLC38A4	MGAM	PNPLA8 (2 of 2)
DENND2A	FAM55C (3 of 3)	OR9A4	DNAJB9
ADCK2	FAM55C (2 of 3)	CLEC5A	AKR1B1*
BRAF	**BRAF**	TAS2R38	AKR1E2*

Table 1. Analysis of human and medaka *braf* gene synteny. First column shows genes present upstream human *braf*, second column shows genes present upstream medaka *braf*, third column shows genes present downstream human *braf* gene and fourth column shows genes present upstream medaka *braf*. No gene present on the human chromosome in the region where *braf* is present was found in the surround region of medaka *braf*. Genes marked with one asterisk (*) are not annotated gene versions of medaka.

4.1.3 Functionality of BRAF constructs

In order to test the wild type and mutagenized *braf* coding sequences for their ability to produce functional proteins, I transfected mouse Melan A cells with either full length medaka *braf* or with the constitutively activated medaka *brafV614E* in the plasmid pCDNA3 under the control of the ß-actin promoter. As shown in Figure 12B, both proteins are produced, as they could be detected by Western Blot with an antibody targeting the human BRAF protein. Preliminary experiments to detect Braf proteins via their Ha or Flag tag were not successful. I also tested, whether BRAF V614E is constructively active. Therefore, I cultivated transfected cells in starving medium in order to lose the external stimulation on BRAF. Non stimulated BRAF is not able to activate MEK, which in turn is not able to phosphorylate MAP-kinase (reviewed in Michaloglou, 2008, Fig. 12A). BRAF V614E does not need stimulation to be active and therefore is able to phosphorylate MAP kinase even in starving medium (Fig. 12B). This enabled me to conclude that the constitutively activated version of BRAF works as expected.
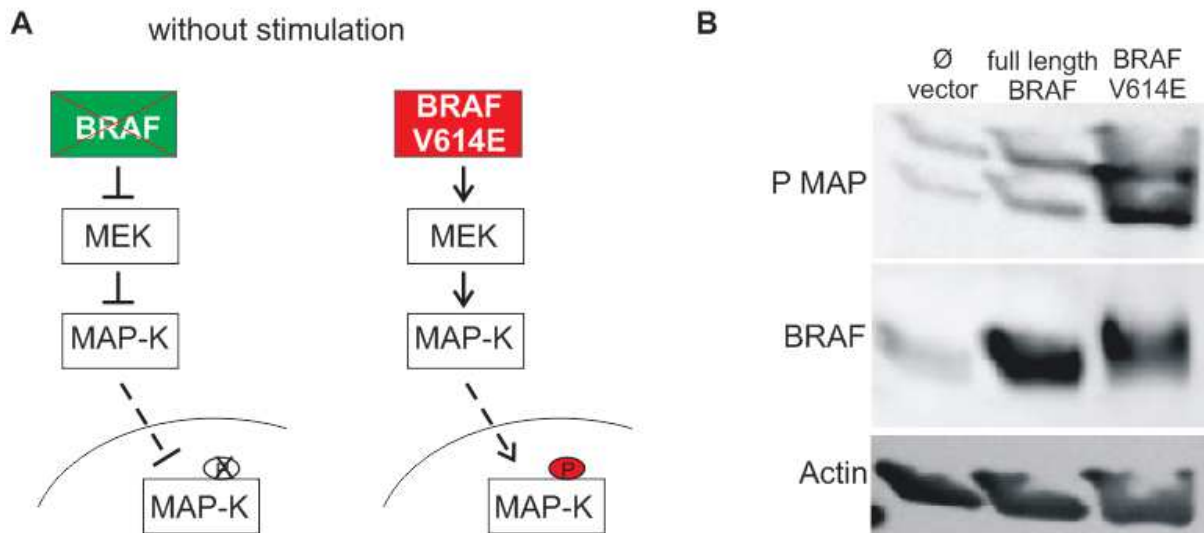
Fig. 12. Test of BRAF constructs functionality. (A) Wild type BRAF needs external signalization to become active and phosphorylate MEK. In a starving medium, no external signal is present, so BRAF is not active. In contrast, BRAF V614E is constitutively active, and therefore it is expected that even without stimulus, it phosphorylates MEK. (B) Western Blot showing the presence of BRAF in Melan A cells transfected with full length BRAF and BRAF V614E but only low amounts in cells transfected with empty vector. In starving medium, only BRAF V614E is able to phosphorylate MAP.

4.1.4 BRAF expression pattern

Using whole mount RNA *in situ* hybridization, I analysed BRAF expression during the early stages of development. RNA expression of BRAF was not detected at medaka development stage 20 (Fig. 13A) by *in situ* hybridization. At stage 28 (Fig. 13B) and 32 (Fig. 13C), a ubiquitous expression of *braf* was observed with raised expression in the otic vesicle (ot), mesencephalon (me) and prosencephalon (pe). As other tissues also show weaker staining, ubiquitous expression is possible. No expression or light blue background coloration was detected in the negative sense control (Fig. 13D-F).
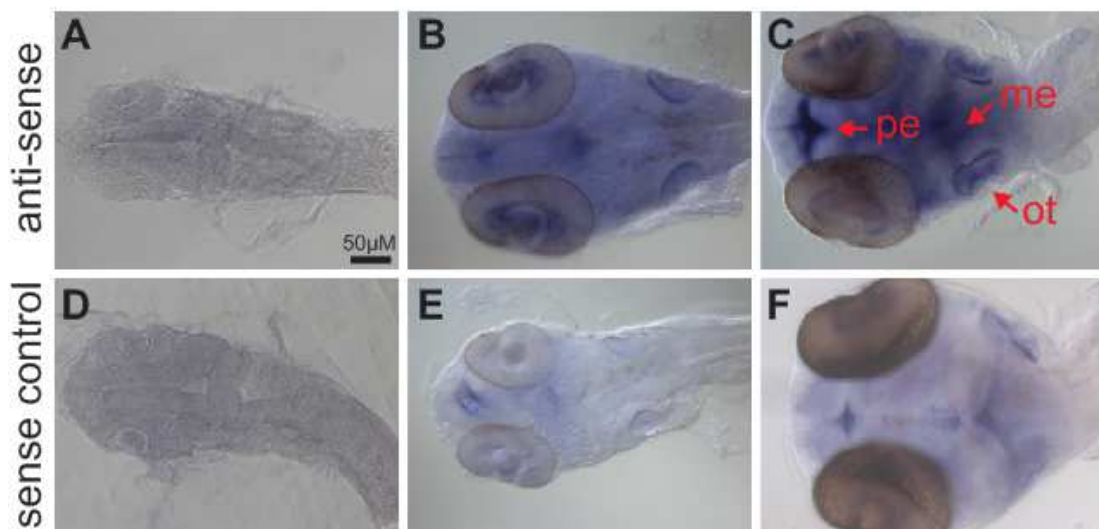

Fig. 13. *In situ* hybridization of medaka embryos using BRAF probes. (A-C) *braf* expression. (D-F) sense control. In stage 28 (B) and 32 (C), expression can be observed in the lens (l), otic vesicle (ot), mesencephalon (me) and prosencephalon (pe).

Braf expression was detected by Real Time PCR (qPCR) in wild type fishes in skin, brain, kidney, liver, testis and muscle. In brain the highest expression level was observed, it was 4 fold higher compared to skin (Fig. 14). No expression was found in eyes and gills.
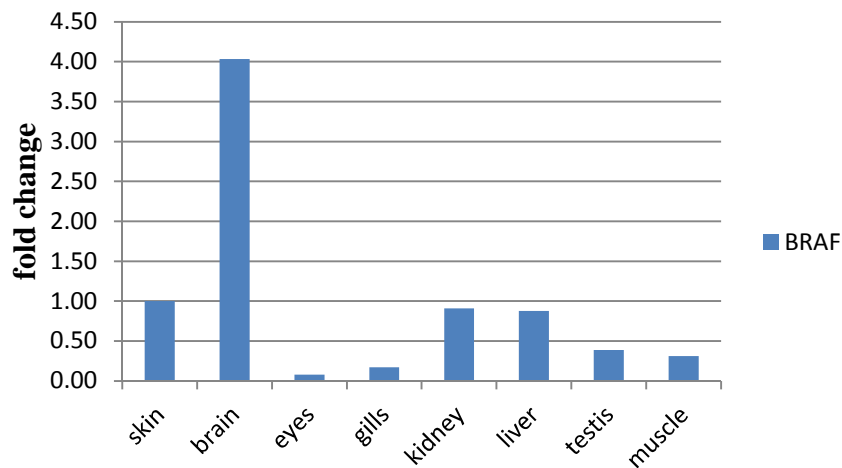

Fig. 14. *braf* expression in different organs from adult medaka fishes. *braf* expression was normalized against skin. The results shown here were calculated by the mean value of a triplicate assay. The expression of medaka *ef1a1* was used as internal cDNA control and standardization.

4.1.5 Generation of BRAF transgenic lines

One of the goals of my thesis was to investigate the effects of deregulated BRAF *in vivo.* Therefore I generated transgenic medaka lines carrying the medaka BRAF full length sequence and a constitutively activated BRAF version under the control of the pigment cell specific MITF promoter. These constructs were used to inject one cell stage medaka embryos to produce transgenic lines. Successfully injected fishes were raised, and progeny of sibling crossings were screened for transmission of transgene via genotyping PCR (section 3.4.6.6). For *mitf:braf*, four different lines transmitted the transgene to the next generation (named BRAF line 1, 2, 3 and 4), for *mitf:braf* V614E, three lines were screened positive (named BRAF V614 line A, B and C). An example of PCR result from generation 1 genotyping can be seen in Figure 15.
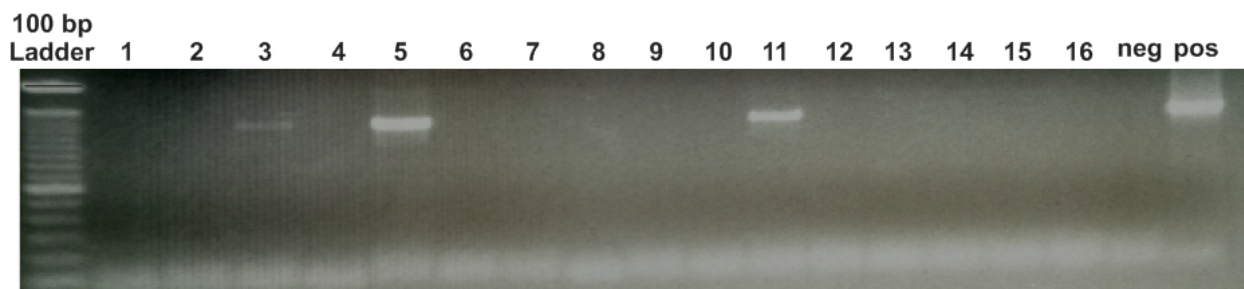

Fig. 15. F0 screen for transgene transmission to siblings. After crossing injected fishes, gDNA of the siblings was extracted. From 1-8, each line corresponds to a pool of hatchlings from fishes injected with wild type BRAF. 8-16 correspond to siblings of fishes injected with BRAF V614E construct. 3, 5 and 11 are positive. Neg = water negative control; pos = plasmid positive control

4.1.6 Analysis of BRAF transgenic lines

Phenotypic investigations of the established lines revealed that all BRAF V614E lines show a more pigmented skin when compared to lines bearing full length BRAF (Fig. 16). BRAF line 3 bearing the full BRAF sequence was used as control (Fig. 16 A-D). Higher pigmentation could be observed in all three BRAF V614E lines produced in this work (Fig. 16 E-P). Constitutive activity of BRAF leads to a stronger pigmentation in the skin of the trunk as well as in the fins, probably due to higher number of melanocytes.
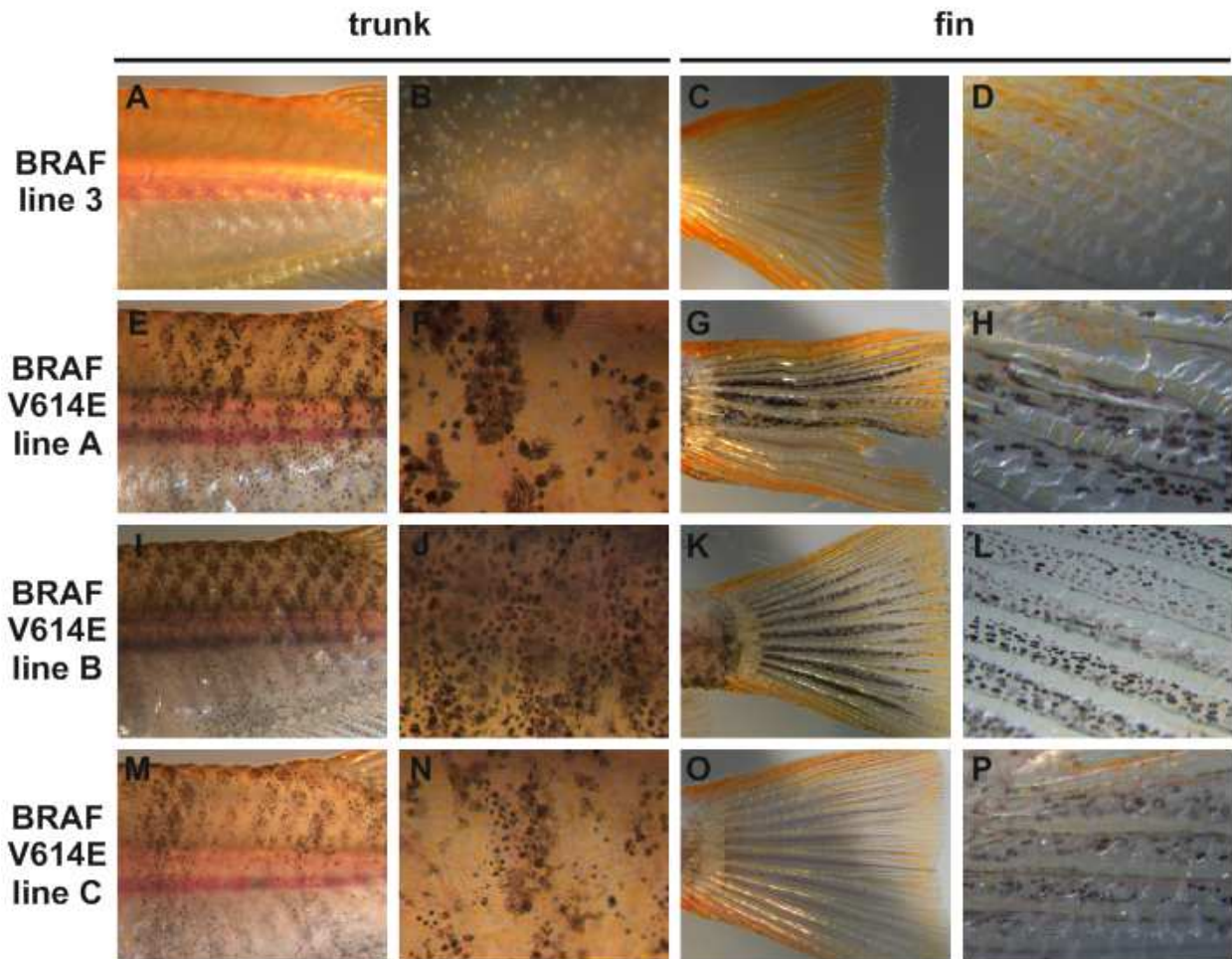

Fig. 16. Phenotypic comparison between BRAF V614E lines show differences in pigmentation. Pictures of trunk (first and second column) and fin (third and fourth column) from adult medakas from BRAF or BRAF V614E F1 lines showing different pigment patterns.

In transiently expressing Braf V614E F0 fishes from line A, a disrupted eye development was observed. To investigate this phenotype, histology on paraffin section was done. In Figure 17 one can easily observe the bigger right lens (indicated with red arrows in Fig. 17A and B) compared to the normal left lens in a Braf V614E specimen. This phenotype is also indicated by a red arrow in the adult fish (Fig. 17C). In another fish a melanin containing tumour like structure was observed (indicated with red arrows in Fig. 17D and E and in the adult fish in 17F). The structure was observed only in the right eye. No disrupted eye phenotype was observed in the wild type control (Fig. 17G-I).
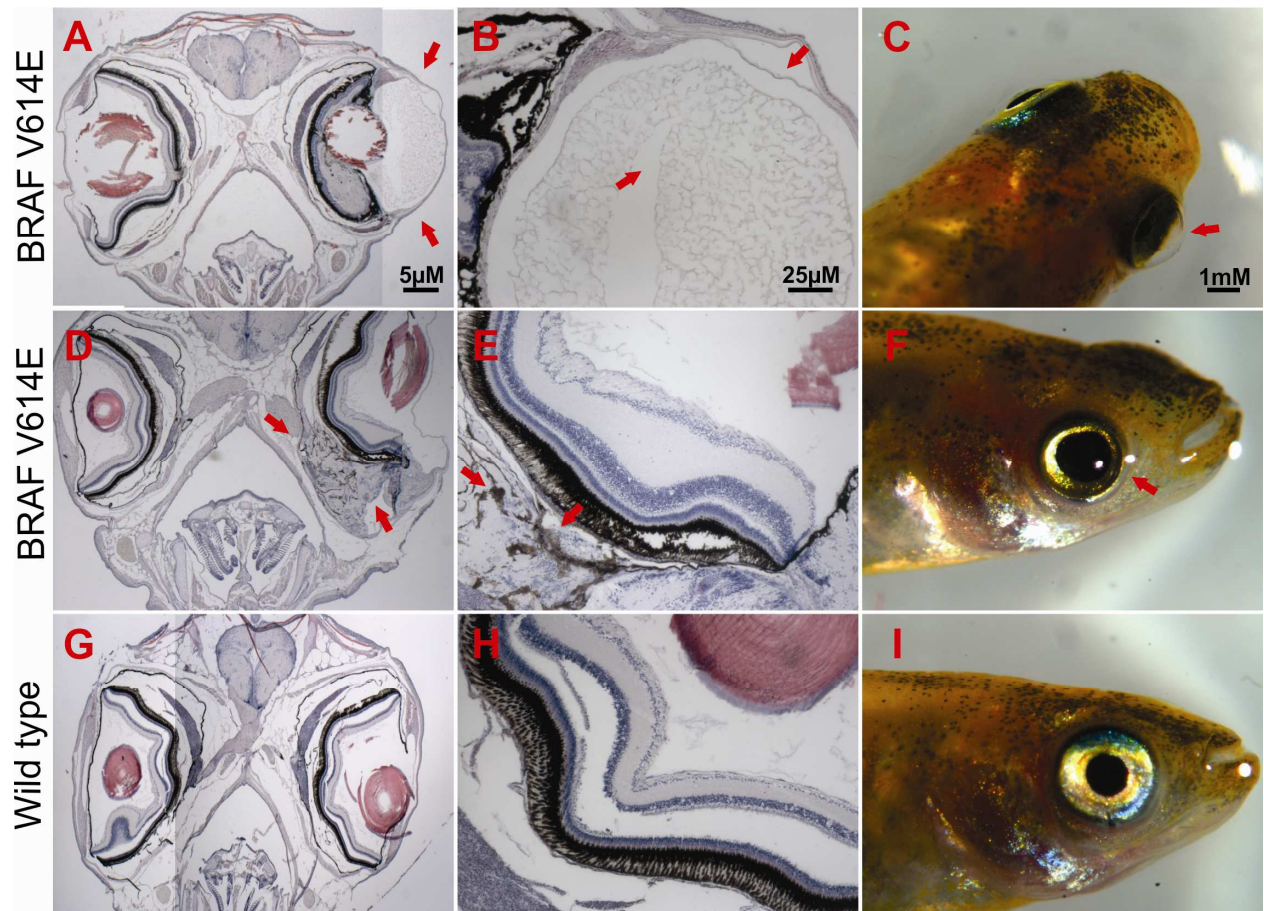
Fig. 17. Disrupted eye phenotype observed in *braf* **V614E transient expressing fishes.** HE staining of *braf* V614E (A-B) and fish (C) showing phenotype at the lens and HE staining of *braf* V614E (D-E) and fish (F) showing a tumour like lesion in the eye. HE staining of wild type (G-H) and wild fish (I) were used as control. Red arrows point to abnormal lens (A and B) and pigmented tumour like structure (C and D) observed in the transgenic fishes.

In summary, I was able to identify and clone medaka *braf* and produce transgenic lines bearing either wild type or a constitutively active BRAF under the control of the pigment cell specific *mitf* promoter. My results also indicate that constitutive activation of BRAF leads to a disrupted eye development and to hyperpigmented skin.

4.2 Stat5

The signal transducer and activator of transcription 5 (Stat5) is constitutively activated in many human cancers affecting gene expression, controlling cell proliferation and cell survival (Ferbeyre and Moriggl, 2011). Understanding Stat5 function in more detail and its role during tumorigenesis will bring new insights into the biology of cancer cells. To gain new knowledge on Stat5 function *in vivo,* I have identified and cloned for the first time both medaka *Stat5* genes. As Stat5 ab/a and Stat5ab/b are not homologues of human Stat5A and Stat5B (see section 4.2.2), they were so named to avoid false correlation with human copies.

4.2.1 Stat5 cloning

4.2.1.1 Medaka full length Stat5ab/a

Medaka *Stat5ab/a* sequence was cloned from cDNA pool from different organs of adult fishes. Protein sequence of full length Stat5ab/a is shown in Figure 18 in comparison with the protein sequence available in ENSEMBL database (ENSORLP00000004950). As mentioned below, the sequence cloned in this work lacks 5 amino acids corresponding to positions 693 to 697 (orange box in Figure 18) of the sequence available in the database. The 2421 nucleotides from Stat5ab/a gene were amplified from the initial ATG with primer Stat5ab/a _mdka_left that includes an XhoI site and primer Stat5ab/a R1 to nucleotide 985. The second part, from nucleotide 851 till 1763, was amplified using primers Stat5ab/a F1 and Stat5ab/a R2. The third part was amplified from nucleotide 1482 until the stop codon with primers Stat5ab/a F2 and Stat5ab/a _mdka_right that includes an EcoRI site.
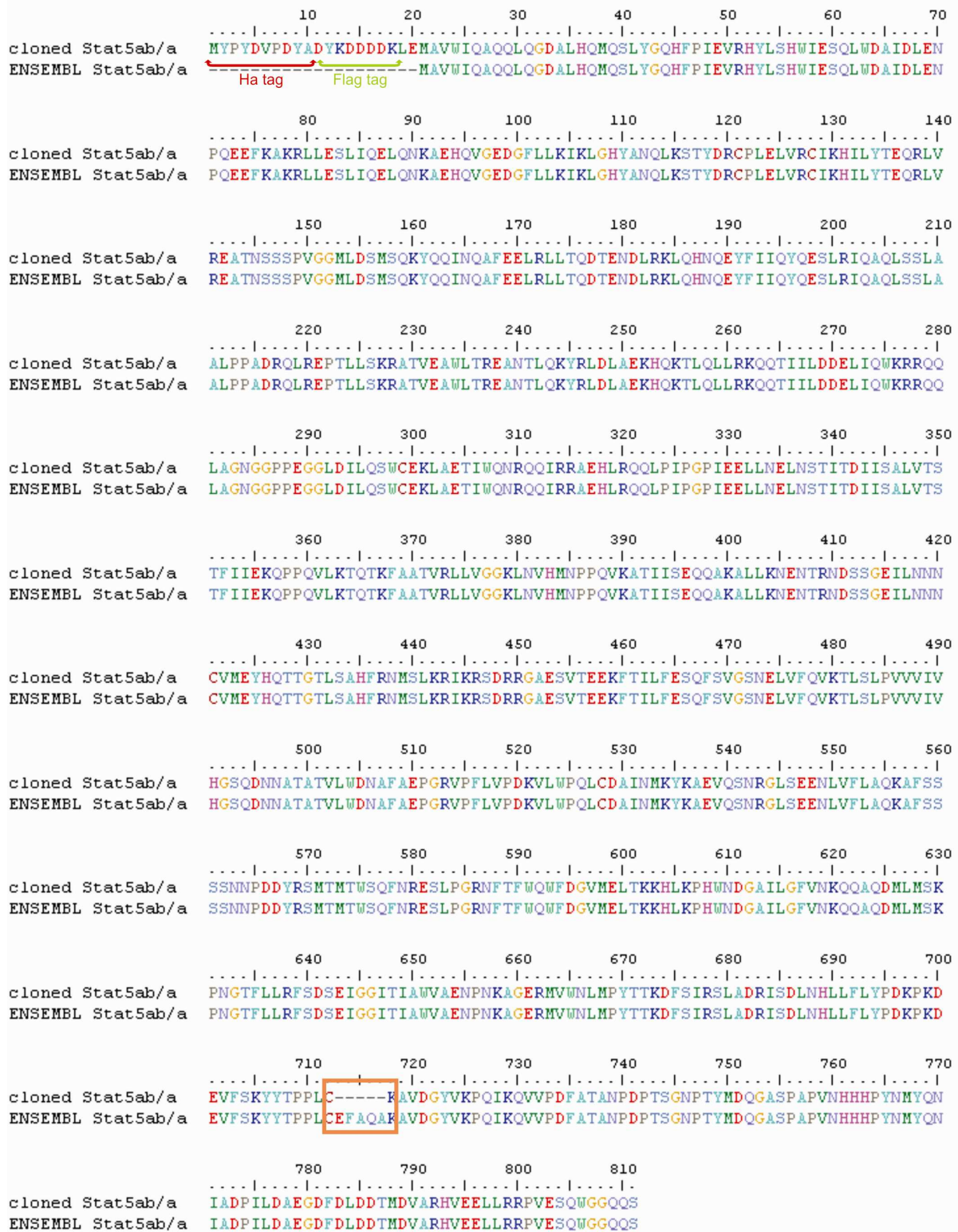
Fig 18. Protein sequence alignment of full length medaka Stat5ab/a gene. Ha (marked in red) and flag (marked in green) tags were added in the C-terminal region of the protein. Orange square marks the difference between the sequence present in ENSEMBL database and the sequence cloned from cDNA clones.

To validate that the cloned cDNA really lack these nucleotides, I aligned 4 independently cloned sequences and noticed that all of them lacked a 15 nucleotide sequence that was present in

ENSEMBL database (ENSORLG00000003961) in between nucleotides 2074 and 2090 (Fig. 19). The sequence used in this work for all analyses was based on the initially cloned Stat5ab/a gene.

Fig. 19. Sequence alignment of different Stat5ab/a clones with ENSEMBL database. All 4 sequenced clones lacked 15 nucleotides corresponding to nucleotides 2074 to 2090 of the ENSEMBL database Stat5a gene. The raw data was used to build this graphic. Sequence variation is due to sequencing error. Every variation was checked, and two picks in the Abi file were detected, always corresponding to amino.

For full length *Stat5ab/a* cloning as schematized in Fig. 20, part one was cut from the corresponding pCRII vector using XbaI and NsiI and the vector was further digested in a way that after purification the only fragment with overlapping ends to the desired receiving vector was the *Stat5* segment. This way, without the need of gel purification, I was able to sub-clone part one into part two previously cut with the same enzymes. After control digestions to confirm the acquisition of the sequence corresponding to the beginning of *Stat5ab/a* in the vector containing the middle sequence, part one and two, now together in the same vector, were cut using XbaI and SacII and added in vector containing the C-terminal part in a similar way as described for the first sub-cloning step (Fig. 20). Ha and Flag tags were added at the full length gene by oligo cloning as described in section 3.3.4. For *Stat5ab/a* constitutive active form, oligos XbaIHAFLAGXhoIFOR and XbaIHAFLAGXhoIREV were designed with respective 5'prime overhang for XbaI and XhoI. Correct construct assembly was controlled by restriction endonuclease digestion and sequencing.

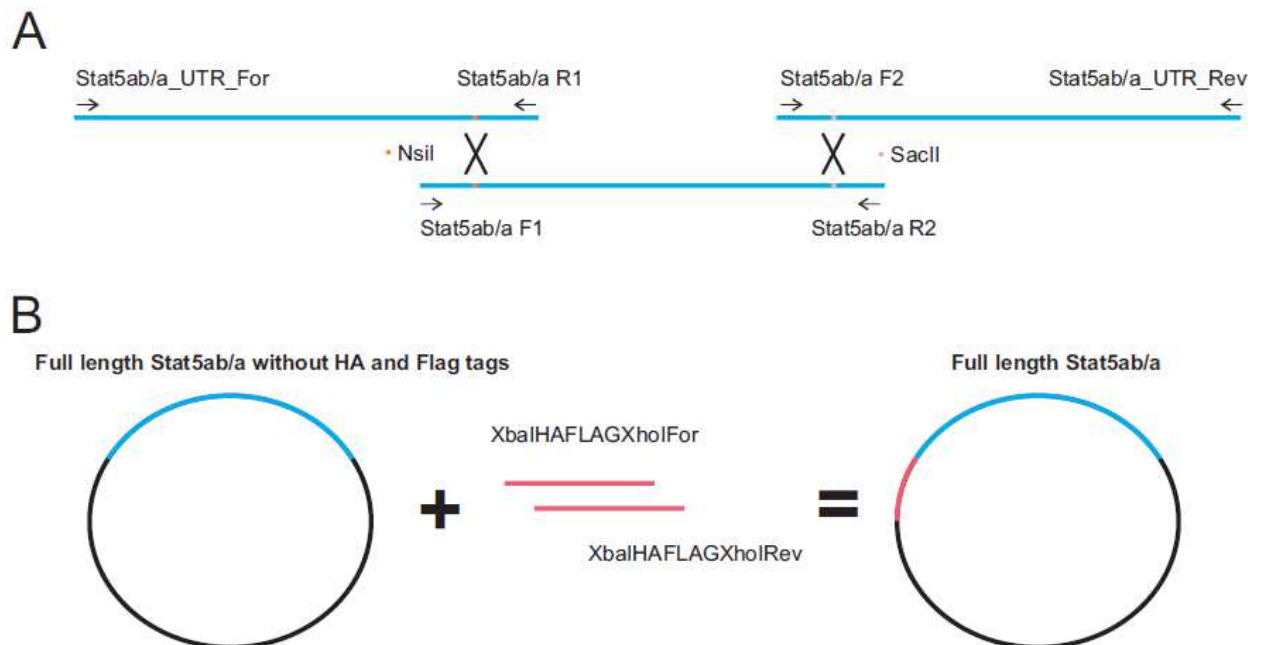**Fig. 20. Schematic representation of Stat5ab/a cloning strategy.** (A) Medaka *stat5ab/a* coding sequence was cloned in three parts, each with overlapping sequences containing restriction endonuclease sites. Those restriction sites were used for sub-cloning all parts together in the same vector. (B) After full length Stat5ab/a sequence was generated, Ha and flag tags were added by oligo cloning.

4.2.1.2 Medaka full length Stat5ab/b cloning

Corresponding to the *stat5ab/a* cloning strategy, the 2358 nucleotides from medaka Stat5ab/b sequence (ENSORLG00000014335) were cloned from cDNA pool from different organs of adult fishes as described in section 3.3. Protein sequence of full length Stat5ab/b is shown in Figure 21 in comparison with the protein sequence available in ENSEMBL database (ENSORLP00000004950). As shown in closer detail in Fig. 22, the sequence cloned in this work has 4 amino acids that are not present in the sequence available in the database between 635 and 636. Also the arginine residue present in ENSEMBLs sequence in position 636 was not found in our cDNA clones, which have instead a glycine (blue box in Fig. 21). In addition, the cloned Stat5ab/b sequence lacked 6 amino acids corresponding to amino acids 688 to 693 of the available Stat5ab/b sequence online (Fig. 21, purple box).

Fig 21. Protein sequence of full length medaka Stat5ab/b gene. Ha (marked in red) and flag (marked in green) tags were added in the C-terminal region of the protein. Blue and purple squares mark the difference between the sequence present in ENSEMBL database and the sequence cloned from my cDNA clones.

To validate the changes in the sequences, I aligned 5 independently sequenced clones of *Stat5ab/b* and noticed that all of them included 12 nucleotides between nucleotides 1909 and 1910 which are not present in the sequence in ENSEMBL's database (Fig. 22A). Also, all sequenced clones

lacked the 12 nucleotide sequence that was present in ENSEMBL database (ENSORLG00000003961) in between nucleotides 2074 and 2090 (Fig. 22B). The sequence used in this work for all analyses was based on cloned Stat5ab/a gene.
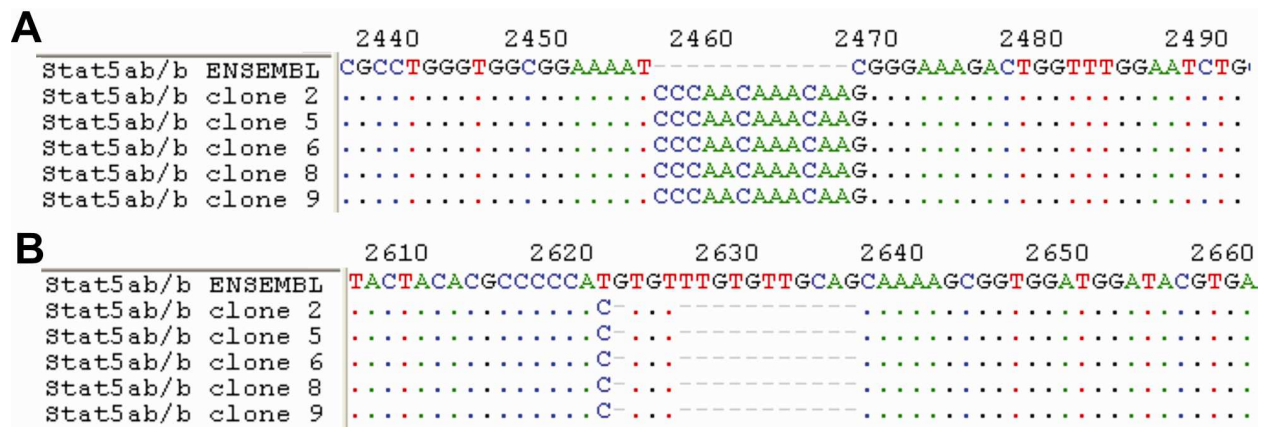

Fig. 22. Sequence alignment of different Stat5ab/b clones with ENSEMBL database sequence. (A) All 5 clones sequenced bore 12 nucleotides between nucleotides 2458 and 2459 of the ENSEMBL database Stat5b sequences. Besides that, all five clones had a guanine at position 2460 instead of a cytosine present in the ENSEMBL database sequence. This modification is responsible for the glycine present in position 661 which differs from the arginine present at the same position in the ENSEMBL data base sequence. (B) Also, cloned Stat5ab/b lacked 12 nucleotides corresponding to nucleotides 2624 and 2628 to 2638 ENSEMBL database Stat5ab/b coding sequence.

Stat5ab/b was amplified from the initial ATG with primer Stat5ab/b_mdka_left that includes an XhoI site and primer Stat5ab/bR1 to nucleotide 843. The second part was amplified from nucleotide 646 until 1765 using primers Stat5ab/bF1 and Stat5ab/bR2. The third part was amplified from nucleotide 1364 until the stop codon with primers Stat5ab/bF2 and Stat5ab/b_mdka_right that includes an EcoRI site.

For full length *Stat5ab/b* cloning, the first part was cut from the vector using XbaI and EcoNI, and the vector was further digested in a way that after purification the only fragment with overlapping ends to the desired receiving vector was the *Stat5ab/b* segment. This way, without the need of gel purification, I was able to sub-clone part one into part two previously cut with the same enzymes. After control digestions to confirm the acquisition of the sequence corresponding to the beginning of *Stat5ab/b* in the vector containing the middle sequence, part one and two, now together in the same vector, were cut using XbaI and HindIII and added in vector containing the C-terminal part in a similar way as described for the first sub-cloning step. Ha and Flag tags were added at the full length gene by oligo cloning as described in section 3.3.4 (Fig. 23). For *Stat5ab/b*, oligos XhoIHAFLAGNdeIfor and XhoIHAFLAGNdeIrev were designed with respective 5'prime overhang for XhoI and NdeI. Correct construct assembly was controlled by restriction endonuclease digestion and sequencing.
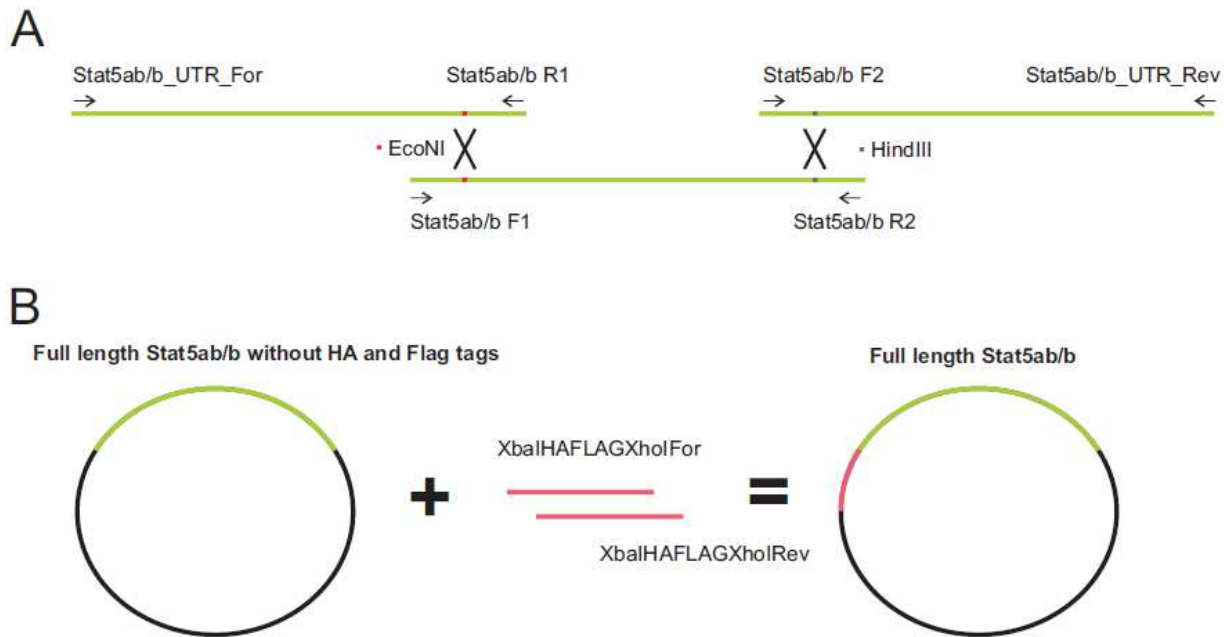
Fig. 23. Schematic representation of Stat5ab/b cloning strategy. (A) Stat5ab/b coding sequence was cloned in three parts, each with overlapping sequences containing restriction endonuclease sites. Those restriction sites were used for sub-cloning all parts together in the same vector. (B) After full length Stat5ab/b sequence was generated, Ha and flag tags were added by oligo cloning.

4.2.1.3 Generation of constitutively activated and dominant negative Stat5ab/a and Stat5ab/b

After full length Stat5ab/a and Stat5ab/b with Ha and Flag tags were generated, a constitutive active version of each was produced as described in section 3.3.5. It is known that a single point mutation in the SH2 domain of human Stat5A (Ariyoshi *et al.*, 2000), leading to an aspargine to histidine substitution at the position 642, is constitutively activated. As aspargine in position 642 in human is conserved in medaka (present in position 646 in Stat5ab/a and 647 in Stat5ab/b), I produced the same mutation by site directed mutagenesis (Fig. 24). Site directed mutagenesis was performed as described in section 4.1.1.2 with *braf* gene. For Stat5ab/a Stat5ab/a_N646H_For and Stat5ab/a_N646H_Rev primers were used. For Statab/b Stat5ab/b_N646H_For and Stat5ab/b_N646H_Rev primers were used.

Figure 24A shows the wild type amino acid (big letters) and nucleotide sequences (small letters) of the region flanking this aspargine in medaka *Stat5ab/a*. Figure 24B shows the amino acid (big letters) and nucleotide (small letters) sequence of the same region after mutagenesis. Figure 24C shows the wild type amino acid (big letters) and nucleotide (small letters) of the region flanking this aspargine in medaka *Stat5ab/b*. Figure 24D shows the amino acid (big letters) and nucleotide (small letters) sequence of the same region after mutagenesis. Also, an alignment of human Stat5A and Stat5B with both medaka Stat5 sequences (Fig. 24E) confirms that the aspargine 642 in humans is conserved in both medaka sequences. The result of the sequencing after mutagenesis of *Stat5ab/a* (Fig. 24F) and *Stat5 ab/b* (Fig. 24G) confirms that the mutagenesis successfully added the desired mutation in medaka sequences.
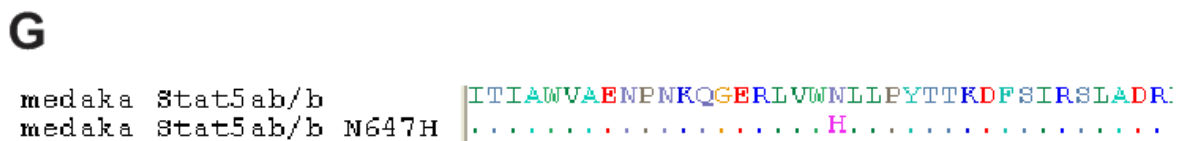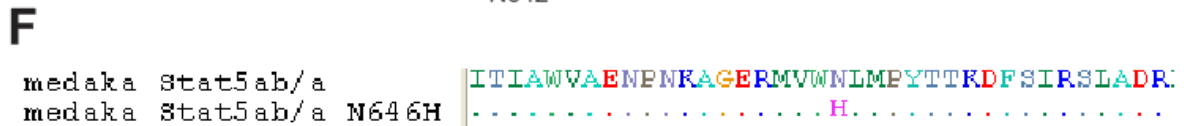
Fig. 24. Comparison of mutagenized *stat5ab/a* and *stat5ab/b* sequences. (A) Wild type Stat5ab/a or (B) Stat5ab/b amino acid (big letters) and nucleotide (small letters) sequence. In red is the amino acid that will be mutagenized. (C) Sequence alignment of human and medaka Stat5ab/a and Stat5ab/b genes showing conservation of human N642 in both species. (D) Alignment of cloned medaka wild type and mutagenized Stat5ab/a and (E) Stat5ab/b sequences showing the successful mutagenesis of an aspargine to histidine.

Deletion of the carboxyl-terminal region of mouse Stat5A leads to sustained DNA-binding and dominant negative phenotype (Moriggl *et al*., 1996). Therefore, dominant negative Stat5 constructs were generated by deletion of the carboxyl-terminal transactivation domain from medaka *Stat5ab/a* and *Stat5ab/b*. The deletion was done by adding a stop codon in the same region as done in mouse Stat5a by PCR and subsequently cloned into pCR2.1 topo (Fig. 25, marked with green arrow). Figure 25 shows an alignment of both mice Stat5 sequences with cloned full length and dominant negative *Stat5ab/a* (Fig. 25A) and *Stat5ab/b* (Fig. 25B).

Fig. 25. Alignment of dominant negative versions of medaka *Stat5* coding sequences. (A) Stat5ab/a and (B) Stat5ab/b alignment with its respective full length sequence showing the lack of the N-terminal region.

4.2.1.4 Sub-cloning of Stat5 genes sequences into pI-SceI plasmid

To produce stable transgenic medaka fish lines, both full length *Stat5ab/a* and *Stat5ab/b* bearing HA and Flag tags in the N-terminal region were sub-cloned into an I-SceI pla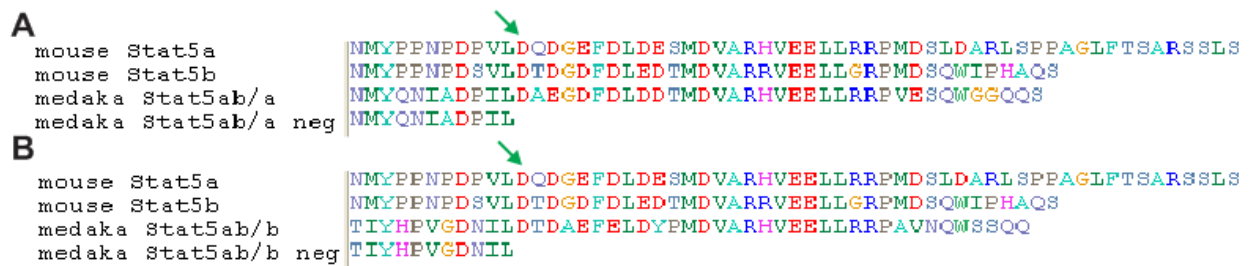smid that has a medaka *mitf* promoter and a SV40 poly A site using XbaI and SpeI restriction endonucleases. (Vector maps can be found in appendix section 7.2)

4.2.2 Stat5 sequence analysis

By comparing amino acids sequences of medaka Stat5ab/a and Stat5ab/b, I observed a high degree of similarities in known conserved Stat5 domains like coiled-coil (83%), DNA binding (92%) and the SH2 domain (92%). As expected, the domain with lower degree of homology is the transactivation domain. Medaka Stat5ab/a have similar levels of homology with both human Stat5A and Stat5B sequences (Table 2).

	medaka Stat5ab/b	human Stat5A	human Stat5B
medaka Stat5ab/a N-term	74%	79%	80%
medaka Stat5ab/a CC	83%	80%	80%
medaka Stat5ab/a DBD	92%	95%	97%
medaka Stat5ab/a LD	78%	74%	76%
medaka Stat5ab/a SH2	92%	75%	72%
medaka Stat5ab/a TA	51%	60%	59%

Table 2. Comparison of Stat5 conserved domains. Conservation of medaka Stat5ab/a and Stat5ab/b and human Stat5A and Stat5B protein sequences. N-term indicates the N-terminal domain. CC indicates the coiled-coil domain. DBD indicates the DNA binding domain. LD indicates the linker domain. SH2 indicates the SH2 domain. TA indicates the transactivation domain.

Figure 26 shows a protein alignment between human Stat5A and Stat5B and medaka Stat5ab/a and Stat5ab/b. Their conserved domains are highlighted based on the known human sequences.

N-terminal domain

```
                    10        20        30        40        50        60        70
human Stat5A    MAGWIQAQQLQGDALRQMQVLYGQHFPIEVRHYLAQWIESQPWDAIDLDNPQDRAQATQLLEGLVQELQK
human Stat5B    ..M.........E..H..A..............S......A..SV.....ENIK...............
medaka Stat5ab/a .M.........H..S...........SH.....L...E..EEFK.KR...I.........N
medaka Stat5ab/b SL........E..H..S...............SVE...AEETK.KR..DN..Q
```

N-terminal domain

```
                    80        90        100       110       120       130       140
human Stat5A    KAEHQVGEDGFLLKIKLGHYATQLQKTYDRCPLELVRCIRHILYNEQRLVREANNCSSPAG-ILVDAMSQ
human Stat5B    .........................N...........M.............G.......-S.A.
medaka Stat5ab/a QV.G.............N.KS.........K...T.........T.V..-GML.S.
medaka Stat5ab/b .QV.G...........T.KS........KQ..QS.........T.V.CGN.LQAM.SL
```

coiled-coil domain

```
                    150       160       170       180       190       200       210
human Stat5A    KHLQINQTFEELRLVTQDTENELKKLQQTQEYFIIQYQESLRIQAQFAQLAQLSPQERLSRETALQQKQV
human Stat5B    ...........................................GP.
medaka Stat5ab/a .YQ.........L........D.R...HN.........LSS..A.P.AD.QL..PT.LS.RA
medaka Stat5ab/b R.Q.........A..E....R...HS.........N......LSS.SS.PAA..SQ...F..S.RA
```

coiled-coil domain

```
                    220       230       240       250       260       270       280
human Stat5A    SLEAWLQREAQTLQQYRVELAEKHQKTLQLLRKQQTIILDDELIQWKRRQQLAGNGGPPEGSLDVLQSWC
human Stat5B    ..............................................................
medaka Stat5ab/a TV...T..N....K.LD...........................G..L..
medaka Stat5ab/b TV...T..S....K.LD..Q......I...E..................QH.G.L.
```

coiled-coil domain   ## DNA binding domain

```
                    290       300       310       320       330       340       350
human Stat5A    EKLAEIIWQNRQQIRRAEHLCQQLPIPGPVEEMLAEVNATITDIISALVTSTFIIEKQPPQVLKTQTKFA
human Stat5B    ..............................................................
medaka Stat5ab/a ....T.........R........I..L.N.L.E
medaka Stat5ab/b .DL........Q...T.....M..L.RKL..D...M.
```

DNA binding domain

```
                    360       370       380       390       400       410       420
human Stat5A    ATVRLLVGGKLNVHMNPPQVKATIISEQQAKSLLKNENTRNECSGEILNNCVMEYHQATGTLSAHFRNM
human Stat5B    .....................................DY........................
medaka Stat5ab/a .....................A.......DS.......N........I.
medaka Stat5ab/b ........M....AM....AM..S.NS.S................N..
```

DNA binding domain

```
                    430       440       450       460       470       480       490
human Stat5A    SLKRIKRADRRGAESVTEEKFTVLFESQFSVGSNELVFQVKTLSLPVVVIVHGSQDHNATATVLWDNAFA
human Stat5B    .......S...........I........G.................N........
medaka Stat5ab/a .......S...........I........G.................N........
medaka Stat5ab/b .......S...........I........G..GLH...M.........N........
```

linker domain

```
                    500       510       520       530       540       550       560
human Stat5A    EPGRVPFAVPDKVLWPQLCEALNMKFKAEVQSNRGLTKENLVFLAQKLFNNSSSHLEDYSGLSVSWSQFN
human Stat5B    ..............................................................
medaka Stat5ab/a .....L.....D.I...Y......SE.......A.SS..NNPD..RSMTMT.P.
medaka Stat5ab/b .....V....K..I....D..Y.MHTT.....E......A.TS..NNP..HNMT...A.
```

linker domain   ## SH2 domain

```
                    570       580       590       600       610       620       630
human Stat5A    RENLPGWNYTFWQWFDGVMEVLKKHHKPHWNDGAILGFVNKQQAHDLLINKPDGTFLLRFSDSEIGGITI
human Stat5B    ......R.................L.................
medaka Stat5ab/a ..S...R.F.........LT...L.........Q.M.MS.
medaka Stat5ab/b ..RSF.........M.LM...L.........Q.M.MS.N.
```
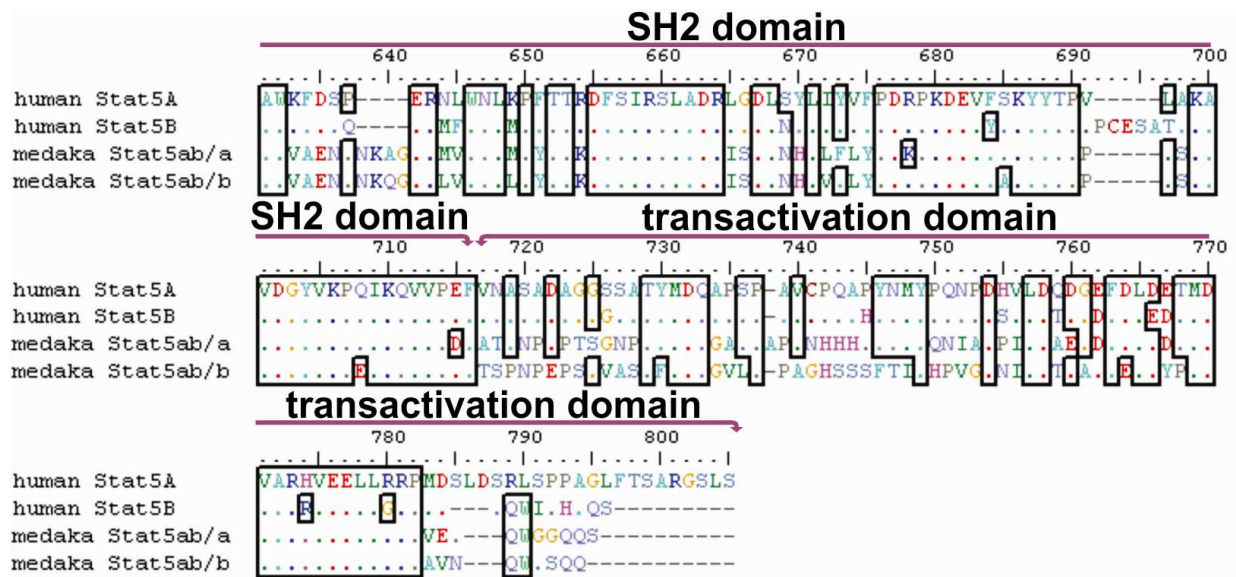
Fig. 26. Protein alignment of full length Stat5A and Stat5B from human and Stat5ab/a and Stat5ab/b from medaka. Conserved domains are marked in purple based on human sequence.

The whole protein sequence of medaka Stat5ab/a is about 80% similar to medaka Stat5ab/b, as well as to both human sequences. Medaka Stat5ab/b sequence is approximately 75% similar with both human sequences. Human Stat5 sequences, when compared to each other are 94% conserved (Table 3).

	Medaka Stat5ab/a	Medaka Stat5ab/b	Human Stat5A
Medaka Stat5ab/b	79%	---	---
Human Stat5A	79%	74%	---
Human Stat5B	80%	75%	94%

Table 3. Comparison of medaka and human Stat5 full length protein sequences. Conserved amino acids of full medaka Stat5ab/a and Stat5ab/b and human Stat5A and Stat5B.

To further analyse the evolutionary relationship of Stat5 genes, I created a phylogenetic tree using medaka Stat5ab/a (ENSORLG00000003961), medaka Stat5ab/b (ENSORLG00000014335), human Stat5a (ENSG00000126561), human Stat5b (ENSG00000173757), mouse Stat5a (ENSMUSG00000004043), mouse Stat5b (ENSMUSG00000020919), zebrafish Stat5.1 (ENSDARG00000019392), zebrafish Stat5.2 (ENSDARG00000055588), stickleback Stat5a (ENSGACG00000008634) and stickleback Stat5b (ENSGACG00000015405) protein sequences (Fig. 27). This analysis revealed that Stat5a and Stat5b from mammals are more related to each other than both fish Stat5 proteins. This indicates that the two Stat5 copies arose through different duplication processes in mammals and in fishes.
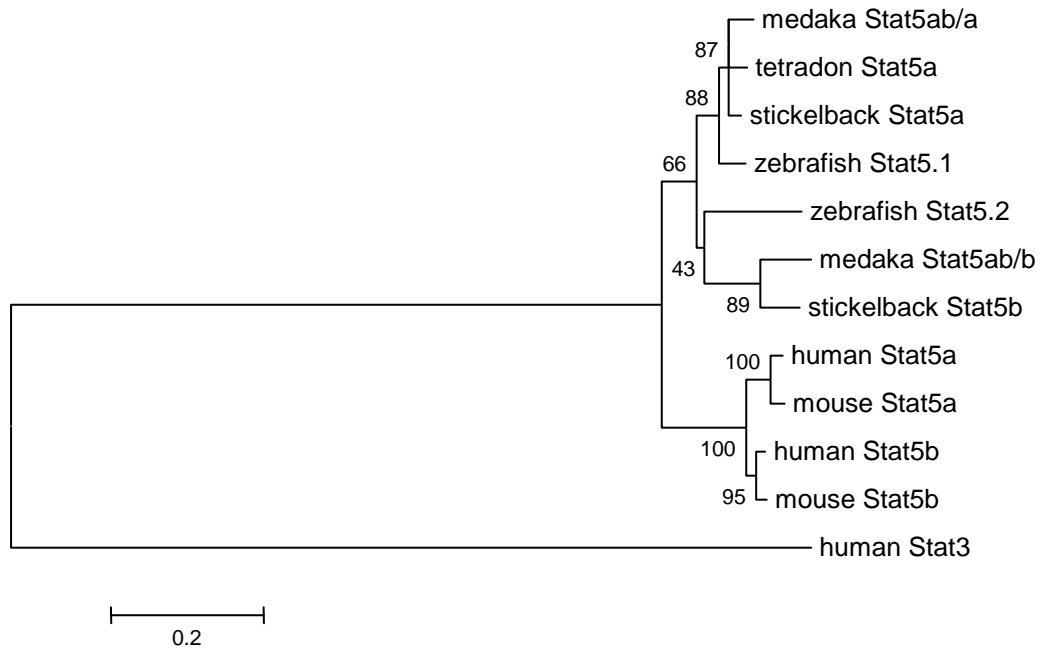
Fig. 27. Phylogenetic tree of vertebrate Stat5 genes. Amino acid sequences were aligned by maximum likelihood method. Human Stat3 sequence was used as out group. Numbers on nodes are bootstrap values out of 100 iterations. The scale bar indicates evolutionary distance.

To further analyse the possibility that human Stat5a and Stat5b arose from a different duplication process than medaka Stat5 genes, additional synteny analyses of the comprising medaka genome regions to the human chromosome 17 where both Stat5 copies are present was performed (Table 4). This analysis showed that medaka Stat5ab/a copy shares a high number of syntenic genes, which is not observed in medaka Stat5ab/b.

Human Stat5A up/down. genes	Medaka Stat5ab/a up/down. genes	Medaka Stat5ab/b up/down. genes
KLHL10	ADAM11 (1 of 2)	USH1G (2 of 2)
KLHL11	FKBP10 (1 of 2)	C17orf28 (2 of 2)
ACLY	NT5C3L (1 of 2)	PLAU
CNP	KLHL11 (1 of 2)	HO ENDOD1
DNAJC7	ACLY*	FMNL1 (2 of 2)
NKIRAS2	CNP	SRCIN1 (2 of 2)
ZNF385C	DNAJC7 (1 of 2)	GRB7
DHX58	NKIRAS2	MAP3K14 (2 of 2)
KAT2A	ZNF385C (1 of 2)	GRN (2 of 2)
HSPB9	DHX58	RACGAP1*
RAB5C	KAT2A	JAKMIP3
KCNH4	RAB5C	MTR
HCRT	KCNH4 (2 of 2)	TFAM
GHDC	HCRT	IPMK
Stat5B	PLCL2*	NAGLU
Stat5A	**Stat5ab/a**	**Stat5ab/b**
STAT3	STAT3	PTRF (1 of 2)
PTRF	PTRF (2 of 2)	ATP6V0A1 (1 of 2)
ATP6V0A1	ATP6V0A1 (2 of 2)	RFNG
HSD17B1P1	STK17B*	EXOC6 (2 of 2)
NAGLU	HSD17B1	EXOC6 (1 of 2)
HSD17B1	COQ10B*	CYP26A1*

77

COASY	L1TD1*	REEP3
MLX	MYLK*	NRBF2
PSMC3IP	FZD2	NHLRC3
FAM134C	CCDC43	EGR2*
TUBG1	C1QL1 (1 of 2)	ADO
TUBG2	RAMP2	BMS1
PLEKHH3	EZH1	MBTD1
CCR1	CNTNAP1	NME1*
CNTNAP1	MYO16*	MRPL27

Table 4. Analysis of human and medaka *Stat5* gene synteny. Human Stat5A and Stat5B genes lay adjacent to each other on the same chromosome. The first column shows genes present upstream and downstream of human *Stat5* genes. The second column shows genes present downstream and upstream of medaka *Stat5ab/a* gene on chromosome 8. The third column shows genes present downstream and upstream of medaka *Stat5ab/b* gene on chromosome 19. Genes marked with one asterisk (*) are not annotated gene versions of medaka. Genes marked in pink represent genes found in the surrounding of human Stat5 genes and medaka Stat5ab/a. The gene marked in green was the only found surrounding human Stat5 genes and medaka Stat5ab/b. Genes marked in blue are genes found in the surrounding of human Stat5 genes and both medaka Stat5 genes.

Synteny analysis of the medaka genome region where Stat5ab/a copy is present with the region from zebrafish containing Stat5.1 gene and the region from stickleback, tetraodon and fugu where Stat5a is present was performed (Table 5). This analysis showed that medaka Stat5ab/a copy shares a high number of syntenic genes with the other fish species analysed.

Medaka Stat5ab/a up/down. genes	Zebrafish Stat5.1 up/down. genes	Stickleback Stat5a up/down. genes	Tetraodon Stat5a up/down. genes	Fugu Stat5a up/down. genes
ADAM11 (1 of 2)	EFTUD2	TUBG2	FAM134C	TUBG2
FKBP10 (1 of 2)	EPS8L1	PLEKHH3	TUBG2	PLEKHH3
NT5C3L (1 of 2)	KCNJ12 (2 of 2)	CNTNAP1	PLEKHH3	CNTNAP1
KLHL11 (1 of 2)	MPRIP	EZH1	CNTNAP1	EZH1
ACLY	SLC6A16 (1 of 2)	RAMP2	EZH1	RAMP2 (2 of 2)
CNP	SLC17A7	C1QL1 (1 of 2)	C1QL1 (1 of 2)	C1QL1 (1 of 2)
DNAJC7 (1 of 2)	HRAS	CCDC43	CCDC43	CCDC43
NKIRAS2	GYS1	FZD2	FZD2	FZD2
ZNF385C (1 of 2)	ASPDH	MYLK	MYLK	MYLK
DHX58	TMEM86B	COQ10A	COQ10A	COQ10A
KAT2A	LRRC3C (2 of 2)	HSD17B1P1	HSD17B1P1	HSD17B1P1
RAB5C	STK17B	STK17B	STK17B	STK17B
KCNH4 (2 of 2)	ATP6V0A1A	ATP6V0A1 (2 of 2)	ATP6V0A1 (2 of 2)	ATP6V0A1 (2 of 2)
HCRT	PTRFA	PTRF (2 of 2)	PTRF (1 of 2)	PTRF (1 of 2)
PLCL2	STAT3	STAT3	STAT3	STAT3
Stat5a/b a	**Stat5.1**	**Stat5a**	**Stat5a**	**Stat5a**
STAT3	PLCL2	PLCL2 (2 of 2)	PLCL2	PLCL2
PTRF (2 of 2)	HCRT	KCNH4 (2 of 2)	HCRT	HCRT
ATP6V0A1 (2 of 2)	RAB5C	RAB5C (2 of 2)	KCNH4 (2 of 2)	KCNH4 (2 of 2)
STK17B	KAT2A	KAT2A	RAB5C (1 of 2)	RAB5C (1 of 2)
HSD17B1	DHX58	DHX58	KAT2A	KAT2A
COQ10B	CNP (2 of 2)	ZNF385C (1 of 3)	DHX58	DHX58
L1TD1	DNAJC7 (1 of 2)	NKIRAS2	ZNF385C	ZNF385C (1 of 2)
MYLK	ZNF385C	DNAJC7 (1 of 2)	STAC2 (2 of 2)	NKIRAS2
FZD2	NKIRAS2	CNP	FBXL20	DNAJC7 (1 of 2)
CCDC43	DNAJC7 (2 of 2)	ACLY (2 of 2)	CDK12	CNP
C1QL1 (1 of 2)	TTC25	KLHL11	NEUROD2	ACLY (1 of 2)
RAMP2	CNP (1 of 2)	NT5C3L (1 of 2)	PPP1R1B	KLHL11
EZH1	ACLYA	FKBP10 (1 of 2)	STARD3	NT5C3L (1 of 2)
CNTNAP1	COQ10A	LEPREL4 (1 of 2)	MREG	FKBP10 (1 of 2)
MYO16	HSD17B1	ADAM11 (2 of 2)	TCAP	LEPREL4 (1 of 2)

Table 5. Analysis of medaka, zebrafish, stickleback, tetraodon and fugu *Stat5a* gene synteny. The first column shows genes present upstream and downstream of medaka *Stat5ab/a* gene. The second column shows genes present downstream and upstream of zebrafish *Stat5.1* gene. The third column shows genes present downstream and upstream of stickleback *Stat5a* gene. The fourth column shows genes present downstream and upstream of tetraodon

Stat5a gene. The fifth column shows genes present downstream and upstream of fugu *Stat5a* gene. Genes marked with the same colour represent genes found in the surrounding of medaka *Stat5ab/a* gene that was also found in the surrounding of *Stat5a* of the other fish species analysed.

Besides that, synteny analyses of the region containing the medaka *Stat5ab/b* gene, the region in zebrafish that contains *Stat5.2* gene and from stickleback that contains *Stat5b* gene was performed (Table 6). This analysis showed that medaka Stat5ab/b copy shares a high number of syntenic genes with stickleback region where Stat5b is present but not with zebrafish region where Stat5.2 is located. The synteny analyses of the region containing *Stat5* genes in different fishes will help to hypothesize whether the different Stat5 copies present in fishes arose from the fish specific genomic duplication.

Medaka Stat5ab/b up/down. genes	Zebrafish Stat5.2 up/down. genes	Stickleback Stat5b up/down. genes
USH1G (2 of 2)	GRID1 (1 of 2)	EGR2 (1 of 2)
C17orf28 (2 of 2)	FAM190B (2 of 2)	NHLRC3
PLAU	PATL2	NRBF2
ENDOD1	CMN	REEP3
FMNL1 (2 of 2)	PAQR4 (2 of 2)	JMJD1C
SRCIN1 (2 of 2)	PELO	CYP26A1
GRB7	PPP1CAB	EXOC6
MAP3K14 (2 of 2)	IRF9	HHEX
GRN (2 of 2)	ATP2A1L	TRUB1
RACGAP1	FAM158A	LRRC45
JAKMIP3	PSME2	RAC3
MTR	LSM5	DCXR
TFAM	RNASEN	RFNG
IPMK	KCNH4	ATP6V0A1 (1 of 2)
NAGLU	GHDCL	PTRF (1 of 2)
Stat5a/b b	**Stat5.2**	**Stat5b**
PTRF (1 of 2)	OPLAH	NAGLU
ATP6V0A1 (1 of 2)	FOXH1	IPMK
RFNG	PPP1R16A	UBE2D1 (1 of 2)
EXOC6 (2 of 2)	ADAM11	TFAM
EXOC6 (1 of 2)	DBF4B	POLR3D
CYP26A1	FKBP10	-
REEP3	KLHL11	-
NRBF2	ACLY (2 of 2)	-
NHLRC3	GPT (2 of 2)	-
EGR2	KBTBD2	-
ADO	AVL9	-
BMS1	MTO1	-
MBTD1	BECN1	-
NME1	NEUROD2	-
MRPL27	PKMYT1	-

Table 6. Analysis of medaka, zebrafish and stickleback *Stat5b* gene synteny. The first column shows genes present upstream and downstream of medaka *Stat5ab/b* gene. The second column shows genes present downstream and upstream of zebrafish *Stat5.2* gene. The third column shows genes present downstream and upstream of stickleback *Stat5b* gene until the end of the scaffold. Genes marked with the same colour represent genes found in the surrounding of medaka *Stat5ab/b* gene that was also found in the surrounding of *Stat5b* of the other fish species analysed.

4.2.3 Expression pattern

Using whole mount RNA *in situ* hybridization, I analysed *Stat5ab/a* and *Stat5ab/b* expression during the early stages of medaka embryonic development. RNA expression of *Stat5ab/a* was detected at medaka development stages 20, 28 and 32 (Fig. 28 A-C). In all stages analysed,

Stat5ab/a expression was detected in the prosencephalon (pe), mesencephalon (me) and otic vesicle (ot). No expression was detected using the sense probe as negative control (Fig. 28 D-F). *Stat5ab/b* expression was detected in all stages analysed, but the expression was restricted to brain vesicles and otic vesicles at stages later than 28 (Fig. 28 G-I). Both genes show a rather ubiquitous expression pattern at stage 20 (Fig. 28 A and G). No expression was detected using *Stat5ab/b* sense probe as negative control (Fig. 28 J-L).
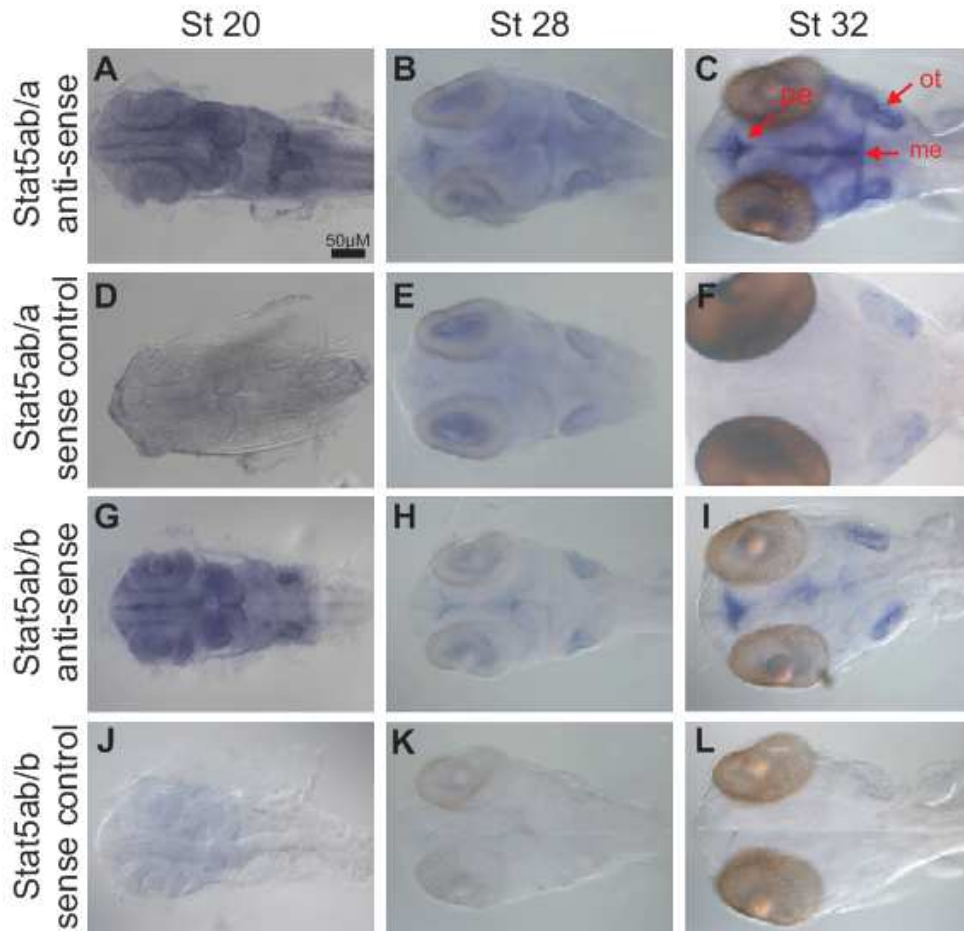
Fig. 28. In *situ* hybridization of medaka embryos using Stat5a/a and Stat5a/b probes. All pictures show dorsal views of the head region. Anterior is orientated to the left side. Arrows indicate regions of expression in the prosencephalon (pe), mesencephalon (me) and otic vesicle (ot).

Additionally *Stat5ab/a* and *Stat5ab/b* expression was investigated by qPCR in skin, brain, kidney and liver of wild type fishes. No expression was observed in eyes, gills, testis and muscle. Both genes had a raised expression in brain. The expression pattern of both genes was very similar to each other (Fig. 29).
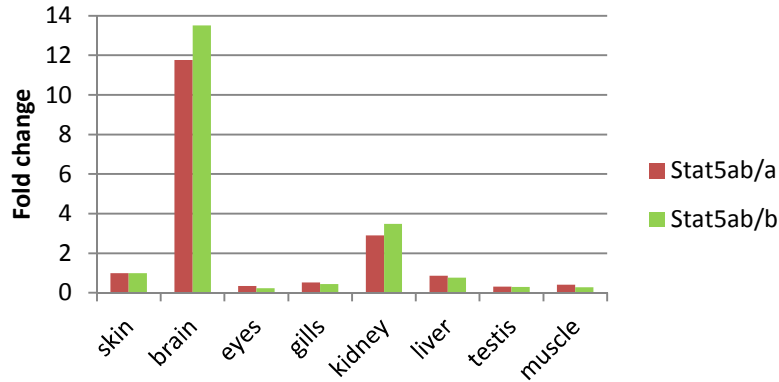
Fig. 29. Real time PCR of different organs from adult medaka fishes. Stat5ab/a and Stat5ab/b expressions were normalized against skin. The results shown here were calculated by the mean value of a triplicate assay. The expression of medaka *ef1a1* was used as internal control.

4.2.4 Generation of Stat5ab/a and Stat5ab/b transgenic lines

To gain new insights on Stat5 function, I generated transgenic medaka lines carrying the medaka *Stat5ab/a* and *Stat5ab/b* full length sequence under the control of the pigment cell specific mitf promoter (Schartl *et al*, 2010). Also, to investigate the consequences of constitutive activation or the lack of Stat5 signalling on cancer progression *in vivo*, I established a constitutively activated version and a dominant negative version of each gene under the control of the same pigment cell specific promoter. Therefore, after cloning full length medaka *Stat5ab/a* and *Stat5ab/b*, producing *Stat5ab/a* N646H and *Stat5ab/b* N647H through site directed mutagenesis and producing *Stat5ab/a* dominant negative and *Stat5ab/b* dominant negative through PCR adding a premature stop codon, I sub-cloned all sequences into the pISce-I containing a *mitf* promoter and a poly A. These constructs were used to inject one cell staged medaka embryos to produce transgenic lines. Positive injected fishes were raised and siblings were screened by genotyping PCR for transmission of transgene; 14 different lines were positive screened (Table 7).

Gene version	Feature	Number of lines	Names
Stat5ab/a	Full length	3	Stat5ab/a 5, 6 and 7
Stat5ab/b	Full length	2	Stat5ab/b 8 and 9
Stat5ab/a N646H	Constitutive active	2	Stat5ab/a N646H D and E
Stat5ab/b N647H	Constitutive active	2	Stat5ab/b N647H F and G
Stat5ab/a neg	Dominant negative	3	Statab/a neg α,ß and γ
Stat5ab/b neg	Dominant negative	2	Statab/b neg δ and ε

Table 7. Different Stat5 transgenic medaka lines established in this work. Gene variant, feature, number of lines and name of each line are listed.

In summary I was able to identify and clone medaka *Stat5ab/a* and *Stat5ab/b* and produce transgenic lines bearing either wild type, a constitutively active and a dominant negative version of each medaka Stat5 gene under the control of the pigment cell specific *mitf* promoter. These lines will help to gain new knowledge on Stat5 function in the normal development and in cancer.

4.3 c-myc

c-myc expression is deregulated in a wide range of human cancers and is often associated with aggressive tumours (Larsson and Henriksson, 2010). Detailed knowledge of C-myc biology is a key premise to understanding its role in cancer initiation, progression and to target it for cancer therapy. To obtain new information on C-myc function, the identification and cloning of one of the medaka *c-myc* genes was performed.

4.3.1 Identification and cloning of a novel *c-myc* gene

By searching available medaka databases I identified two *c-myc* genes, positioned on chromosomes 17 (*c-myc17*, ENSEMBL database identifier: ENSORLT00000008816) and on chromosome 20 (*c-myc20*, chromosome location 20:19323350-19324300). The sequence of *c-myc17* (which was cloned by Cornelia Schmidt) differs from the one found in the ENSEMBL database. Marked with a green square in Figure 30 is an exon, which is present in the database, but was not found in our cDNA clones. According to the c-myc sequences from tetraodon, zebrafish, stickleback and fugu present in the same database, these other fish species also lack this extra sequence. Also, the last amino acids (marked in red in Figure 30) differ between our sequence and the database. All the results shown in this work refer to experiments obtained with the sequence from our cDNA clones.
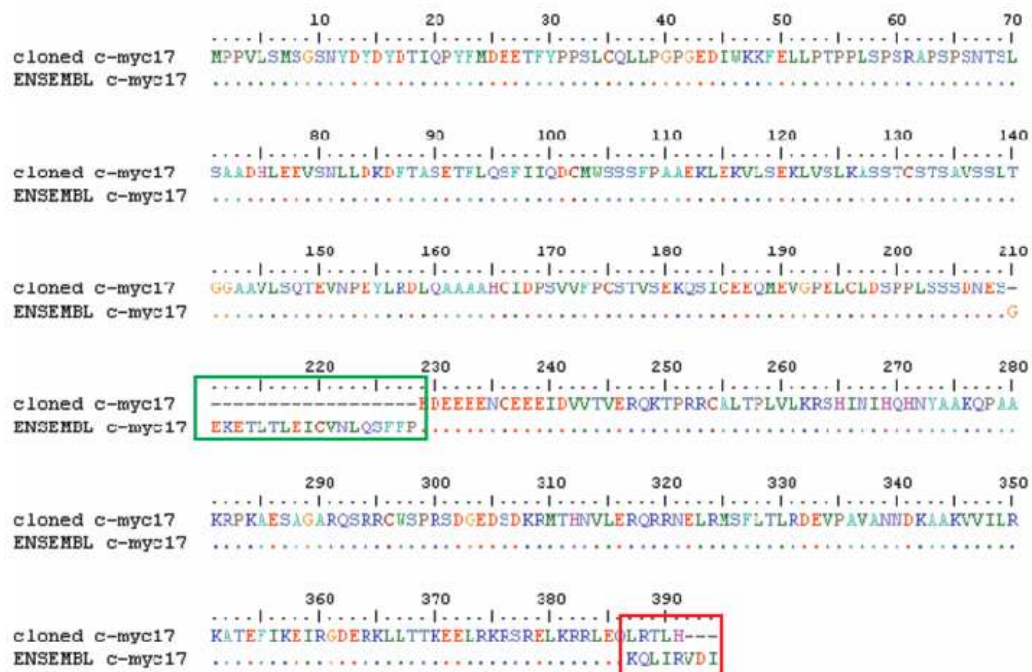
Fig. 30. Protein sequence alignment of full length medaka *c-myc17* gene. Green and red squares mark the differences between the sequence present in ENSEMBL database and the cDNA clones sequences.

Medaka *c-myc20* was not annotated in the ENSEMBL database. By blasting the human *c-myc* gene in NBRP cDNA database (http://www.shigen.nig.ac.jp/medaka/) two different orthologues were found. And by blasting this second copy in ENSEMBL lastetgp database, I found out that it lays on medaka chromosome 20. After alignment with *c-myc* sequence from different fish species, I observed that 120 amino acids were missing (marked in purple in Fig. 31). Using primers

flanking this gap (mdk_cmyc20_gap_for and mdk_cmyc20_gap_rev) I was able to obtain full length *c-myc20* sequence (Fig. 31). Newly identified medaka c-*myc17* and *c-myc20* coding sequences have been submitted to Genebank (*c-myc17*: GeneBank-nr. JN542547; *c-myc20*: GeneBank-nr. JN634762).
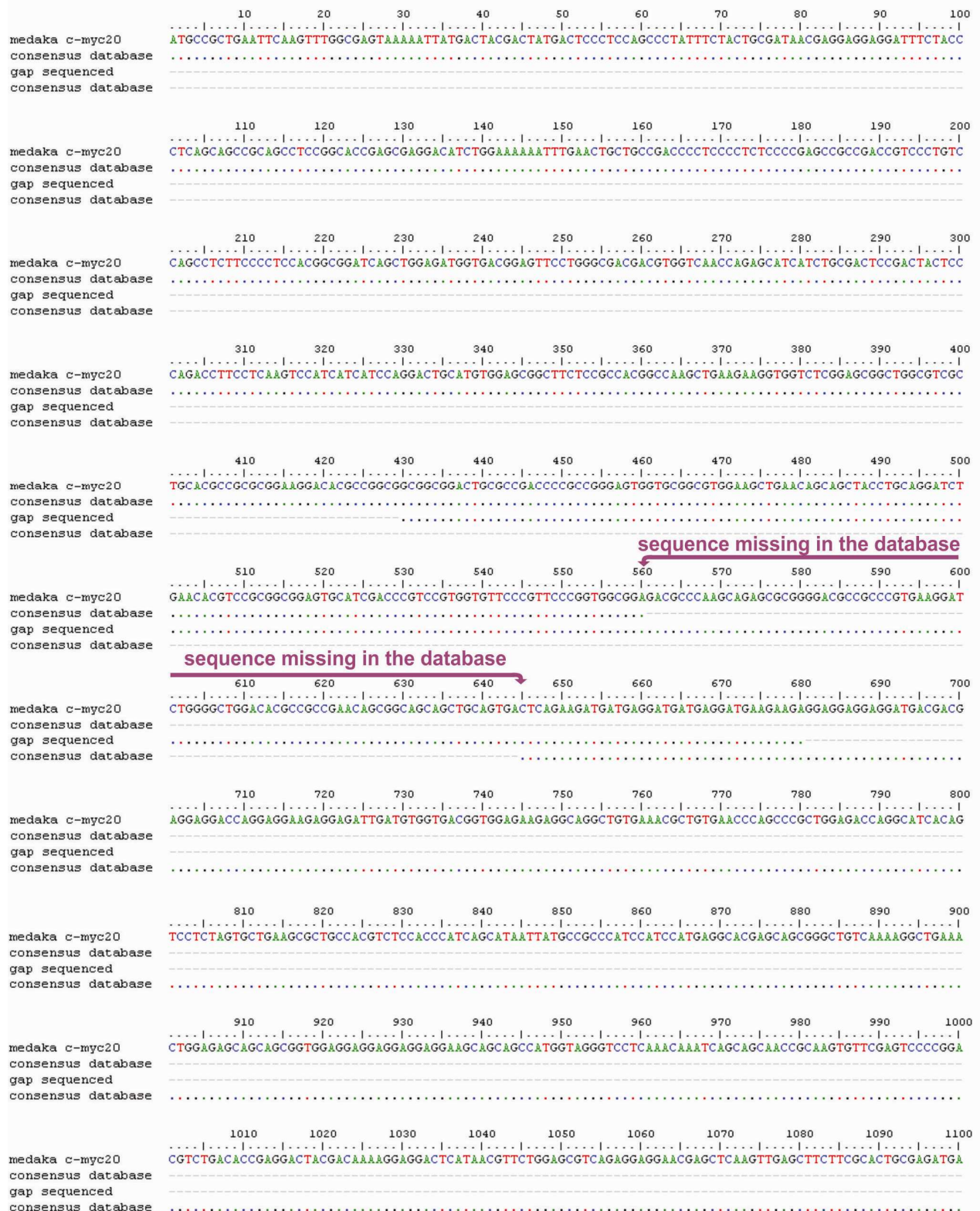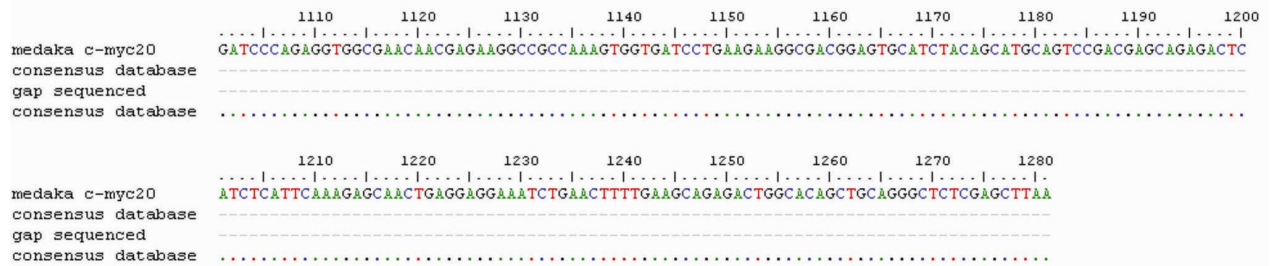
Fig. 31. Nucleotide alignment of c-*myc20* sequences. The consensus sequences were obtained from NBRP cDNA database. The sequence missing was obtained by direct sequencing using a PCR product of a reaction using primers flanking the gap. This way the full length *c-myc20* coding sequence was obtained.

Medaka *c-myc17* sequence was PCR amplified from pooled medaka organ cDNA using ReproFast polymerase (Genaxxon) with primers inserting HindIII restriction site downstream and BamHI site upstream the gene. To compare homology among different vertebrates, C-myc protein sequences from human, mouse, fugu and both medaka copies were aligned (Fig. 32). The DNA binding domain, the helix-loop-helix domain and the leucine-zipper domain share an overall high rate of conservation throughout all investigated vertebrates (purple lines in Fig. 32).
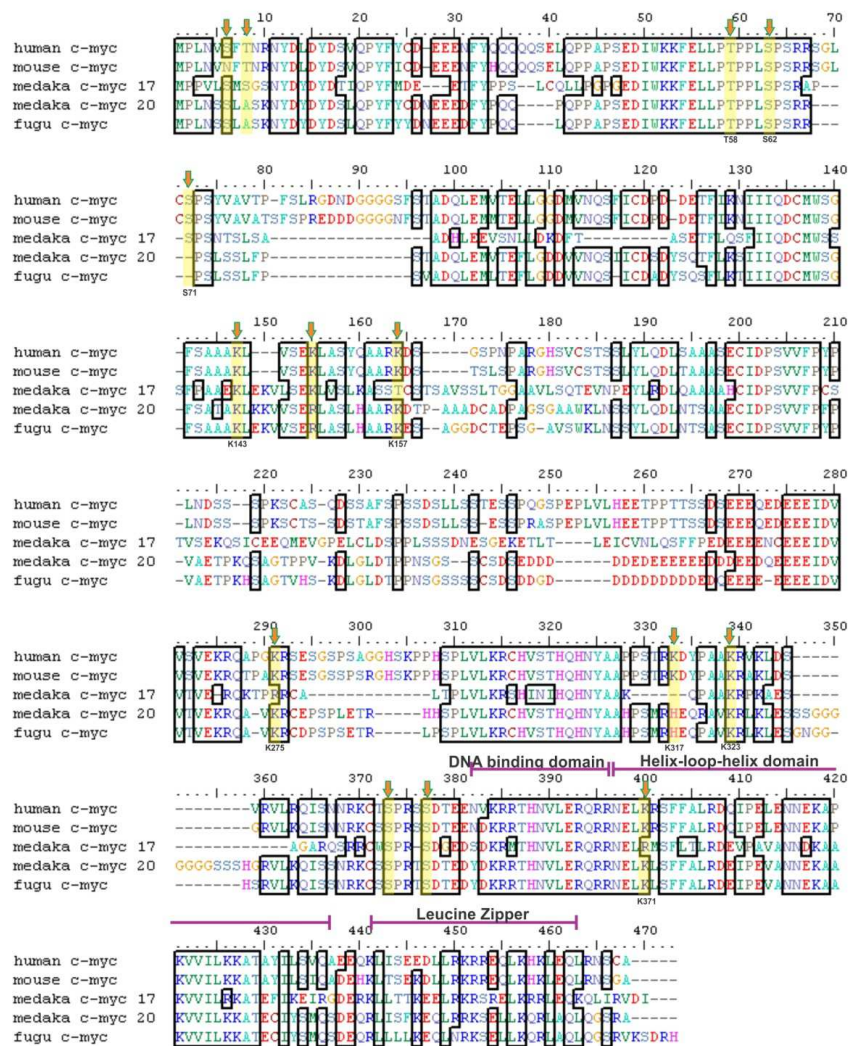
Fig. 32 Alignment of C-myc protein sequences. Human, mouse and fugu C-myc protein sequences were aligned with medaka C-myc17 and medaka C-myc20. Black boxes highlight conserved amino acid residues (more than 75% conservation in all sequences). Yellow arrows indicate known amino acid sites for posttranslational modifications in the human Myc protein, e.g. phosphoserine and N6-acetyllysine modifications, as stated in the UniProt database.

Table 8A lists the degree of similarity between both medaka C-myc protein sequences and human, fugu and the three zebrafish protein sequences. Human C-myc basic-helix-loop-helix (BHLH) domain is 78% similar to C-myc20 and 55% similar to C-myc17 (Table 8B). The DNA binding domain is 100% equal to C-myc20 and 92% similar C-myc17. Interestingly, the leucine-zipper, which is responsible for the interaction with MAX, is only 50% similar to C-myc20 but 68% similar to C-myc17.

A

	c-myc17	c-myc20
c-myc17	---	47%
Human c-myc	46%	55%
Fugu c-myc	51%	84%
Zebrafish c-myca	49%	70%
Zebrafish c-mycb	48%	69%
Zebrafish c-mych	31%	43%

B

	c-myc17	c-myc20
Human c-myc HLH	55%	78%
Human DBD	92%	100%
Human LZ	68%	50%
c-myc17 HLH	---	68%
c-myc17 LZ	---	61%
c-myc17 DBD	---	93%

Table 8. Comparison of medaka C-myc sequences. (A) Conserved amino acids of full human, fugu and zebrafish C-myc sequences in comparison with medaka C-myc17 and 20. (B) Conservation of C-myc17 and 20 motifs compared between themselves and with human sequences. HLH indicates helix-loop-helix domain; DBD indicates DNA binding domain; LZ indicates Leucine-zipper domain.

Furthermore the alignment in Figure 32 shows that known C-myc phosphorylation sites for the human protein (Adhikary and Eilers, 2005), like T58, targeted by glycogen synthase GSK3, and S62, targeted by MAP kinase, are conserved in both medaka orthologues. Apparently differences between the two medaka Myc proteins could be determined. S71, targeted by Rho-dependent kinase and related with transcriptional repression by Myc, is only conserved in C-myc17 but not in C-myc20. Apart from the phosphorylation sites, there are six lysine residues on human C-Myc that are direct substrates for acetylation by p300 (Zhang *et al.*, 2005). Two of these are conserved in both medaka *c-myc* genes: K143 within Myc homology box 1 and K323 within the nuclear localization signal. Three lysine modification sites are only present in C-myc20: K157 located next to the Myc homology box 2, K275 not linked to functionally important Myc domains and K371 within the BHLH domain. One site is not present in both medaka copies K317 next to the nuclear localization signal. These results indicate that essential functional domains and amino acid residues of C-Myc have been conserved in both Medaka genes, but some changes in posttranslational regulatory amino acid motifs, especially those of N-6 acetyllysine modification sites in C-myc17, may have resulted in functional divergence of these orthologues.

4.3.2 Syntenic and phylogenetic analysis of *c-myc* orthologues in medaka

To further analyse the relation between both medaka C-myc orthologues and the human C-myc, I performed syntenic analyses of C-myc corresponding genome regions on medaka chromosome 17 and 20 and the human chromosome 8 (Tables 9 and 10). Most of the genes present upstream human C-myc are present either on medaka chromosome 11 or 16. Homologues of genes downstream human C-myc are present either on chromosome 11, 16 or 17. Interestingly, no homologue present on medaka chromosome 20 was found (Table 9).

human myc up. genes	medaka chromosome	human myc down. genes	medaka chromosome
POU5F1B	12	GSDMC	not present
FAM84B	11 and 16	FAM49B	17
TRIB1	11	ASAP1	not present
NSMCE2	not present	ADCY8	17
TMEM65	11 and 16	EFR3A	not present
NDUFB9	11	OC90	not present
KLHL38	11 and 16	HHLA1	not present
FAM91A1	11	KCNQ3	17
MTSS1	11 and 16	LRRC6	17
TRMT12	10	TMEM71	not present
RNF139	not present	NDRG1	11 and 16
TATDN1	not present	PHF20L1	not present
ZNF572	not present	ZFAT	16
SQLE	16	KHDRBS3	11
KIAA0196	16	COL22A1	11
FER1L6	21	KCNK9	11
WDR67	16	PTK2	16
C8orf76	16	SLC45A4	16
ZHX1	11	CHRAC1	11
ATAD2	16	TRAPPC9	11

Table 9. Analysis of *c-myc* gene synteny between human and medaka genomes. First column shows genes present upstream human c-myc locus, while the second column indicates the position of the corresponding gene orthologue on the medaka chromosomes. Third column shows genes present downstream of the human c-myc and fourth column the chromosome in which they are found in medaka.

The synteny analysis of medaka chromosome 17 and 20 in comparison with human C-myc locus (Fig. 33) confirms that more genes are conserved between human chromosome 8 and medaka chromosome 17 than 20 (blue lines, Fig. 33A). Figure 33B shows a magnified picture illustrating the corresponding chromosome regions around human and medaka c-myc. Medaka C-myc20 is not present in the analysis because it is not annotated in the used databases.
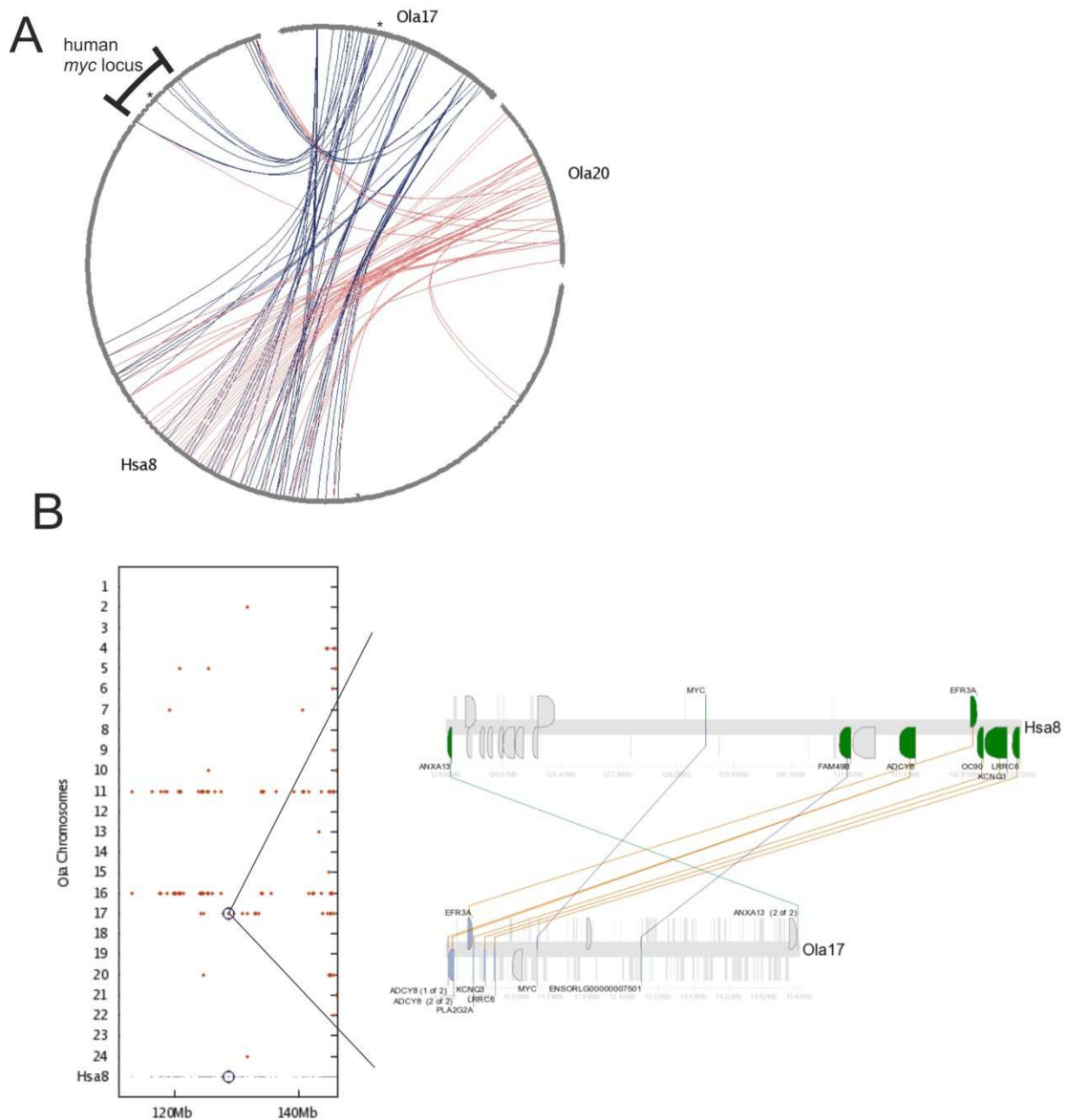
Fig. 33. Synteny analysis of the medaka cmyc in comparison to human. Analysis of *c-myc* gene synteny was performed utilizing the ENSEMBL database and the Synteny database. (A) Blue lines show conserved loci between human chromosome 8 and medaka chromosome 17. Red lines show conserved loci between human chromosome 8 and medaka chromosome 20. The asterisk (*) indicates *c-myc* genes on human and medaka chromosomes. The human cmyc locus, 10MB around the human *c-myc* gene, is indicated. (B) shows on the x-axis the complete human chromosome 8, while the y-axis represents all medaka chromosomes. Red dots indicate syntenic regions between species. Blue rings mark the position of human *c-myc* at 8q24 and potential regions of *c-myc* homologues in the medaka. The magnified picture illustrates the corresponding chromosome regions, containing neighbouring genes on the human and the medaka loci. Medaka c-myc20 is not present in the analysis because it is not annotated in the used databases.

Additional syntenic analyses of the comprising medaka genome regions to another fish species, the fugu, showed that *c-myc17* and *c-myc20* lie in regions of high evolutionary conservation (Table 10), hinting to a common origin by the fish specific genome duplication.

c-myc17 up./down. genes	c-myc20 up./down. genes	fugu c-myc up./down. genes	orthologue in medaka chr.
trimm55*	ankh	ankh	20
crh*	vps41	fam105b	20
q9w7r1	mrpll5	orf36c7	20
adhfe1	oprk1**	pou6f2	20
cd3e	chmp5**	vps41	20
ttc19	c7orf36	esco1	20
slc39a6	fastkd3	sox17	20
cd3e	myom1	rpl11	not present
pla2g2a	lpin2**	sox17	20
kcnq3	pou6f2	mrpl15	20
lprc6	smchd1	rgs20	17/20
ift57	emilin2**	opk1	20
murc*	esco1	chmp5	17/20
proc	mettl4	fastkd3	20
vcpip1	fam1b	myom1	20
dnajc5b	sox17	lpin2	17/20
slc4a2*	lypla1	emilin2	20
tmub1	rgs20**	adcyap1	17/20
afg3l2	yes1	yes1	17/20
adcy8	ensof1	enosf1	20
slco5a1*	myom1**	tyms	20
c-myc17	c-myc20	fugu c-myc	-
cap7b1	smarcd3	fam49b	17
wdr33	chpf2	gtbp2	1/15
sft2d3	abcf2	asap1	not present
mfn1	slc4a2**	nfx1	not present
fam132b	nrp2	smarcd3	20
pex51	puf60	abcf2	20
armc1*	scrib	chpf2	20
smg7	cdv3	slc4a2	17/10
rasal2	lztfl1	-	-
dhx9	topbp1	-	-
nmnat2	dnajc13	-	-
phb2	gli3	-	-
bfsp2	prpf4b	-	-
opn4	c6orf145	-	-
tmx3*	tmx3**	-	-
c16orf80	dsel	-	-
c7orfl1	cdh19	-	-
atg10	cdh7**	-	-
tmem70	impa1**	-	-
cyp7a1	fbxl7	-	-
impa1*	rala	-	-
cdh7*	ralyl**	-	-

Table 10. Analysis of medaka c-myc17 and c-myc20 gene synteny. First column shows genes present upstream and downstream c-myc17, second column shows genes present upstream and downstream c-myc20, third column shows genes present upstream and downstream fugu c-myc gene and fourth column shows in which chromosome from medaka the orthologue in fugu is present. Genes marked with one asterisk (*) are genes present on medaka chromosome 17 that are duplicate in the medaka genome and where its corresponding copy is present on chromosome 20. Genes marked with two asterisks (**) are genes present on medaka chromosome 20 that are duplicated in the medaka genome and where its corresponding copy is present on chromosome 17. Black lines indicate corresponding gene orthologues between the different genomic regions.

To assess the evolutionary relation of the *c-myc* genes of medaka in more detail, phylogenetic comparison of human, mouse, xenopus, tetraodon, stickleback, fugu and zebrafish *myc* genes with both medaka sequences was performed (Fig. 34).
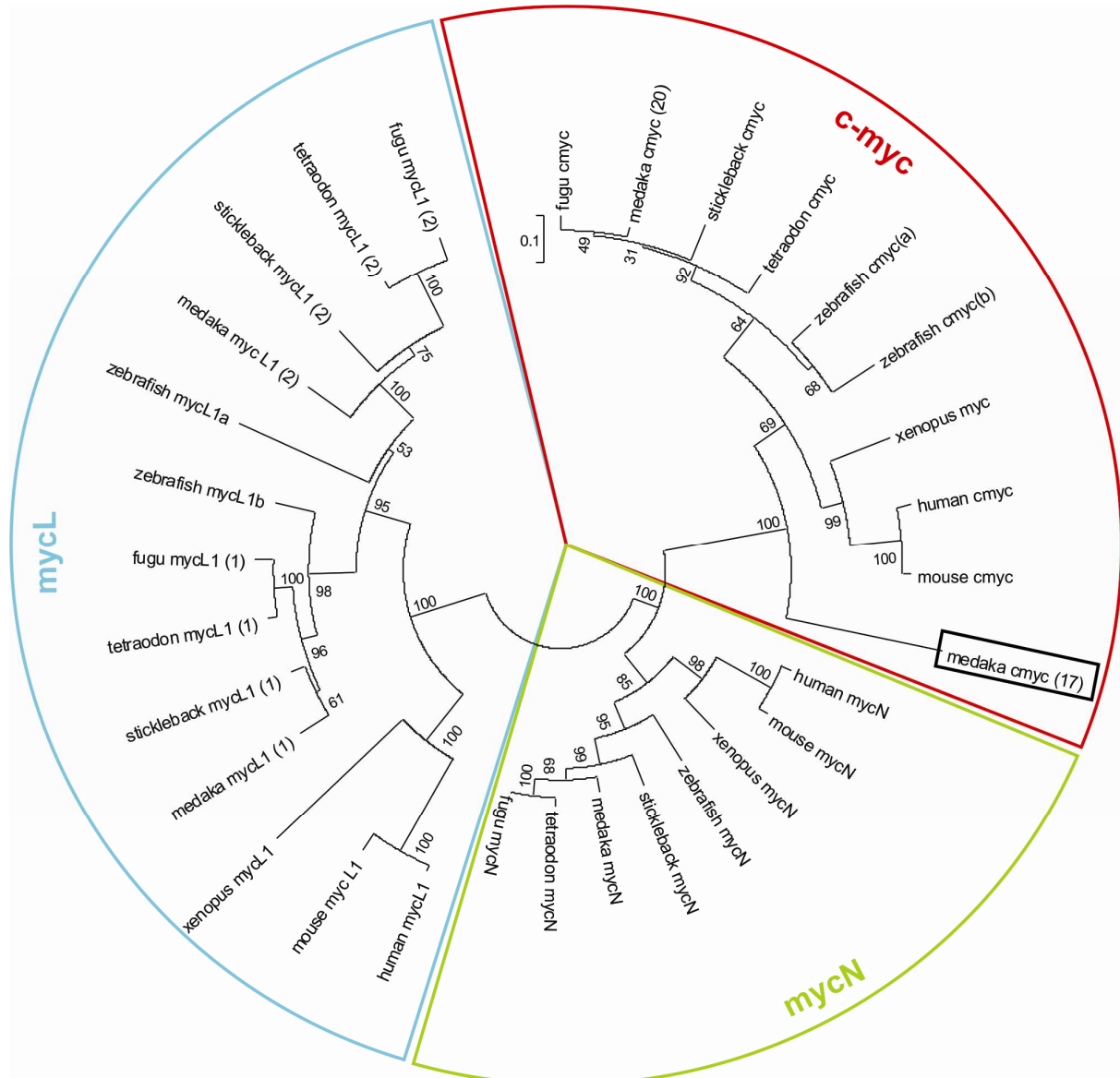

Fig. 34. Unrooted phylogenetic tree of myc family genes. Amino acid sequences were aligned by maximum likelihood method. Numbers on nodes are bootstrap values out of 100 iterations.

These analyses revealed that the medaka *c-myc* genes cluster together with the vertebrate C-myc family and not with mycN or mycL (Fig. 34). Moreover the phylogenetic tree revealed that the copy present on medaka chromosome 20 clusters closely with sequences from other vertebrates, while the copy on medaka chromosome 17 seems to be unique as it branches off relatively early (black box in Figure 34). This unexpected result indicates that c-myc17 of medaka is a highly divergent or an aberrant gene version.

In summary, these results strongly suggest that medaka *c-myc17* is an evolutionary modified *myc* gene version apart of all vertebrate *c-myc* genes, harbouring possible different functions.

4.3.3 Production of transgenic lines and expression pattern

To exclude that *c-myc17* is a non functional, not expressed pseudogene, expression studies of both medaka *c-myc* genes were performed by RT-PCR (Fig. 35). Expression of both genes was detected in all analysed developmental stages (10, 18, 21, 24, 30, 34 and 38; Fig. 35A). In adult tissues (Fig. 35B), expression of both medaka *c-myc* genes was detected in all analysed tissues. Expression was lower in gills and liver when compared to brain, eyes, muscle, skin and testis. This result shows that the c-*myc* copy present on medaka chromosome 17 had a similar expression pattern to *c-myc20* during development.
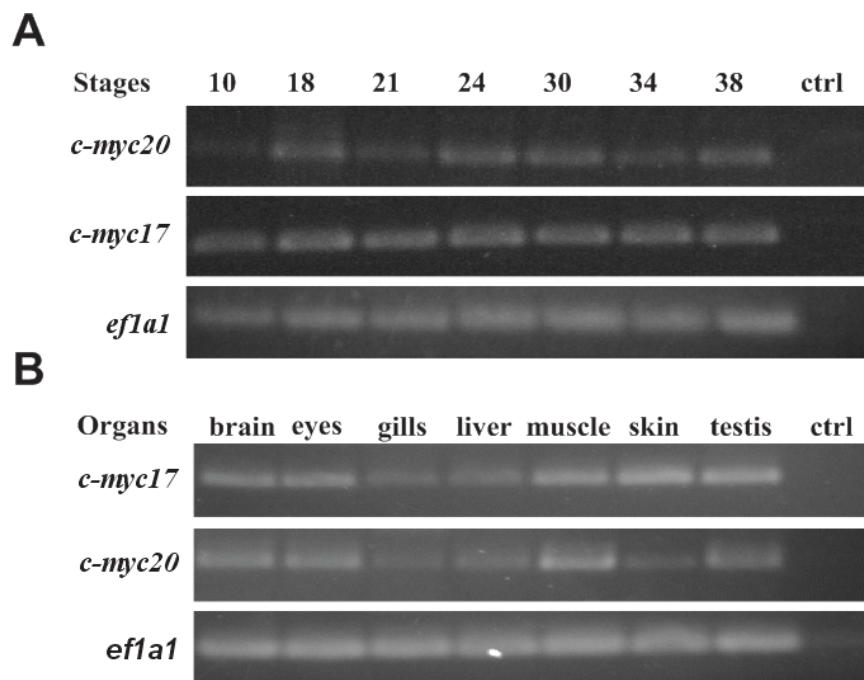
Fig. 35. Reverse transcript PCR of both *c-myc* copies present in Medaka (A) in different developmental stages and (B) in different adult organs. PCR reaction was performed using as template cDNA from different medaka stages of development.

To analyse in detail functions of this novel *c-myc17* gene and to compare these to the human *C-myc* gene, I established a novel inducible *in vivo* model in medaka. The coding region of *c-myc17* lacking the stop codon was fused to the hormone-binding domain of the mouse estrogen receptor (from vector pWZLneoG525R, a gift from Martin Eilers and performed by Cornelia Schmidt), which enables induction of the transcription factor at a chosen time point by addition of tamoxifen. For ubiquitous expression of the construct, the cytoskeletal-actin promoter of *Xenopus borealis* was utilized (Lakin *et al*., 1993). The *c-myc17*-ER construct was then sub-cloned into the pI-SceI vector, containing the cytoskeletal-actin promoter and a SV40-poly A, and named *c-myc17*-ER I-SceI plasmid. This construct was injected into one cell stage medaka embryos. Integration of the construct into the genome resulted in two independent transgenic lines, named *c-myc* line 1 and 2.

Transgene expression in both lines was determined by qPCR. The transgenic medaka line 1 showed a 7 fold higher expression of the transgene only in the gills when compared to the other

organs examined (Fig. 36A). In line 2, brain, eyes, gills and muscle have at least 6 fold increased expression when normalized to liver. Direct comparison of both lines indicates that line 2 has an overall higher *c-myc* RNA expression than line 1. To additionally test whether the protein is produced in both lines, western blot analyses were conducted. In both lines the fusion protein could be detected by using an antibody directed against the mouse ER (Fig. 36B).
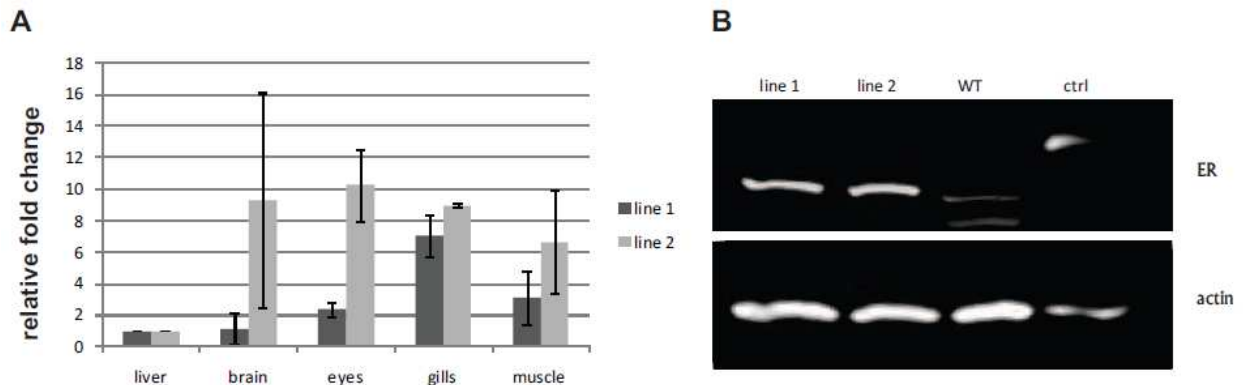

Fig. 36. Expression of c-mycER transgene in established medaka transgenic lines. (A) Real time PCR analysis of c-mycER transgene from liver, brain, eyes, gills and muscle from adult fishes. Levels from the transgene were normalized against *ef1a1* in each tissue. Histograms with T-bars indicate the mean standard deviation based on triplicate assays. (B) Western blot analysis of the c-mycER protein fusion. Protein samples extracted from wild type (WT) and two transgenic fishes immuno-stained with anti-ER antibody. Protein extract containing human c-mycER was used as control (crtl).

4.3.4 *In vitro* induction of c-*myc* in medaka primary cells

To test whether the inducible *c-myc17*ER system works in the established transgenic medaka lines, dissociated fibroblast cells from tail fins were cultured for five days followed by 24h treatment with 4-hydroxytamoxifen (4-OHT). Immunofluorescence of these cells using an anti-ER antibody shows nuclear translocation only in the presence of 4-OHT, confirming the functionality of the inducible *c-myc*ER system in medaka (Fig. 37A). Differences of nuclear to cytoplasm fluorescence intensity enabled me to quantify nuclear translocation (Fig. 37B) and demonstrate that in line 1 a 10 fold higher rate of nuclear myc-ER was detected after 4-OHT treatment, while in line 2 the ratio was only 2,7 fold increased.
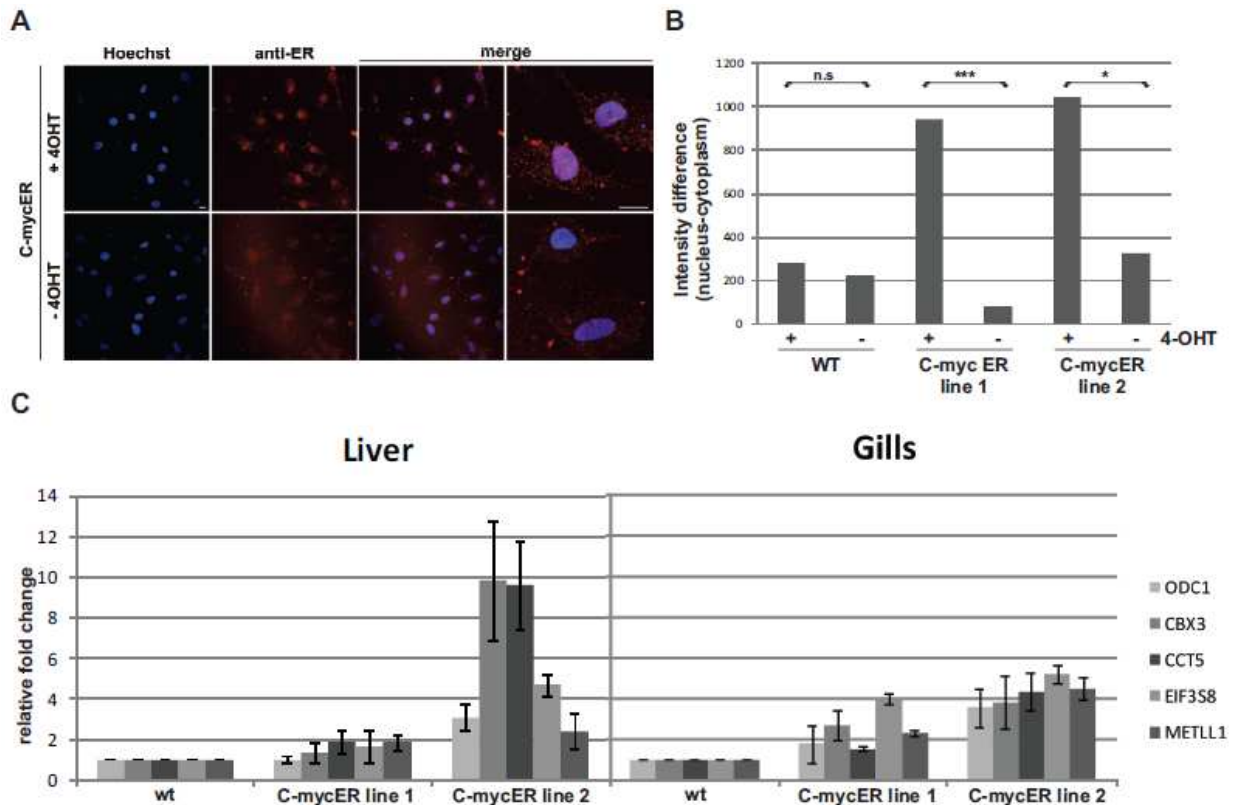
Fig. 37. Functionality tests of c-mycER transgenic lines. (A) Immunofluorescence of c-mycER line 2 in medaka fin primary cell culture in the presence or absence of 4-OHT using anti-ER antibody and nuclear counterstaining with Hoechst. Scale bar: 10µM. (B) Quantification of mean intensity differences (n=7 cells per treatment). Each cell was measured at two independent regions in the nucleus and the cytoplasm. Mean values were subtracted to calculate cytoplasmic to nuclear difference. (C) Direct c-myc target gene expression, ODC1, CBX3, CCT5, EIF3S8 and MTLL1, in different organs via qPCR analysis after 4OHT treatment. Relative fold change levels for each gene were normalized against *ef1a1* in each tissue separately. Histograms with T-bars indicate the mean standard deviation based on duplicate assays.

In addition, I was able to quantify the expression of five target genes that are up-regulated by human *c-myc* (Dang *et al*., 2006; Mao *et al*., 2003; Wagner *et al*, 1993; Zeller *et al*, 2003): ornithine decarboxylase 1(ODC1), chromobox homolog 3 (CBX3), chaperonin containing TCP1, subunit 5 (CCT5), translation initiation factor 3, subunit 8 (EIF3S8) and methyltransferase-like 1 (METLL1). Expression of the Medaka orthologues genes was determined in different adult tissues from *c-myc17*ER lines after 4-OHT treatment. This analysis revealed induced expression in almost all investigated tissues compared to control samples (Fig. 37C). Differences between the two established lines are obvious, as tissue samples of line 2 always show a stronger transcriptional induction of all five genes compared to line 1. Nuclear translocation of the C-myc17ER and induction of target gene expression after 4-OHT treatment show functionality of the transgene.

4.3.5 Function of novel C-myc17

By initially investigating the medaka c-*myc* gene copy present on chromosome 17, I could observe that this less conserved copy is expressed (Fig. 35 and 36) and that it is able to translocate to the nucleus (Fig. 37 A and B). In addition, I could notice that this protein is also able to induce

expression of known C-myc target genes (Fig. 37C). To further understand its function, I performed proliferation and apoptosis assays and looked for its possible role in cancer initiation.

4.3.5.1 Proliferation

I investigated whether ectopic expression of *c-myc17*ER leads to increased cell proliferation *in vivo*, one hallmark function of human C-myc. Distinct higher BrdU incorporation was detected in 4-OHT treated individuals of both transgenic lines in comparison to EtOH treated control fish (Fig. 38A). Quantification of BrdU incorporation after C-myc17 induction (Fig. 38B) revealed that line 1, which has a lower transgene expression level, has a higher rate of proliferation than line 2. For example in liver, line 1 has 3.1% of BrdU positive cells when treated with tamoxifen and 0.49% in the EtOH control. 4-OHT treated line 1 has 2.04% of proliferative cells while EtOH treated cells have 0.58%. In gills, tamoxifen treated fishes present 6.55% (line 1) and 4.07% (line 2) of BrdU positive cells. Control of line 1 and line 2 show 3.13% and 2.88% of proliferating cells.
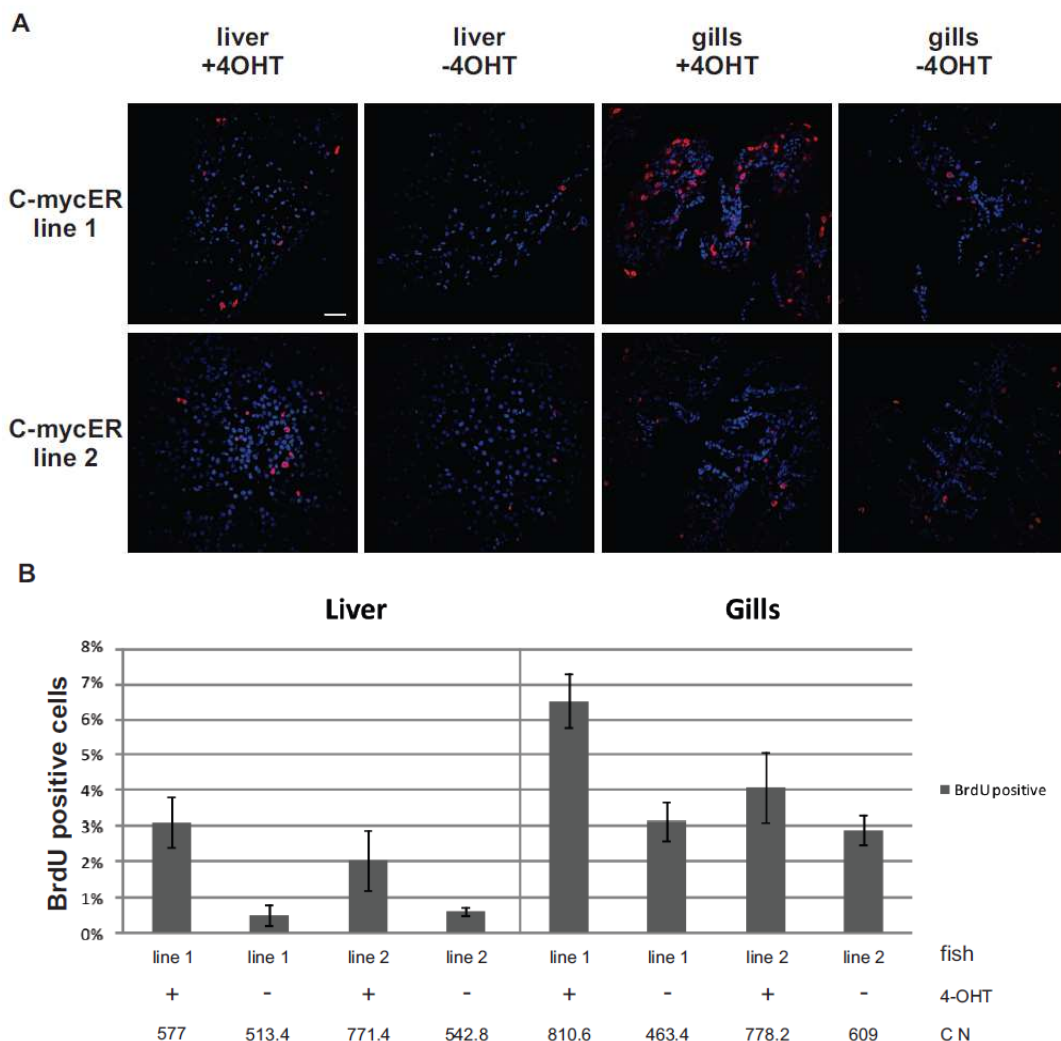

Fig. 38. Cell proliferation after c-myc activation *in vivo*. (A) BrdU staining on sections of liver (upper panel) and gills (lower panel) in the presence or absence of 4-OHT. Scale bar: 10 μM. (B) Quantification of BrdU positive cells in liver (left graphic) and gills (right graphic) in both c-mycER lines. Histograms with T-bars indicate the mean

percentage of BrdU positive cells of two independent experiments with their corresponding standard deviation. C N indicates average cell number counted from 5 different sections.

4.3.5.2 Apoptosis

In contrast to the proliferational potential, line 2 had a higher *in vitro* apoptosis rate after 4-OHT treatment when compared to line 1 in primary cells (Fig. 39A and B) and *in vivo* in liver and gills (Fig. 40 A and B). In primary cell culture from medaka fins, 4-OHT and EtOH treated cells from line 1 showed 7.27% and 2.61% apoptosis rate, respectively. Line 2 presented11.49% and 1.8%, respectively, in treated versus non treated cells.
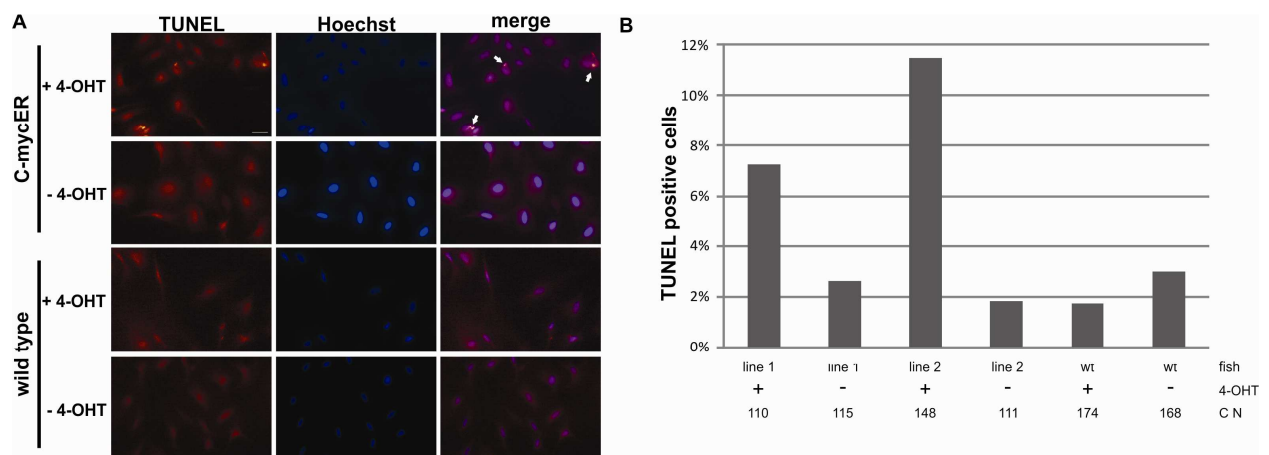

Fig. 39. Effects of C-myc activation on cell death *in vitro*. (A) Detection of apoptosis in primary cell culture (arrows indicate TUNEL positive cells). Cells were treated for five hours with 4-OHT before fixation. Nuclei were counterstained with Hoechst. Scale bar: 100 µM. (B) Quantification of apoptotic cells in primary cultures derived of both C-mycER lines and wild type fishes in presence or absence of 4-OHT in the media. C N indicates total cell number for each assay.

A similar observation was made when looking at adult tissues from transgenic fishes (Fig. 40). For example, livers from fishes from line 2 had 11.61% TUNEL positive cells after treatment with tamoxifen, while EtOH treated control fish had only 2.52%. In gills, the amount of apoptotic cells was 21.39% of 4-OHT treated cells. In contrast, the amount of TUNEL positive cells in non treated gills was 1.58%. In summary, our functional experiments show that in both transgenic lines C-myc17 can induce proliferation and apoptosis. Additionally, I could confirm differences in potency of both lines to induce these effects. Line 1 shows a higher rate of proliferative cells, while line 2 is more potent to drive cells into apoptosis.
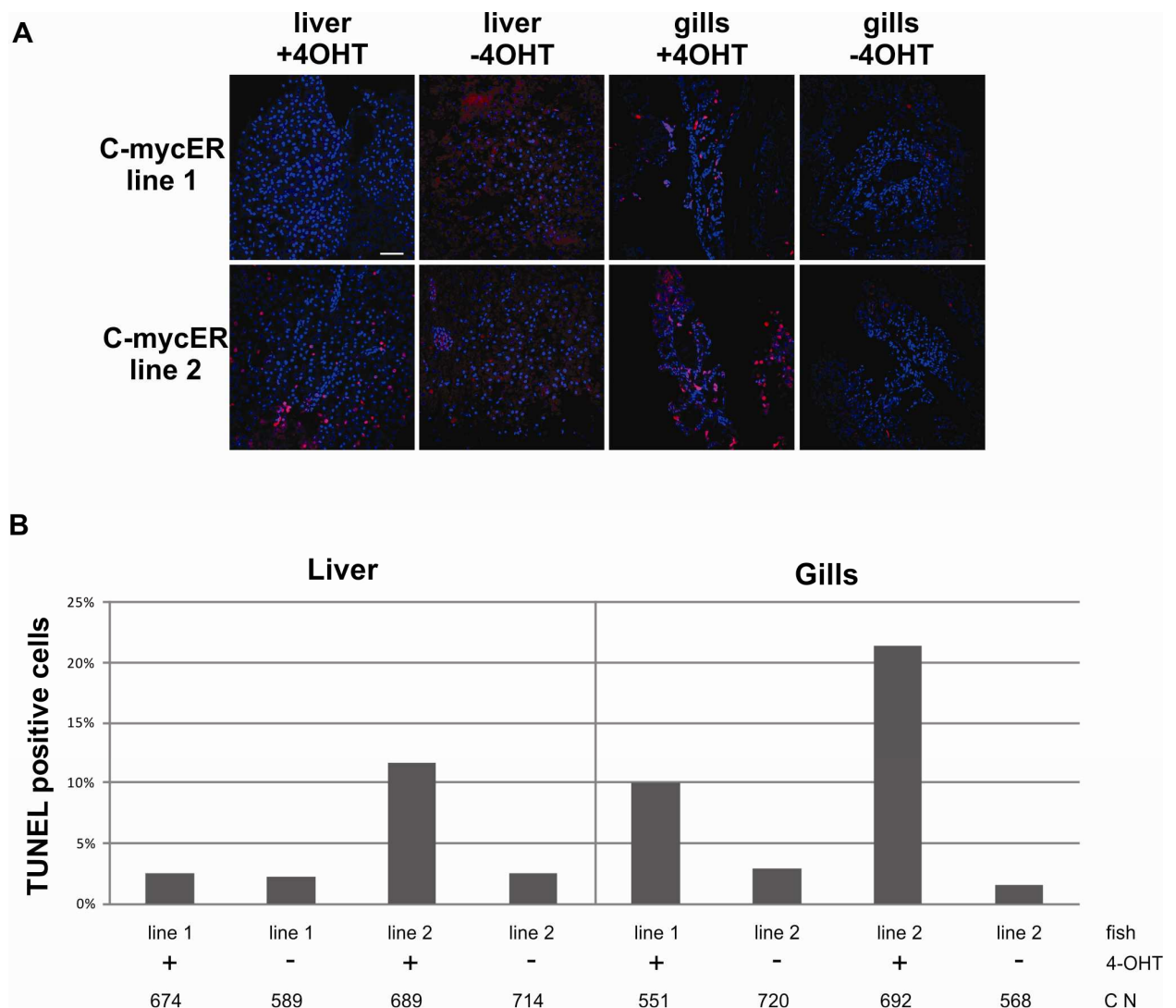
Fig. 40. Induction of apoptosis after C-myc activation *in vivo*. (A) Detection of apoptosis by TUNEL assays in liver and gills sections from adult fishes. Fishes were treated for 24 hours with 4-OHT to induce y-myc17 function.. DNA fragmentation is visible as red spots colocalizing with nuclei, which are stained with Hoechst. Scale bar: 10µM. (B) Quantification of apoptotic cells in liver (left panel) and gills (right panel) of both C-mycER lines fishes in presence or absence of 4-OHT. C N indicates total cell number for each assay.

4.3.5.3 Hyperplasia

I conducted long time C-myc activation experiments of several individuals of both c-myc17 lines to investigate potential pathological changes. Figures 41 A and B show liver histology from both transgenic lines after 4 weeks of treatment with tamoxifen. I observed hyperplasia, a raised number of cells, in the liver from c-myc line 1 and 2 when compared to either wild type fishes treated or non treated with 4-OHT (Fig. 41 C and D). I counted an average of 890 and 794 cells per section in C-mycER fishes after 4-OHT treatment. Wild type fishes had an average of 354 and 397 cells per section in fishes treated and non treated with tamoxifen (Fig. 41 E). Cell nuclei of C-mycER fishes after 4-OHT treatment were smaller (average 2 µm) when compared to cell nucleus of treated and non treated wild type fishes (average 3.8 µm). All visible cells on a picture were counted. Three not overlapping tissue parts, each with an area of approximately 87410µm^2, were

used for counting. This result indicates that long time activation of Cmyc17 does lead to tissue hyperplasia *in vivo*. Interestingly, no differences in both lines were detectable.
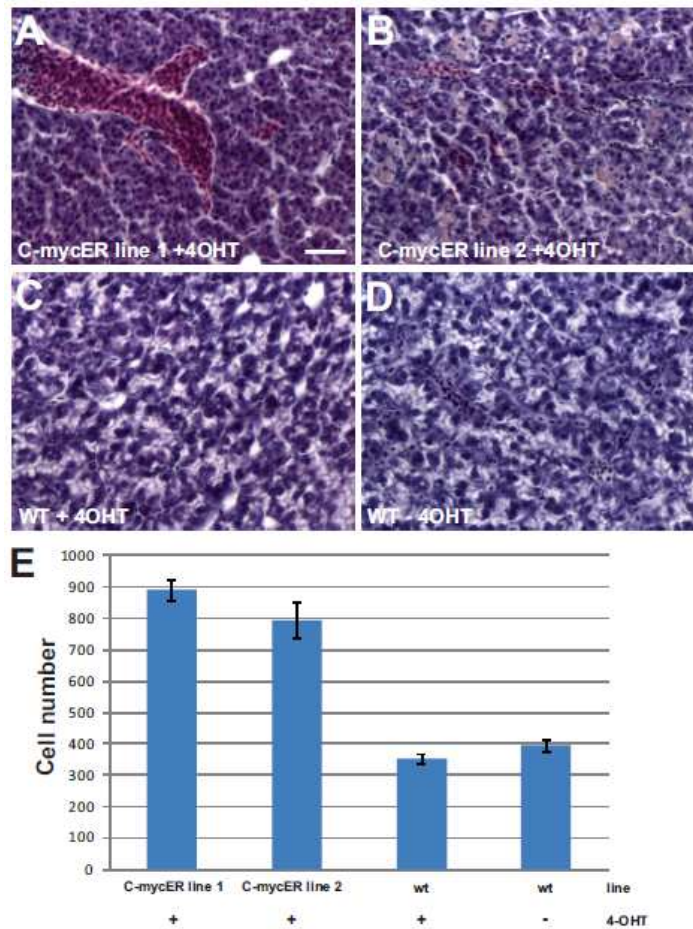

Fig. 41. Constant c-myc activation triggers liver cell hyperplasia *in vivo*. Images show haematoxylin and eosin stained sections of liver from adult transgenic fishes from line 1 (A), line 2 (B) and wild type (C) treated for four weeks with tamoxifen or non treated wild type (D). Scale bar: 20μM. (E) Cell number per section in both C-mycER lines and in wild type fishes treated or not treated with tamoxifen.

In summary, I generated a tamoxifen inducible *in vivo* model for the medaka *c-myc* gene present on chromosome 17. Using this model I showed that C-myc17 leads, when activated, to increased proliferation and to apoptosis in a dose dependent manner, similar to human Myc. It also triggers hyperplasia in adult liver after long-term activation.

5. DISCUSSION

5.1 BRAF

5.1.1 Identification and sequence analysis of medaka BRAF hint to evolutionary conservation

BRAF is a serine threonine kinase found mutated at high incidence in human tumours like malignant melanoma, thyroid cancer, colorectal carcinoma and ovarian cancer, and in low incidence in tumours like colon cancer, lung adenocarcinoma, breast cancer and lymphoma (Garnett and Marais, 2004). Analysis of the medaka *braf* gene is expected to bring new information on BRAF structure and conserved domains that can reflect its different or similar function between different organisms. In this work, I have identified and cloned the medaka *braf* gene for the first time. To analyse the similarities between different fish species, including medaka and other higher vertebrates, I aligned the amino acid sequences of the medaka BRAF, cloned in this work, and the ones from fugu, tetraodon, stickleback, zebrafish, xenopus, mouse and human, which are available in online databases (Figure 11). BRAF protein domains are highly conserved among vertebrates. The high similarity between all BRAF domains suggests the maintenance of function between different organisms. Although human and medaka BRAF protein sequences are highly conserved, synteny analysis (Table 1) comparing human BRAF locus on chromosome 7 and the corresponding medaka locus on chromosome 23 revealed no syntenic conservation between these species. One evolutionary reason for this observation might be a regional translocation in the corresponding medaka region where, during evolution, BRAF jumped out from the chromosome region where it belonged and was inserted in a totally new area.

5.1.2 Medaka BRAF has similar expression pattern as mouse

Analysis of murine *braf* mRNA expression by RT-PCR in different organs revealed a high expression of *braf* in brain and testis and a low expression in eye and liver (Barnier *et al*, 1995). In the same work, no expression was observed in kidney. This result is in accordance with the high *braf* expression in medaka brain found in this work in adult tissues by qPCR (Fig. 14). I also observed expression in the mesencephalon and prosencephalon by *in situ* hybridization during larval development (Fig. 13). Through these experiments, I also detected expression in the eye and liver in adult fishes (Fig. 14). However, I found a moderate expression in kidney, which disagrees with the results from Barnier *et al*. The mouse *braf* gene encodes multiple protein isoforms with tissue specific expression (Barnier *et al*, 1995). So far, no study to identify different BRAF isoforms in medaka has been performed.

5.1.3 Medaka transgenic lines support known BRAF functions

BRAF phosphorylates and thereby activates MEK, which subsequently phosphorylates and activates MAPK, which in turn phosphorylates several cytoplasmatic and nuclear targets (Wellbrock *et al*, 2004). BRAF mutations were found in approximately 66% of human

melanomas, and the most common is a T-A transversion leading to a valine to glutamic acid substitution, BRAF V600E (Michaloglou, 2008). This mutation results in a constitutive active BRAF and therefore induces constitutive MEK/MAPK signalling, resulting in enhanced proliferation (Fecher *et al*., 2008). To obtain more information of BRAF function *in vivo* in medaka and to take advantage of laboratory fish models to answer some of the remaining open questions of BRAF function, I established a medaka transgenic model carrying the medaka *braf* gene. To accomplish this, I produced transgenic lines carrying the wild type medaka gene and a constitutive active form. The constitutive active medaka BRAF showed to be able to transduce the MAPK signalling, since I was able to detect phosphorylated MAPK even without stimulus. This experiment also proved that medaka BRAF has the same function as mammalian BRAF in the propagation of signals through the MAPK pathway. Moreover, this experiment showed that the BRAF carrying the valine to glutamic acid mutation in the fish homologue of the human V600E (position 614, in medaka) is constitutively active. These results show that the medaka homologue of *braf* is able to fulfil similar functions to mammalian proteins, and that a fish specific mutation V614E can resemble a known human property.

5.1.4 BRAF plays a role in skin pigmentation

I observed disrupted pigmentation phenotype in transgenic BRAF V614E medaka fishes, as individuals of these lines show darker body pigmentation (Fig. 16). This phenotype was expected since a role of BRAF in pigmentation has been elucidated in zebrafish, where constitutively activated BRAF also plays a role in melanocyte development (Patton *et al*, 2005). In this work, transgenic zebrafishes showed focal sites of melanocyte proliferation, and BRAF activation was sufficient to promote nevus formation. However, although dramatic changes in zebrafish pigment pattern were observed, no tissue invasion was apparent. In conclusion, expression of BRAF V600E can cause the expansion of melanocytes, but additional mutations are required for melanoma formation. In accordance to this study, no tumour formation was observed in my BRAF V614E medaka fishes. In the same study, Patton *et al* (2005) observed that in a background without the function of the tumour suppressor p53, activated BRAF can lead to melanoma formation. In medaka, a p53 negative background or the loss of another tumour suppressor like *cdkn2* would probably also lead to melanoma formation, but this remains to be elucidated. Although results from fish models may not necessarily be directly extrapolated to the human situation, they will still be very informative to determine the effect of BRAF V600E in melanocytes also in the context of other cancer-predisposing lesions. In addition, medaka fishes have the advantage to enable close visualization of pigmentation during every stage of development and the possibility to screen for chemical compounds. It is important to notice that no correlation between *braf* overexpression and skin pigmentation in mammals has been drawn so far, which could constitute a specific fish BRAF function. In addition, it is known that BRAF not only stimulates melanocyte proliferation but also induces senescence in human melanocytes *in vitro* (Michaloglou *et al*, 2005) and in mice melanocyte *in vivo* (Dhomen *et al*, 2009). It remains to be elucidated whether the hyperpigentation spots present in medaka BRAF V614E lines are made up of senescent melanocytes.

5.1.5 Role of BRAF in the eye development?

Tissue specific *in vivo* manipulation of gene expression from a new species that was never analysed before will bring new insights into the genes's function. Unexpectedly, I observed a disrupted eye development in some fishes transiently expressing the constitutively active *brafV614E* gene under the control of the *mitf* promoter (Fig. 17). The vertebrate eye is formed by cells of the ectoderm origin, which gives rise to the retina, the epithelium of the iris and the lens (Chow and Lang, 2001). A number of genes that play a role in retina and lens development have been identified (reviewed in Cvekl and Mitton, 2010). Among these, the pigment cell master regulator MITF is known to play a role in retinal development (Hallsson *et al*., 2004). Also, Pax6 function is essential for normal eye development (Ashery-Padan and Gruss, 2001) and it is phosphorylated by MAPK, enhancing its transcriptional activity (Lang, 2004; Mikkola *et al*, 1999). Additionally, MAPK induces degradation of Mitf protein and thereby represses differentiation (Delfgaauw, 2003). As BRAF phosphorylates MEK, which in turn phosphorylates MAPK, I hypothesize that through constant activation of this pathway by BRAF V600E normal eye development is deregulated. Further studies will confirm or reject this theory by investigating pax6 phosphorylation and mitf stability. Besides that, *braf* mutations were observed in 14-40% of conjunctiva melanoma (Gear *et al*, 2004), showing a relation of BRAF with ocular melanoma. However, *braf* mutations are absent in uveal melanoma (Rimoldi *et al*., 2003).

5.1.6 Importance of BRAF animal models

Temporal and spatial control on BRAF expression and activity, in particular uncontrolled levels of oncogene expression and function, promote different effects in cell behaviour, like quiescence, proliferation or senescence (Woods *et al*., 1997; Zhu *et al*, 1998). BRAF regulates not only melanoma initiation and progression, but also general tumour progression (Hoeflich *et al*., 2006), which favours BRAF as a therapeutic target for the treatment of melanoma. Both proto-oncogenes activation and tumour-suppressor inactivation are implied in cellular transformation and tumour progression in melanoma (Polsky and Cordon-Cardo, 2003). Inhibitors of MEK in a background expressing mutant BRAF, like U0126 (Calipel *et al*., 2003) or CI 1040 (Solit *et al*., 2006), reduce phosphorylated MAPK and inhibit proliferation and oncogenic transformation, which can be easily explained since BRAF V600E signal via MEK and MAPK. Another BRAF inhibitor, sorafenib, inhibits BRAF and BRAF V600E as well as other protein kinases and retards the growth of human melanoma cells and complete inhibits MEK phosphorylation (Karasarides *et al*., 2004). However sorafenib is not efficient in preventing lung metastasis in a mouse model (Sharma *et al*, 2006). Recently a new drug, which is still investigated by a clinical trial, has been developed. PLX-4032, an inhibitor designed to target specifically BRAF V600E, is highly selective for this mutated form, demonstrating a 10 fold greater potency for the mutated BRAF than for the wild type in kinase assays and more than 100 fold in cell proliferation assays (Tsai *et al*., 2008). In several tumour xerograph models of BRAF V600E expressing melanoma, PLX-4032 treatment caused partial or complete tumour regression in a dose dependent manner (Yang *et al*, 2010). Phase 1 clinical study in melanoma patients showed that PLX-4032 treatment led to tumour regression in cancer patients. However, tumour re-growth occurs in many of the patients

and the cancer is then resistant to PLX-4032 treatment (Bollag *et al*, 2010). Clearly, inhibition of BRAF has a prominent role in melanoma therapy. The medaka BRAF V614E model generated in this work could be very helpful for drug selection and new BRAF target genes search, due to the fact that fish can be more easily screened when compared to mouse models. Also, the medaka model established here can be used to investigate the melanoma resistance (Nazarian *et al*, 2010) after treatment with PLX-4032.

To further understand BRAF function, other BRAF V600E models have been generated in different species. The BRAF V600E zebrafish model (Patton *et al*, 2005) was the first described model organism used to study constitutive BRAF activation. Although this group worked with a fish species, transgenic zebrafishes were carrying the human BRAF gene. Besides the zebrafish models, several BRAF V600E models have been generated in other species. A transgenic mouse expressing BRAF V600E under the control of the bovine thyroglobulin promoter, which drives the expression of the transgene in thyroid cells, shows increased MAPK signalling and an enlarged thyroid as well as poorly differentiated carcinomas (Knauf *et al*., 2005). This result indicates that BRAF V614E can serve as a tumour initiator and promote progression to carcinomas.

In addition, two Cre recombinase inducible BRAF V600E knock in mice have been generated. In one model, the constitutive activation of BRAF during embryonic development resulted in embryonic lethality due to bone marrow failure (Mercer *et al*., 2005). This model indicated that in some primary mouse cells, constitutive activation of BRAF is able to induce several hallmarks of transformation, like morphologic transformation, hyperproliferation and loss of contact inhibition, without the involvement of a second cooperating oncogene. However, for the development of cancer *in vivo,* the situation is more complex, since BRAF V600E mutations are frequently found in nevi which remain senescent and do not progress to tumour formation (Pollock *et al*., 2003). Although BRAF is the most prominent oncogene in melanoma and the acquisition of an activation mutation in BRAF creates an advantage in the proliferation of melanocytes, the constant signalling from BRAF itself is not sufficient to fully transform normal melanocytes. In the second model, BRAF V600E is expressed in the lung epithelium and leads to lung adenomas (Dankort *et al*., 2007). In that work, lesions appear to be dependent on MEK/MAPK signalling, since pharmacological inhibition of MEK prevents adenoma formation. But without pharmacological inhibition, adenomas grow rapidly for about 8 weeks followed by a reduction in proliferative activity and senescence. In this model adenomas rarely progress to adenocarcinomas unless either p53 or CDKN2 is deleted. The model that I established now opens up the possibility to resolve the cell fate decision of *braf* overexpressing cells by investigation of pigment cell development over the full life time of an individual fish. In addition, the medaka mitf:BRAF can be crossed to the melanoma developing *Xmrk* line to understand in details the role of BRAF in melanoma initiation and progression. Also, BRAF V614E fishes can be used in screens for melanoma-suppressing or enhancing genes as well as for testing novel melanoma therapeutics.

5.2 Stat5

5.2.1 Evolution of Stat5 genes

The signal transducer and activator of transcription 5 works as a cytoplasmatic signal transducer and a nuclear transcription factor. It has been linked with myeloid cell transformation, breast, prostate, lung, neck, head and liver cancers and melanoma (Ferbeyre and Moriggl, 2011). Understanding of Stat5 biology in detail helps to elucidate its function in cancer initiation and progression and comprises the possibility of its usage as a target for cancer therapy. To further investigate Stat5 function in vertebrates I have identified and cloned the medaka Stat5ab/a (ENSORLG00000003961) and Stat5ab/b (ENSORLG00000014335) genes. It has been proposed that all members from the Stat5 family have arisen from a series of gene duplications, the most recent of which generated the two Stat5 genes (Copeland *et al*., 1995). The human Stat5A (ENST00000345506) and Stat5B (ENST00000293328) genes show high sequence identity (Fig. 26 and Table 3) and lie adjacent to each other in close proximity to Stat3 gene (position: 17:40350565-40540000) on chromosome 17. The two medaka Stat5 proteins showed higher rates of homology to each other than to human Stat5A and Stat5B, suggesting that they do not represent human Stat5A and Stat5B equivalents but have arisen independently. The same is observed with the two Stat5 genes from zebrafish (Lewis and Ward, 2004) and stickleback (ENSEMBL database) indicating that this represents a fish specific duplication. However, other fish species like fugu (Lewis and Ward, 2004) and tetraodon (Sung *et al*., 2003) only have one Stat5 copy. Synteny analysis of the comprising medaka genome regions to the human chromosome 17 where both Stat5 copies are present (Table 4) revealed that Stat5ab/a copy shares a high number of syntenic genes with human, which is not observed in medaka Stat5ab/b. This also suggests that the second copy from medaka Stat5 gene arose from a different duplication process than the human. Also, further syntenic analysis of Stat5 genes from different fish species (Tables 5 and 6) suggests that the second copy of medaka Stat5 gene arises from the fish specific duplication event due to the high number of syntenic genes between zebrafish, stickleback, tetraodon, fugu and medaka Stat5 genes.

5.2.2 Conservation of functional motifs of medaka Stat5 genes

To further analyse medaka Stat5 genes and their possible correlation with human Stat5 function, I analysed the level of similarities between known Stat5 conserved domains. The Stat5 family of proteins contains six conserved domains: the N-terminal domain, a transactivation domain, a DNA binding domain, a linker domain, a Src homology 2 (SH2) domain and the coiled-coil domain (Lim and Cao, 2006). Stat5 proteins show evolutionary conservation from *Drosophila* to mammals (Miyoshi *et al*., 2001). Comparison of amino acid sequences of medaka Stat5ab/a and Stat5ab/b revealed a high degree of similarity between the two medaka Stat5 in the DNA binding domain and in the SH2 domain. Also, the N-terminal domain, the coiled-coil domain and the linker domain showed moderate levels of similarity (Table 2). Since the transactivation domain is known to be the least conserved domain of the whole Stat5 family (Paukku and Silvennoinen, 2004), it was no surprise that this domain was the least conserved among both medaka Stat5 genes sharing only 51% of equal amino acid. Comparison of medaka Stat5ab/a and Stat5ab/b

protein sequences with human Stat5A (Figure 26 and Table 3) revealed highest homology in the DNA binding domain: 95% and 90% respectively. Besides the ability to bind to DNA, this domain is also involved in nuclear translocation (Lim and Cao, 2006). Further work remains to be performed to test whether both medaka Stat5 proteins are able to translocate to the nucleus and act as a transcription factor, but the high similarity indicates that this is the case. As expected, the transactivation domain from both medaka proteins is also the least conserved in their amino acid sequences when compared to human Stat5A. Medaka Stat5ab/a and Stat5ab/b are 60% and 51% similar to the human Stat5A protein sequence, respectively.

5.2.3 Medaka *Stat5* genes have similar expression pattern to other vertebrates

Additional characterization of gene expression also brings new information that can be useful for understanding the function of a given gene. Stat5a and Stat5b were found at similar levels in 6 week old mice by reverse transcription PCR in heart, kidney, liver, lung, ovary and spleen (Liu *et al*., 1995). In the same study, only Stat5b was found to be expressed in brain and muscle. During my work, I observed similar expression patterns of both medaka *Stat5* genes in all tissues analysed, including brain and muscle (Fig. 29). The reason for this can be the different origins of mammal and medaka Stat5 genes. Both medaka Stat5 genes could have arisen from the duplication of one of the human/mouse Stat5, which would explain the similar expression pattern observed among both Stat5 copies in medaka. The expression of the single Stat5 gene found in *Tetraodon fluviatilis* was detected in all analysed organs including gills, heart, liver, intestine, kidney and testis by reverse transcription PCR (Sung *et al*., 2003). *In situ hybridization* of the single *Stat5* gene found in *Xenopus laevis* revealed *Stat5* expression in the evaginating eye (Pascal *et al*, 2001). In the same study, *Stat5* expression was observed on the ventral part of the embryo at Xenopus stage 28. The expression pattern observed by these authors in Xenopus greatly differs from the expression pattern I observed in medaka embryos by *in situ hybridization* (Fig. 28) where expression was detected in the otic vesicle, prosencephalon and mesencephalon. However, the developmental stages in medaka and the ones in xenopus are too different to make a clear statement about the differences.

5.2.4 Stat5 function during melanoma development

Xmrk signalling leads to *Stat5* activation in *Xiphophorus* melanoma (Wellbrock *et al*., 1998). Melanoma developing medaka fishes carrying the *Xmrk* under the *mitf* promoter show a correlation of *Stat5* activation and MITF and BCL-X levels with more aggressive stages of the malignancy (Schartl *et al*., 2010). Stat5 has been shown to contribute to anti-apoptosis signalling through up-regulation of BCL-X and to trigger proliferation also in human melanoma cell lines (Morcinek *et al*., 2002). All investigations studying phosphorylated Stat5 were based on the phosphorylation on Tyr694 of the human protein, which is conserved between both human and medaka Stat5 proteins. This means that no difference between different copies of Stat5 was found in this study. To obtain more information on Stat5 function *in vivo* in medaka and to investigate the different roles of each gene copy, I established medaka lines carrying the full length medaka

Stat5ab/a and *Stat5ab/b* gene (Table 7). In addition to these lines, lines carrying constitutive active and dominant negative versions of each gene were generated. The established lines in this work will be important to test whether both medaka Stat5 copies play a role in melanoma and to investigate different function of each gene in a whole organism.

5.2.5 Importance of Stat5 animal models

Stat5a was first identified as a prolactin-induced mammary gland factor (Gouilleux *et al.*, 1994). Subsequent studies identified a closely related gene, Stat5b that shares more than 90% similarity, diverging only in their carboxy-terminal region (Azam *et al.*, 1995). To further decipher their functions *in vivo*, Stat5a and Stat5b single knockout mice were generated. Stat5a knockout mice are normal in appearance, size, weight and fertility but they have impaired mammary gland development and females fail to lactate due to loss of prolactin responsiveness (Liu *et al.*, 1997). Stat5b knockout mice revealed that this protein is required to maintain sexual dimorphism of body growth rates and liver gene expression due to defects in growth hormone signalling (Udy *et al.*, 1997). A study on combined Stat5a -/- and Stat5b -/- mice during fetal development revealed that embryos were severely anemic (Socolovsky *et al*, 1999). Also, double knockouts for both Stat5 genes have severe alterations in different bone marrow progenitor populations (Snow *et al.*, 2003).

Due to the severe defects observed in the established mouse models, investigations of Stat5 function during processes like cancer *in vivo* are still elusive. In this work, Stat5 transgenic fishes were generated for the first time. The different generated medaka Stat5 lines will help in the future to determine if any specific functional division of medaka Stat5 proteins has occurred. The constitutively active Stat5ab/a and Stat5ab/b constitute the first animal models to bear gain of developmental function of Stat5 proteins. Also, the dominant negative lines of both medaka Stat5 genes will help to gain new insight on fish Stat5 function as well as serve for comparison with higher vertebrate models.

5.2.6 Stat5: possible target for gene therapy?

To be an ideal target for cancer therapy, a transcription factor needs to fulfil four main criteria. First, it must be overactive in a large percentage of cells in different tumour types. Second, this activity should determine gene expression patterns that not only promote cancer cell survival and proliferation, but also promote other malignant properties such as tumour angiogenesis and immune evasion. Third, good therapeutic targets must also be susceptible to specific inhibition by small molecule drugs. And fourth, tumour cells should be more dependent on activity of the target than normal cells (Yu and Jove, 2004). Stat5 has been correlated *in vitro* with all of these categories. However, no studies involving a living organism have been reported. The Stat5 lines generated here constitute a nice model to test Stat5 as a cancer therapy agent since medaka fishes can be easily crossed with cancer developing lines, like the melanoma developing *Xmrk* fishes, to

produce a double transgenic bearing the different Stat5 versions. A double mutant for both stat5 versions in one individual would be useful to study the role of Stat5 in cancer progression.

5.3 C-myc

5.3.1 Evolution of c-myc genes in medaka

In my PhD work, I have identified two medaka C-myc genes, named C-myc17 (Fig. 30) and C-myc20 (Fig. 31). In addition, I have further cloned and characterized the *c-myc17* gene. The amino acid sequence alignments indicated that the two medaka *c-myc* genes are orthologues of the human C-myc (Fig. 32). Analyses of the available sequenced teleost genomes revealed that just the zebrafish genome has kept two *c-myc* copies besides medaka (Schreiber-Agus, *et al,*1993). Their evolutionary origin from the fish specific genome duplication (Meyer and Schartl, 1999) was clearly established from synteny analysis comparing C-myc17 and 20 with the human *myc* locus at chromosome 8q24 and the corresponding fugu locus, which revealed a high degree of conservation between these species (Table 9). The phylogenetic analysis revealed also that both medaka *c-myc* genes are bona-fide members of the *c-myc* gene family (Fig. 34). However, *c-my17* differs significantly from other vertebrate c-*myc* genes as it branches off very basal in the phylogenetic tree (box in Fig. 34), while both zebrafish genes come out closely together within the teleost branch. This indicated a high degree of diversification of this gene copy. Unless the presence of an extra gene product is advantageous, two genes with identical functions are unlikely to be stably maintained in the genome (Nowak *et al*, 1997). Duplicated genes can be maintained when they differ in some aspects of their functions, which can, for example, occur by subfunctionalization. During this process, each gene copy adopts parts of the functions of their parental genes (Zhang, 2003). Another (non-exclusive) possibility is that one of the two versions adopts a novel function. Our studies of C-myc17 indicate that after the duplication process of the locus, the structure, and to a minor extent the expression of the medaka *myc* genes, changed. However, the essential Myc functions even after significant structural and amino acid changes are maintained. Further experiments will reveal whether the two medaka *c-myc* genes have compensating or overlapping functions or might differ in more subtle aspects of their overall function.

5.3.2 Conservation of functional motifs of medaka C-myc genes

By comparing amino acid sequences of the human DNA binding domain with C-myc17 and C-myc20, I observed 92% and 100% similarities, suggesting that both copies retained the ability to bind to DNA. Moreover, the leucine-zipper, which is responsible for interaction with Max, is only 50% similar to C-myc20 and 68% similar to C-myc17 (Table 8B). Since medaka has two Max copies (ENSORLG00000019517 and ENSORLG00000016817), it is likely that each medaka C-myc copy binds to a specific Max for activation of gene transcription. This hypothesis remains to be elucidated. In addition, C-myc function in inducing gene transcription has been shown to be conserved in medaka C-myc17 (Fig. 37C). As in humans, medaka homologues of *odc1*, *cbx3*,

cct5, *eif3s8* and *metll1*, were up regulated after C-myc activation by 4-OHT treatment in the established C-mycER17 fishes. Thereby, these results show transcriptional activity of C-myc17.

Additionally, the protein alignment indicated the loss or change of essential residues in Cmyc17 responsible for posttranslational regulation of C-myc function and stability (indicated as yellow arrows in Fig. 32). These changes did not ablate the transcriptional function of C-myc17 *in vivo*, but may result in altered potential of Myc function during cell transformation by influencing Myc's life time (Spencer and Groudine, 1991). In human cancers, stabilized versions of Myc act as main reasons for malignant transformation and cancer progression (Junttila and Westermarck, 2008). Phosphorylation (Westermarck, 2010) and ubiquitination (Gregory and Hann, 2000) are key regulators of Myc turnover. Besides these modifications, acetylation of Myc by histone acetyltransferases, like p300/CBP, Tip60 and GN5, (Vervoorts *et al*, 2003; Patel *et al*, 2004) is critical for protein stabilization. My analysis indicates that C-myc17 lost a number of these conserved modification sites hinting to a reduction of stability by reduced acetylation and a faster turnover rate. Interestingly, C-myc20 displays a higher rate of residue conservation, pointing to differences in posttranscriptional regulation and subsequent different protein stability rates between the two medaka orthologues.

A correlation to known tumour related human SNP changes in MYC indicated that a number of conserved residues, for example P57 and P59 residues, found mutated in Burkitt Lymphoma (Bhatia, 1993) are unchanged in medaka. Other human regulatory residues are not conserved, like E39 and N86, in both versions of C-myc in medaka. Functional consequences of these changed residues in fish are not observed, but can be investigated by future mutational analyses.

5.3.3 C-myc17 plays a role in apoptosis and proliferation

It is known from higher vertebrates that activation of C-myc leads to cell proliferation through its ability to activate expression of genes involved in cell cycle progression (Steiner *et al*., 1995), in repression of CDK inhibitors (Staller *et al*., 2001) and also in chromatin remodelling (Amati *et al*., 2001). Deregulated C-myc activation may also lead to cell growth arrest and subsequent apoptosis under certain conditions (Evan *et al*., 1992). To test the ability of C-myc17 to perform established C-myc functions, I generated two transgenic medaka lines expressing a mouse estrogen receptor coupled version of the gene under the ubiquitously expressed *beta-actin* promoter. In the absence of a ligand, C-mycER fusion protein is bound to the heat-shock protein Hsp90 and therefore located in the cytoplasm, hence inactive. 4OHT has higher affinity to the estrogen receptor than Hsp90, and therefore after its administration, 4OHT binds to ER instead (Tian *et al*, 2006). C-myc ER is then free to translocate to the nucleus and act as a transcription factor. The two C-myc lines generated in this work showed to be efficiently activable on 4OHT administration since C-myc nuclear translocation (Fig. 37A and B) and activation of known C-myc target genes (Fig. 37C) were only observed after 4-OHT treatment.

Interestingly, the two independently generated medaka lines displayed differences in the amount of transgene expression (Fig. 36A) and showed clearly distinguishable functional differences after

activation. Line 1, which had a lower c-*myc17ER* transgene expression, showed a raised proliferative rate when compared to line 2 (Fig. 38). Vice versa, line 2 had a higher transgene expression level and appeared to induce higher apoptosis rates than line 1 (Fig. 39 and 40). A comparable observation was obtained by Murphy *et al* (2008) in mice, where the activation of C-myc under the weak Rosa26 promoter triggered proliferation, while the more powerful rat insulin promoter, when driving C-myc expression, led to apoptosis. This indicated that cellular fate decisions are obviously taken depending on different threshold levels of C-myc. My work supports this view since the ability to induce higher proliferation or higher apoptosis rates was related to the differences in the level of transgene expression in the two medaka lines, which were otherwise genetically identical. What is not clear is how different levels of Myc trigger such different biological outputs. Murphy *et al* suggest two possibilities. First, it is possible that Myc induced proliferation and apoptosis are mediated by a distinct set of target genes. Low and high levels of Myc might engage proliferative and proapoptotic target genes, respectively. This might be due to changed affinity to promoter elements. So, with low levels of Myc, only proliferation target genes achieve the threshold that leads to cell proliferation. On the other hand, high levels of Myc would make the target genes involved in apoptosis cross the threshold and trigger cell death. A second explanation would be that proliferation and apoptosis themselves have a different threshold. Low levels of Myc would lead to low levels of both sets of target genes (proliferative and pro apoptotic), which would achieve only the proliferation execution threshold. By contrast, high levels of Myc regulate the same genes but in a greater extend, achieving the higher apoptosis execution threshold. It seems that the level of Myc required to trigger apoptosis is not fixed, but depends on each cell's microenvironment. The two C-myc lines established in my PhD work will be helpful in further studies aiming to understand how the mechanisms of Myc triggering proliferation and/or apoptosis work.

5.3.4 A possible role for C-myc17 in tumorigenesis

Although a link between C-myc and cancer is well established, the molecular and cellular mechanisms of C-myc mediated transformation are not yet fully understood (Wang *et al*, 2011). C-myc is thought to contribute to tumorigenesis by deregulating gene expression and abrogating cell cycle checkpoints, thereby driving uncontrolled cellular growth and promoting cell proliferation. Additional effects on cellular adhesion, angiogenesis, metabolism and genomic instability have been described and are key elements of tumour progression (Lutz *et al*, 2002). Nevertheless, Myc induced cellular alterations can lead to apoptosis and senescence as a mechanism to protect the organism from proliferation of damaged and abnormal cells that could be progenitors of cancer cells (Evan *et al*., 1992). In an oncogenic background, with additional mutations that activate anti-apoptotic signals, Myc can lead to neoplasms and subsequently to malignant transformation (Nilsson and Cleveland, 2003). To give one example, C-myc was shown to collaborate with loss of p53 (Blyth *et al*., 2000) or Arf (Jacobs *et al*., 1999) in mouse lymphoma genesis.

To further decipher Myc functions and cell fate decisions, genetic models utilizing inducible protein versions have been established in higher vertebrates and recently in zebrafish. Two

examples from transgenic mice are an activable C-myc version in mouse epidermis (Pelengaris *et al*., 1999) and in adult mouse pancreatic ß-cells (Pelengaris *et al*., 2002). Both mouse models greatly differ in the potential of inducing apoptosis, proliferation and their dependence on additional mutations. Although laboratory fish systems offer several experimental advantages in comparison to mice, such as the possibility to perform large scale screens and *in vivo* visualization of tumour progression, a similar inducible myc-ER system, like the one presented in this work, has been established only recently for lymphomas (Gutierrez *et al*., 2011). Prior to this study, mouse or human C-myc was used in zebrafish to induce T-cell acute lymphoblastic leukemia (T-ALL, Langenau *et al*., 2003). The examination of molecular pathways activated in response to C-myc overexpression closely resembled the most common subclass of human leukemia and thereby indicates great overlap in the underlying signals between humans and fishes (Langenau *et al*., 2004). Lymphoid malignancy in zebrafish also requires additional events of transformation, such as *tal1* and *lmo2* deregulation. Gutierrez *et al*. (2011) show that ablation of Myc activation results in regressions of T-ALL and tumour regression depending on Akt/Pten singling. In contrast to these published zebrafish models, my work presents a more general tumorgenesis model to induce Myc function in other organs than blood in an evolutionary divergent laboratory fish species by using a species specific *c-myc* orthologue.

As a first indication of cellular transformation caused by C-myc activation, hyperplasia, but not tumour formation, was observed in livers of *c-myc17*-ER transgenic medaka individuals after 4-OHT treatment. Interestingly, no difference in the degree of liver hyperplasia between line 1 and line 2 was observed. Based on the studies mentioned above, I can hypothesize that Cmyc17 would need an additional anti-apoptotic event to function as a viable tumour model. In accordance with our findings in medaka, sustained overexpression of *c-myc* in the liver of transgenic mice led to cancer only after 12 months (Santoni-Rugiu *et al*., 1996). In zebrafish, constantly expressed oncogenic Kras, an upstream factor of C-myc in the Map-kinase-signalling pathway (Gupta and Davis, 1994; Jin *et al*, 2004), was sufficient to drive liver tumorigenesis (Nguyen *et al*., 2011). These fishes exhibit a similar histological phenotype as observed in our C-myc medaka.

Data from animal models support the idea that the liver is more susceptible to neoplastic transformation during stages of liver growth and regeneration (Heindryckx *et al*, 2009). Using a tetracycline regulated conditional mouse model it was postulated that C-myc's ability to induce mitotic division and tumorigenesis in the liver is developmentally regulated (Beer *et al*., 2004). In an embryonic or neonatal liver, in which hepatocytes are actively undergoing cellular division, *c-myc* overexpression further increases mitosis and results in liver tumorigenesis. In contrast, when *c-myc* is overexpressed in adult murine hepatocytes, cellular growth but no tumour formation was observed.

In summary, the medaka model established here, utilizing a teleost *c-myc*, opens up the possibility to decipher transition from hyperplasia to liver cancer. Medaka can be easily manipulated to produce double transgenic individuals lacking anti-apoptotic factors, for example p53 mutants (Taniguchi *et al*., 2006) to induce tumor growth. Additionally, this model is suitable for large scale genetic and chemical compound screens to screen anticancer agents. It also facilitates the

investigation of cell fate decision and their consequences during early steps of tumorigenesis and development in closer detail.

6. REFERENCES

Adhikary, S. and Eilers, M. (2005). Transcriptional regulation and transformation by Myc proteins. *Nature reviews. Molecular cell biology*, *6*(8), 635-45.

Amati, B., Brooks, M. W., Levy, N., Littlewood, T. D., Evan, G. I., and Land, Hartmut. (1993). Oncogenic activity of the c-Myc protein requires dimerization with Max. *Cell*, *72*, 233-245.

Amati, B., Frank, S. R., Donjerkovic, D., and Taubert, S. (2001). Function of the c-Myc oncoprotein in chromatin remodelling and transcription. *Biochimica et biophysica acta*, *1471*, 135-145.

Amsterdam, A., and Hopkins, N. (2006). Mutagenesis strategies in zebrafish for identifying genes involved in development and disease. *Trends in genetics : TIG*, *22*(9), 473-8.

Ariyoshi, K., Nosaka, T., Yamada, K., Onishi, M., Oka, Y., Miyajima, A., et al. (2000). Constitutive activation of STAT5 by a point mutation in the SH2 domain. *J. Biol. Chem.*, *275*, 24407-24413.

Arnold, I., and Watt, F. M. (2001). c-Myc activation in transgenic mouse epidermis results in mobilization of stem cells and differentiation of their progeny. *Current biology : CB*, *11*(8), 558-68.

Arvanitis C, Felsher DW. 2006. Conditional transgenic models define how MYC initiates and maintains tumorigenesis. *Semin Cancer Biol*. Aug;16(4):313-7.

Ashery-Padan, R., and Gruss, P. (2001). Pax6 lights-up the way for eye development. *Current opinion in cell biology*, *13*(6), 706-14.

Azam, M., Erdjument-bromage, H., Kreider, B. L., Xia, M., Quelle, F., Basu, R., et al. (1995). lnterleukin-3 signals through multiple isoforms of. *EMBO Journal*, *14*(7), 1402-1411.

Bardeesy, N., Bastian, B. C., Hezel, A., Pinkel, D., DePinho, R. A., Chin, L. (2001). Dual inactivation of RB and p53 pathways in RAS-induced melanomas. *Mol Cell Biol*. Mar;21(6):2144-53.

Bardeesy, N., Wong KK, DePinho RA, Chin L. (2000). Animal models of melanoma: recent advances and future prospects. *Adv Cancer Res*. 79:123–156.

Barnier, J. V., Papin, C., Eychène, A., Lecoq, O., and Calothy, G. (1995). The mouse B-raf gene encodes multiple protein isoforms with tissue-specific expression. *The Journal of biological chemistry*, *270*(40), 23381-9.

Baudler, M., Schartl, M., and Altschmied, J. (1999). Specific Activation of a STAT Family Member in Xiphophorus Melanoma Cells locus is the Xmrk oncogene encoding a subclass I re-. *Experimental Cell Research*, *220*, 212-220.

Becker, J. C., Houben, R., Schrama, D., Voigt, H., Ugurel, S., Reisfeld, R. A. (2010). Mouse models for melanoma: a personal perspective. *Exp Dermatol*. Feb;19(2):157-64.

Beer, S., Zetterberg, A., Ihrie, R. a, McTaggart, R. a, Yang, Q., Bradon, N., et al. (2004). Developmental context determines latency of MYC-induced tumorigenesis. *PLoS biology*, *2*(11), e332.

Bennett, D. C. (1987). Mechanisms of differentiation in melanoma cells and melanocytes. *Environ Health Perspect.* Mar;80:49-59.

Berghmans, S., Murphey, R. D., Wienholds, E., Neuberg, D., Kutok, J. L., Fletcher, C. D. M., et al. (2005). Tp53 Mutant Zebrafish Develop Malignant Peripheral Nerve Sheath Tumors. *Proceedings of the National Academy of Sciences of the United States of America*, *102*(2), 407-12.

Berkelhammer, J., Oxenhandler, R. W., Hook, R. R. J., Hennessy, J. M. (1982). Development of a new melanoma model in C57BL/6 mice. *Cancer Res.* 42:3157–3163.

Bhatia, K., Huppi, K., Spangler, G., Siwarski, D., Iyer, R., Magrath, I. (1993). Point mutations in the c-Myc transactivation domain are common in Burkitt's lymphoma and mouse plasmacytomas. *Nat Genet*. Sep;5(1):56-61.

Bittner, M., Meltzer, P., Chen, Y., Jiang, Y., Seftor, E., Hendrix, M., et al. (2000). Molecular classification of cutaneous malignant melanoma by gene expression profiling. *Nature*, Aug 3;406(6795):536-40.

Blackwood, E. M., and Eisenman, R. N. (1991.). Max : A Helix-Loop-Helix Zipper Protein That Complex with Myc. *Science*. Mar 8;251(4998):1211-7.

Blyth, K., Stewart, M., Bell, M., James, C., Evan, G, Neil, J. C., et al. (2000). Sensitivity to myc-induced apoptosis is retained in spontaneous and transplanted lymphomas of CD2-mycER mice. *Oncogene*, *19*(6), 773-82.

Blyth K, Terry A, O'Hara M, Baxter EW, Campbell M, Stewart M, Donehower LA, Onions DE, Neil JC, Cameron ER. (1995). Synergy between a human c-myc transgene and p53 null genotype in murine thymic lymphomas: contrasting effects of homozygous and heterozygous p53 loss. *Oncogene*. May 4;10(9):1717-23.

Bollag, G., Hirth, P., Tsai, J., Zhang, J., Ibrahim, P. N., Cho, H., Spevak, W., Zhang, C., Zhang, Y., Habets, G., *et al*. (2010). Clinical efficacy of a RAF inhibitor needs broad target blockade in BRAF-mutant melanoma. *Nature*. Sep 30;467(7315):596-9.

Bouchard, C., Thieke, K., Maier, A., Saffrich, R., Hanley-Hyde, J., Ansorge, W., et al. (1999). Direct induction of cyclin D2 by Myc contributes to cell cycle progression and sequestration of p27. *The EMBO journal*, *18*(19), 5321-33.

Bouchard, C., Dittrich, O., Kiermaier, A., Dohmann, K., Menkel, A., Eilers, Martin, et al. (2001). Regulation of cyclin D2 gene expression by the Myc / Max / Mad network : Myc-dependent TRRAP recruitment and histone acetylation at the cyclin D2 promoter. *Genes and Development*, 2042-2047.

Bowman, T., Garcia, R., Turkson, J., and Jove, R. (2000). STATs in oncogenesis. *Oncogene*, *19*(21), 2474-88.

Bromberg, J. F. (2001). Activation of STAT proteins and growth control. *BioEssays : news and reviews in molecular, cellular and developmental biology*, 23(2), 161-9.

Bradl, M., Klein-Szanto, A., Porter, S., Mintz, B. (1991). Malignant melanoma in transgenic mice. *Proc Natl Acad Sci USA*. 88:164–168.

Brummer, T., Martin, P., Herzog, S., Misawa, Y., Daly, R. J., and Reth, M. (2006). Functional analysis of the regulatory requirements of B-Raf and the B-Raf(V600E) oncoprotein. *Oncogene*, 25(47), 6262-76.

Calipel, A., Lefevre, G., Pouponnot, C., Mouriaux, F., Eychène, A., and Mascarelli, F. (2003). Mutation of B-Raf in human choroidal melanoma cells mediates cell proliferation and transformation through the MEK/ERK pathway. *The Journal of biological chemistry*, 278(43), 42409-18.

Catchen, J. M., Conery, J. S., Postlethwait, J. H. (2009). Automated identification of conserved synteny after whole-genome duplication. *Genome Res.* Aug;19(8):1497-505.

Ceol, C. J., Houvras, Y., Jane-Valbuena, J., Bilodeau, S., Orlando, D. A., Battisti, V., Fritsch, L., Lin, W. M., Hollmann, T. J., Ferré, F., Bourque, C. *et al* (2011). The histone methyltransferase SETDB1 is recurrently amplified in melanoma and accelerates its onset. *Nature*. Mar 24;471(7339):513-7.

Cheon, D. J., and Orsulic, S. (2011). Mouse models of cancer. *Annual review of pathology*, 6, 95-119.

Chin, L. (2003). The genetics of malignant melanoma: Lessons from mouse and man. *Nat. Rev. Cancer*, 3, 559-570.

Chin, L., Garraway, L. A., and Fisher, D. E. (2006). Malignant melanoma: genetics and therapeutics in the genomic era. *Genes and Development*. 2149-2182.

Chin, L., Pomerantz, J., Polsky, D., Jacobson, M., Cohen, C., Cordon-Cardo, C., Horner, J. W. DePinho, R. A. (1997). Cooperative effects of INK4a and ras in melanoma susceptibility in vivo. *Genes Dev*. Nov 1;11(21):2822-34.

Chong, H., Vikis, H. G., and Guan, K.-L. (2003). Mechanisms of regulating the Raf kinase family. *Cellular Signalling*, 15(5), 463-469.

Chow, R. L., and Lang, R. A. (2001). Early eye development in vertebrates. *Annu Rev Cell Dev Biol. 2001;17:255-96*.

Copeland, N. G., Gilbert, D. J., Schindler, C., Zhong, Z., Wen, Z., Darnell, J. E., et al. (1995). Distribution of the mammalian Stat gene family in mouse chromosomes. *Genomics*. Sep 1;29(1):225-8

Cree, I. A. (2011). Cancer Biology. *Methods Mol Biol.*, Vol.371.

Cvekl, A., and Mitton, K. P. (2010). Epigenetic regulatory mechanisms in vertebrate eye development and disease. *Heredity*, 105(1), 135-51.

Dang, C. V., O`Donnell, K. A., Zeller, K. I., Nguyen, T., Osthus, R. C., and Li, F. (2006). The c-Myc target gene network. *Seminars in cancer biology*, *16*(4), 253-64.

Dankort, D., Curley, D. P., Cartlidge, R. A., Nelson, B., Karnezis, A. N., Damsky, W. E. Jr, You, M. J., DePinho, R. A., McMahon,. M., Bosenberg, M. (2009). Braf (V600E) cooperates with Pten loss to induce metastatic melanoma. *Nat Genet*. May;41(5):544-52.

Dankort, D., Filenova, E., Collado, M., Serrano, M., Jones, K., and McMahon, Martin. (2007). A new mouse model to explore the initiation, progression, and therapy of BRAFV600E-induced lung tumors. *Genes and development*, *21*(4), 379-84.

Davies, H., Bignell, G. R., Cox, C., Stephens, P., Edkins, S., Clegg, S., et al. (2002). Mutations of the BRAF gene in human cancer. *Nature*, *417*(6892), 949-54.

Davis, A. C., Wims, M., Spotts, G. D., Hann, S. R., and Bradley, a. (1993). A null c-myc mutation causes lethality before 10.5 days of gestation in homozygotes and reduced fertility in heterozygous female mice. *Genes and Development*, *7*(4), 671-682.

Delfgaauw, J. (2003). MITF-M plays an essential role in transcriptional activation and signal transduction in Xiphophorus melanoma. *Gene*, *320*, 117-126.

Dhomen, N., Reis-Filho, J. S., da Rocha Dias, S., Hayward, R., Savage, K., Delmas, V., Larue, L., Pritchard, C. and Marais, R. (2009). Oncogenic Braf induces melanocyte senescence and melanoma in mice. *Cancer Cell*. Apr 7;15(4):294-303.

Dissanayake, S. K., Wade, M., Johnson, C. E., Connell, M. P. O., Leotlela, P. D., French, A. D., et al. (2008). The Wnt5A/protein kinase C pathway mediates motility in melanoma cells via the inhibition of metastasis suppressors and initiation of an epithelial to mesenchymal transition. *J Biol Chem*, *282*(23), 17259-17271.

Dovey, M., White, R. M., and Zon, L. I. (2009). Oncogenic NRAS cooperates with p53 loss to generate melanoma in zebrafish. *Zebrafish*, *6*(4), 397-404.

Eilers, M., and Eisenman, R. N. (2008). Myc's broad reach. *Genes and Development*, 2755-2766.

Eilers, M., Picard, D., Yamamoto, K. R., Bishop, J. M.(1989). Chimaeras of myc oncoprotein and steroid receptors cause hormone-dependent transformation of cells. *Nature*. Jul 6;340(6228):66-8.

Eischen, C. M., Weber, J. D., Roussel, M. F., Sherr, C. J., Cleveland, J. L. 1999. Disruption of the ARF-Mdm2-p53 tumor suppressor pathway in Myc-induced lymphomagenesis. *Genes Dev.* 13 2658–2669.

Eischen, C. M., Woo, D., and Roussel, M. F. (2001). Apoptosis Triggered by Myc-Induced Suppression of Bcl-X L or Bcl-2 Is Bypassed during Lymphomagenesis. *Society*, *21*(15), 5063-5070.

Emuss, V., Garnett, M., Mason, C., and Marais, R. (2005). Mutations of C-RAF are rare in human cancer because C-RAF has a low basal kinase activity compared with B-RAF. *Cancer research*, *65*(21), 9719-26.

Estep, A. L., Palmer, C., McCormick, F., and Rauen, K. A.. (2007). Mutation analysis of BRAF, MEK1 and MEK2 in 15 ovarian cancer cell lines: implications for therapy. *PloS one*, *2*(12), e1279.

Evan, G. I., Wyllie, A. H., Gilbert, S., Littlewood, T. D., Land, Hartmut, Brooks, M., et al. (1992). Induction of Apoptosis by c-myc Protein in Fibroblasts. *Cell*, *69*, 119-128.

Fecher, L. A., Amaravadi, R. K., and Flaherty, K. T. (2008). The MAPK pathway in melanoma. *Current opinion in oncology*, *20*(2), 183-9.

Feil, R., Brocard, J., Mascrez, B., LeMeur, M., Metzger, D., and Chambon, P. (1996). Ligand-activated site-specific recombination in mice. *Proceedings of the National Academy of Sciences of the United States of America*, *93*(20), 10887-90.

Feng, H., Langenau, D. M., Madge, J. A., Quinkertz, A., Gutierrez, A., Neuberg, D. S., Kanki, J. P., Look, A. T. (2007). Heat-shock induction of T-cell lymphoma/leukaemia in conditional Cre/lox-regulated transgenic zebrafish. *Br J Haematol*. Jul;138(2):169-75.

Ferbeyre, G., and Moriggl, R. (2011). The role of Stat5 transcription factors as tumor suppressors or oncogenes. *Biochimica et biophysica acta*, *1815*(1), 104-14.

Field, J., Nikawa, J., Broek, D., MacDonald, B., Rodgers, L., Wilson, I. a, et al. (1988). Purification of a RAS-responsive adenylyl cyclase complex from Saccharomyces cerevisiae by use of an epitope addition method. *Molecular and cellular biology*, *8*(5), 2159-65.

Flicek, P., Amode, M. R., Barrell, D., Beal, K., Brent, S., Chen, Yuan, et al. (2011). Ensembl 2011. *Nucleic acids research*, *39*(Database issue), D800-6.

Frank, S. R., Schroeder, M., Fernandez, P., Taubert, S., and Amati, B. (2001). Binding of c-Myc to chromatin mediates mitogen-induced acetylation of histone H4 and gene activation. *Genes and Development*, 2069-2082.

Fukushima, T., Suzuki, S., Mashiko, M., Ohtake, T., Endo, Y., Takebayashi, Y., et al. (2003). BRAF mutations in papillary carcinomas of the thyroid. *Oncogene*, *22*(41), 6455-7.

Furutani-Seiki, M., Sasado, T., Morinaga, C., Suwa, H., Niwa, K., Yoda, H., et al. (2004). A systematic genome-wide screen for mutations affecting organogenesis in Medaka, Oryzias latipes. *Mechanisms of development*, *121*(7-8), 647-58.

Garnett, M. J., and Marais, R. (2004). Guilty as charged: B-RAF is a human oncogene. *October*, *6*(October), 313-319.

Garraway, L. A., Widlund, H. R., Rubin, M. A., Getz, G., Berger, A. J., Ramaswamy, S., et al. (2005). Integrative genomic analyses identify MITF as a lineage survival oncogene amplified in malignant melanoma. *Nature*, *436*(7047), 117-22.

Gartel, A. L., Ye, X., Goufman, E., Shianov, P., Hay, N., Najmabadi, F., et al. (2001). Myc represses the p21(WAF1/CIP1) promoter and interacts with Sp1/Sp3. *Proc Natl Acad Sci U S A*, *21*.

Gear, H., Williams, H., Kemp, E. G., and Roberts, F. (2004). BRAF mutations in conjunctival melanoma. *Investigative ophthalmology and visual science*, *45*(8), 2484-8.

Gilchrest, B. A., Eller, M. S., Geller, A. C., Yaar, M. (1999). The pathogenesis of melanoma induced by ultraviolet radiation. *N Engl J Med.* Apr 29;340(17):1341-8.

Gómez, A., Wellbrock, C., Gutbrod, H., Dimitrijevic, N., and Schartl, M. (2001). Ligand-independent dimerization and activation of the oncogenic Xmrk receptor by two mutations in the extracellular domain. *The Journal of biological chemistry*, *276*(5), 3333-40.

Gómez, A., Volff, J. N., Hornung, U., Schartl, M., Wellbrock, C. (2004). Identification of a second egfr gene in Xiphophorus uncovers an expansion of the epidermal growth factor receptor family in fish. *Mol Biol Evol.* Feb;21(2):266-75.

Gordon, M. (1947). Melanomas in the hybrid offspring of two species of swordtails, Xiphophorus montezumae and Xiphophorus hellerii. *Anat Rec.* Dec;99(4):613.

Gouilleux, F, Wakao, H., Mundt, M., and Groner, B. (1994). Prolactin induces phosphorylation of Tyr694 of Stat5 (MGF), a prerequisite for DNA binding and induction of transcription. *The EMBO journal*, *13*(18), 4361-9.

Grabher, C., and Wittbrodt, J. (2007). Meganuclease and transposon mediated transgenesis in medaka. *Genome Biology*, *8*(Suppl 1), 1-7.

Grandori, C., Cowley, S. M., James, L. P., and Eisenman, R. N. (2000). The Myc/Max/Mad network and the transcriptional control of cell behavior. *Annu Rev Cell Dev Biol*. 16:653-99.

Gray-schopfer, V., Wellbrock, C. and Marais, R. (2007). Melanoma biology and new targeted therapy. *Nature*. Feb 22;445(7130):851-7.

Gregory, M. A., Hann, S. R. (2000). c-Myc proteolysis by the ubiquitin-proteasome pathway: stabilization of c-Myc in Burkitt's lymphoma cells. *Mol Cell Biol*. Apr;20(7):2423-35.

Guldberg, P., Straten, P., and Birck, A. (1997). Disruption of the MMAC1/PTEN Gene by Deletion or Mutation Is a Frequent Event in Malignant Melanoma. *Cancer Research*, 3660-3663.

Gupta, S., and Davis, R. J. (1994). MAP kinase binds to the NH2-terminal activation domain of c-Myc. *FEBS letters*, *353*(3), 281-5.

Gutierrez, A., Grebliunaite, R., Feng, H., Kozakewich, E., Zhu, S., Guo, F., et al. (2011). Pten mediates Myc oncogene dependence in a conditional zebrafish model of T cell acute lymphoblastic leukemia. *The Journal of experimental medicine*. Aug 1;208(8):1595-603.

Hall, T. A. (1999). BioEdit a user-friendly biological sequence alignment editor and analysis. *Nucleic Acids Symposium Series*, Vol. 41 (1999), pp. 95-98

Hallsson, J. H., Haflidadóttir, B. S., Stivers, C., Odenwald, W., Arnheiter, H., Pignoni, F., et al. (2004). The basic helix-loop-helix leucine zipper transcription factor Mitf is conserved in Drosophila and functions in eye development. *Genetics*, *167*(1), 233-41.

Hassel, J. C., Fischer, P., Becker, J., Vetter, C. S., Behrmann, I., and Schartl, M.. (2005). STAT5 Contributes to Interferon Resistance of Melanoma Cells. *Current Biology*, *15*, 1629-1639.

Hassel, J. C., Winnemo, D., Schartl, M., and Wellbrock, C. (2008). STAT5 contributes to antiapoptosis in melanoma. *Melanoma Research*, 378-385.

Heindryckx, F., Colle, I., and Van Vlierberghe, H. (2009). Experimental mouse models for hepatocellular carcinoma research. *International journal of experimental pathology*, *90*(4), 367-86.

Hermeking, H., Rago, C., Schuhmacher, M., Li, Q., Barrett, J. F., Obaya, a J., et al. (2000). Identification of CDK4 as a target of c-MYC. *Proceedings of the National Academy of Sciences of the United States of America*, *97*(5), 2229-34.

Hirobe, T. (2011). How are proliferation and differentiation of melanocytes regulated? *Pigment Cell Melanoma Res*. Jun;24(3):462-78.

Hoeflich, K. P., Gray, D. C., Eby, M. T., Tien, J. Y., Wong, L., Bower, J., et al. (2006). Oncogenic BRAF is required for tumor growth and maintenance in melanoma models. *Cancer research*, *66*(2), 999-1006.

Hoek, K., Rimm, D. L., Williams, K. R., Zhao, H., Ariyan, S., Lin, A., et al. (2004). Expression profiling reveals novel pathways in the transformation of melanocytes to melanomas. *Cancer research*, *64*(15), 5270-82.

Ito, S., Wakamatsu, K. (2003). Quantitative analysis of eumelanin and pheomelanin in humans, mice, and other animals: a comparative review. *Pigment Cell Res.* Oct;16(5):523-31.

Iwamatsu, T. (2004). Stages of normal development in the medaka Oryzias latipes. *Mech Dev.*, *121*, 605-618.

Izumi, H., Molander, C., Penn, L Z, Ishisaki, a, Kohno, K., and Funa, K. (2001). Mechanism for the transcriptional repression by c-Myc on PDGF beta-receptor. *Journal of cell science*, *114*(Pt 8), 1533-44.

Jacobs, J. J., Scheijen, B., Voncken, J. W., Kieboom, K., Berns, a, and Lohuizen, M. van. (1999). Bmi-1 collaborates with c-Myc in tumorigenesis by inhibiting c-Myc-induced apoptosis via INK4a/ARF. *Genes and development*, *13*(20), 2678-90.

Jin, Z., Gao, F., Flagg, T., and Deng, X. (2004). Tobacco-specific nitrosamine 4-(methylnitrosamino)-1-(3-pyridyl)-1-butanone promotes functional cooperation of Bcl2 and c-Myc through phosphorylation in regulating cell survival and proliferation. *The Journal of biological chemistry*, *279*(38), 40209-19.

Junttila, M. R., Westermarck, J. (2008). Mechanisms of MYC stabilization in human malignancies. *Cell Cycle.* Mar 1;7(5):592-6.

Karasarides, M., Chiloeches, A., Hayward, R., Niculescu-Duvaz, D., Scanlon, I., Friedlos, F., et al. (2004). B-RAF is a therapeutic target in melanoma. *Oncogene*, *23*(37), 6292-8.

Kawakami, K. (2005). Transposon tools and methods in zebrafish. *Developmental dynamics : an official publication of the American Association of Anatomists*, *234*(2), 244-54.

Klapproth, K., and Wirth, T. (2010). Advances in the understanding of MYC-induced lymphomagenesis. *British journal of haematology*, *149*(4), 484-97.

Kligman, L. H., Elenitsas, R. (2001). Melanoma induction in a hairless mouse with short-term application of dimethylbenz[a]anthracene. *Melanoma Res*. 11:319–324.

Knauf, J. A., Ma, X., Smith, E. P., Zhang, L., Mitsutake, N., Liao, X.-H., et al. (2005). Targeted expression of BRAFV600E in thyroid cells of transgenic mice results in papillary thyroid cancers that undergo dedifferentiation. *Cancer research*, *65*(10), 4238-45.

Kolch, W. (2000). Meaningful relationships: the regulation of the Ras/Raf/MEK/ERK pathway by protein interactions. *The Biochemical journal*, *351 Pt 2*, 289-305.

Kraehn, G. M., Utikal, J., Udart, M., Greulich, K. M., Bezold, G., Kaskel, P., et al. (2001). Extra c-myc oncogene copies in high risk cutaneous malignant melanoma and melanoma metastases. *British journal of cancer*, *84*(1), 72-9.

Kusewitt, D. F., Applegate, L. A., and Ley, R.D. (1991). Ultroviolet radiation-induced skin tumors in a south American opossum (*Monodelphis domestica*).*Vet. Pathol.* 28:55-65.

Lai, S. Y., Johnson, F. M. (2010). Defining the role of the JAK-STAT pathway in head and neck and thoracic malignancies: implications for future therapeutic approaches. *Drug Resist Updat*. Jun;13(3):67-78.

Lakin, N. D., Boardman, M., and Woodland, H. R. (1993). Determination of the sequence requirements for the expression of a Xenopus borealis embryonic/larval skeletal actin gene. *European journal of biochemistry / FEBS*, *214*(2), 425-35.

Lang, R. A.. (2004). Pathways regulating lens induction in the mouse. *The International journal of developmental biology*, *48*(8-9), 783-91.

Langenau, D. M., Ferrando, A. A., Traver, D., Kutok, J. L., Hezel, J.-P. D., Kanki, J. P., et al. (2004). In vivo tracking of T cell development, ablation, and engraftment in transgenic zebrafish. *Proceedings of the National Academy of Sciences of the United States of America*, *101*(19), 7369-74.

Langenau, D. M., Traver, D., Ferrando, A. a, Kutok, J. L., Aster, J. C., Kanki, J. P., et al. (2003). Myc-induced T cell leukemia in transgenic zebrafish. *Science*. *299*(5608), 887-90.

Larsson, L.-G., and Henriksson, M. A. (2010). The Yin and Yang functions of the Myc oncoprotein in cancer development and as targets for therapy. *Experimental cell research*, *316*(8), 1429-37.

Lee, J. W., Soung, Y. H., Kim, S. Y., Park, W. S., Nam, S. W., Min, W. S., et al. (2005). Mutational analysis of the ARAF gene in human cancers. *APMIS : acta pathologica, microbiologica, et immunologica Scandinavica*, *113*(1), 54-7.

Levy, C., Khaled, M., and Fisher, D. E. (2006). MITF: master regulator of melanocyte development and melanoma oncogene. *Trends in molecular medicine*, *12*(9), 406-14.

Lewis, R. S., Stephenson, S. E. M., and Ward, A. C. (2006). Constitutive activation of zebra sh Stat5 expands hematopoietic cell populations in vivo. *Experimental Hematology*, *34*, 179-187.

Lewis, R. S., and Ward, A. C. (2004). Conservation, duplication and divergence of the zebrafish stat5 genes. *Gene*, *338*, 65 - 74.

Li, G., Schaider, H., Satyamoorthy, K., Hanakawa, Y., Hashimoto, K., and Herlyn, M. (2001). Downregulation of E-cadherin and Desmoglein 1 by autocrine hepatocyte growth factor during melanoma development. *Oncogene*, *20*(56), 8125-35.

Lim, C. P., and Cao, X. (2006). Structure, function, and regulation of STAT proteins{. *Signal Transduction*, (August), 536-550.

Lister, J. A., Robertson, C. P., Lepage, T., Johnson, S. L., Raible, D. W. (1999). Nacre encodes a zebrafish microphthalmia-related protein that regulates neural-crest-derived pigment cell fate. *Development*. 126:3757–3767

Liu, X., Robinson, G. W., Gouilleux, F., Groner, B., and Hennighausen, L. (1995). Cloning and expression of Stat5 and an additional homologue (Stat5b) involved in prolactin signal transduction in mouse mammary tissue. *Proceedings of the National Academy of Sciences of the United States of America*, *92*(19), 8831-5.

Liu, X., Robinson, G. W., Wagner, K. U., Garrett, L., Wynshaw-Boris, A., and Hennighausen, L. (1997). Stat5a is mandatory for adult mammary gland development and lactogenesis. *Genes and Development*, *11*(2), 179-186.

Liu, Z. J., Xiao, M., Balint, K., Smalley, K. S. M., Brafford, P., Qiu, R., et al. (2006). Notch1 signaling promotes primary melanoma progression by activating mitogen-activated protein kinase/phosphatidylinositol 3-kinase-Akt pathways and up-regulating N-cadherin expression. *Cancer research*, *66*(8), 4182-90.

Lutz, W., Leon, J., and Eilers, M.. (2002). Contributions of Myc to tumorigenesis. *Biochimica et biophysica acta*, *1602*(1), 61-71.

Lynn Lamoreux, M., Kelsh, R. N., Wakamatsu, Y., and Ozato, K. (2005). Pigment pattern formation in the medaka embryo. *Pigment cell research*. *18*(2), 64-73.

Lüscher, B. (2001). Function and regulation of the transcription factors of the Myc/Max/Mad network. *Gene*, *277*(1-2), 1-14.

Lüscher, B., and Larsson, L.-G. (1999). The basic region / helix - loop - helix / leucine zipper domain of Myc proto-oncoproteins : Function and regulation. *Oncogene*, 2955-2966.

Maddodi, N. and Setaluri, V. (2008). Role of UV in cutaneous melanoma. *Photochemistry and photobiology*, *84*(2), 528-36.

Mao, D. Y., Watson, J. D., Yan, P. S., Barsyte-lovejoy, D., Khosravi, F., Wong, W. W., et al. (2003). Analysis of Myc Bound Loci Identified by CpG Island Arrays Shows that Max Is Essential for Myc-Dependent Repression. *Current*, *13*, 882-886.

Mason, C. S., Springer, C J, Cooper, R. G., Superti-Furga, G., Marshall, C J, and Marais, R. (1999). Serine and tyrosine phosphorylations cooperate in Raf-1, but not B-Raf activation. *The EMBO journal*, *18*(8), 2137-48.

McMahon, S. B., Van Buskirk, H. a, Dugan, K. a, Copeland, T. D., and Cole, M. D. (1998). The novel ATM-related protein TRRAP is an essential cofactor for the c-Myc and E2F oncoproteins. *Cell*, *94*(3), 363-74.

Meierjohann, S., and Schartl, M.. (2006). From Mendelian to molecular genetics: the Xiphophorus melanoma model. *Trends in genetics : TIG*, *22*(12), 654-61.

Meierjohann, S., Schartl, M., and Volff, J.-N. (2004). Genetic, biochemical and evolutionary facets of Xmrk-induced melanoma formation in the fish Xiphophorus. *Comparative biochemistry and physiology. Toxicology and pharmacology : CBP*, *138*(3), 281-9.

Mercer, K., Giblett, S., Green, S., Lloyd, D., DaRocha Dias, S., Plumb, M., et al. (2005). Expression of endogenous oncogenic V600EB-raf induces proliferation and developmental defects in mice and transformation of primary fibroblasts. *Cancer research*, *65*(24), 11493-500.

Meredith, P., Sarna, T. (2006). The physical and chemical properties of eumelanin. *Pigment Cell Res*. Dec;19(6):572-94.

Meyer, N., and Penn, L. Z. (2008). Reflecting on 25 years with MYC. *Nat. Rev. Cancer*. Dec;8(12):976-90.

Michaloglou, C. (2008). BRAF E600 in benign and malignant human tumours. *Oncogene*, 877-895.

Michailidou, C., Jones, M., Walker, P., Kamarashev, J., Kelly, A., and Hurlstone, A. F. L. (2009). Dissecting the roles of Raf- and PI3K-signalling pathways in melanoma formation and progression in a zebrafish model. *Disease models and mechanisms*, *2*(7-8), 399-411.

Michaloglou, C., Vredeveld, L. C., Soengas, M. S., Denoyelle, C., Kuilman, T., van der Horst, C. M., Majoor, D. M., Shay, J. W., Mooi, W. J., Peeper, D. S. (2005). BRAFE600-associated senescence-like cell cycle arrest of human naevi. *Nature*. Aug 4;436(7051):720-4.

Mikkola, I., Bruun, J. A., Bjorkoy, G., Holm, T., and Johansen, T. (1999). Phosphorylation of the transactivation domain of Pax6 by extracellular signal-regulated kinase and p38 mitogen-activated protein kinase. *The Journal of biological chemistry*, *274*(21), 15115-26.

Mikula, M., Schreiber, M., Husak, Z., Kucerova, L., Rüth, J., Wieser, R., et al. (2001). Embryonic lethality and fetal liver apoptosis in mice lacking the c-raf-1 gene. *The EMBO journal*, *20*(8), 1952-62.

Mione, M. C., Trede, N. S. (2010). The zebrafish as a model for cancer. *Dis Model Mech*. Sep-Oct;3(9-10):517-23.

Mirmohammadsadegh, A., Hassan, M., Bardenheuer, W., Marini, A., Gustrau, A., Nambiar, S., et al. (2006). STAT5 phosphorylation in malignant melanoma is important for survival and is mediated through SRC and JAK1 kinases. *The Journal of investigative dermatology*, *126*(10), 2272-80.

Miyoshi, K., Cui, Y., Riedlinger, G., Robinson, P., Lehoczky, J., Zon, L., et al. (2001). Structure of the mouse Stat 3/5 locus: evolution from Drosophila to zebrafish to mouse. *Genomics*, *71*(2), 150-5.

Morcinek, J. C., Weisser, C., Geissinger, E., and Schartl, M. (2002). Activation of STAT5 triggers proliferation and contributes to anti-apoptotic signalling mediated by the oncogenic Xmrk kinase. *Oncogene*, 1668-1678.

Moriggl, R., Gouilleux-gruart, V., Jähne, R., Berchtold, S., Gartmann, C., Xiuwen, L. et al. (1996). Deletion of the Carboxyl-Terminal Transactivation Domain of MGF-Stat5 Results in Sustained DNA Binding and a Dominant Negative Phenotype. *Mol. Cel. Biol.*, *16*(10), 5691-5700.

Murphy, D. J., Junttila, M. R., Pouyet, L., Karnezis, A., Shchors, K., Bui, D. a, et al. (2008). Distinct thresholds govern Myc`s biological output in vivo. *Cancer cell*, *14*(6), 447-57.

Nakajima, H., Brindle, P. K., Handa, M., and Ihle, J. N. (2001). Functional interaction of STAT5 and nuclear receptor co-repressor SMRT: implications in negative regulation of STAT5 dependent transcription. *The EMBO journal*, *20*(23), 6836-44.

Nasevicius, A., Ekker, S. C. (2000). Effective targeted gene "knockdown" in zebrafish. *Nature genetics*, *26*(2), 216-20.

Nazarian, R., Shi, H., Wang, Q., Kong, X., Koya, R. C., Lee, H., Chen, Z., Lee, M. K., Attar, N., Sazegar, H., et al. (2010). Melanomas acquire resistance to B-RAF(V600E) inhibition by RTK or N-RAS upregulation. *Nature*. Dec 16;468(7326):973-7.

Nesbit, C. E., Tersak, J. M., and Prochownik, E V. (1999). MYC oncogenes and human neoplastic disease. *Oncogene*, *18*(19), 3004-16.

Netscher, D. T., Leong, M., Orengo, I., Yang, D., Berg, C. and Krishnan, B. (2011). Cutaneous malignancies: melanoma and nonmelanoma types. *Plastic and reconstructive surgery*, *127*(3), 37e-56e.

Nguyen, A. T., Emelyanov, A., Koh, C. H. V., Spitsbergen, J. M., Lam, S. H., Mathavan, S., et al. (2011). A high level of liver-specific expression of oncogenic KrasV12 drives robust liver tumorigenesis in transgenic zebrafish. *Disease models and mechanisms*. Jul 4.

Nilsson, J. A., and Cleveland, J. L. (2003). Myc pathways provoking cell suicide and cancer. *Oncogene*, *22*(56), 9007-21.

Nobori, T., Miura, K., Wu, D. J., Lois, A., Takabayashi, K., Carson, D. A. (1994). Deletions of the cyclin-dependent kinase-4 inhibitor gene in multiple human cancers. *Nature*. Apr 21;368(6473):753-6.

Nowak, M. a, Boerlijst, M. C., Cooke, J., and Smith, J. M. (1997). Evolution of genetic redundancy. *Nature*, *388*(6638), 167-71.

Onishi, M., Nosaka, T., Misawa, K., Mui, A. L., Gorman, D., Mcmahon, M., et al. (1998). Identification and characterization of a constitutively active STAT5 mutant that promotes cell proliferation. *Mol. Cell Biol.*, *18*, 3871-3879.

Palmer, J. S., Duffy, D. L., Box, N. F., Aitken, J. F., O`Gorman, L. E., Green, A. C., et al. (2000). Melanocortin-1 receptor polymorphisms and risk of melanoma: is the association explained solely by pigmentation phenotype? *American journal of human genetics*, *66*(1), 176-86.

Parichy, D. M. (2006). Evolution of danio pigment pattern development. *Heredity*, *97*(3), 200-10.

Pascal, A., Riou, J. F., Carron, C., Boucaut, J. C., and Umbhauer, M. (2001). Cloning and developmental expression of STAT5 in Xenopus laevis. *Mechanisms of development*, *106*(1-2), 171-4.

Patel, J. H., Du, Y., Ard, P. G., Phillips, C., Carella, B., Chen, C. J., Rakowski, C., Chatterjee, C., Lieberman, P. M., Lane, W. S., Blobel, G. A., McMahon, S. B. (2004). The c-MYC oncoprotein is a substrate of the acetyltransferases hGCN5/PCAF and TIP60. *Mol Cell Biol*. Dec;24(24):10826-34.

Patrick, R. J., Fenske, N. A. and Messina, J. L. (2007). Primary mucosal melanoma. *Journal of the American Academy of Dermatology*, *56*(5), 828-34.

Patton, E. E., and Zon, L. I. (2001). The art and design of genetic screens: zebrafish. *Nature reviews. Genetics*, *2*(12), 956-66.

Patton, E. E., Mitchell, D. L., and Nairn, R. S. (2010). Genetic and environmental melanoma models in fish. *Pigment cell and melanoma research*, *23*(3), 314-37.

Patton, E. E., Widlund, H. R., Traver, D., and Fletcher, C. D. M. (2005). BRAF Mutations Are Sufficient to Promote Nevi Formation and Cooperate with p53 in the Genesis of Melanoma. *Current*, *15*, 249-254.

Paukku, K., and Silvennoinen, O. (2004). STATs as critical mediators of signal transduction and transcription: lessons learned from STAT5. *Cytokine and Growth Factor Reviews*, *15*, 435-455.

Pelengaris, S., Littlewood, T., Khan, M., Elia, G., and Evan, G. I. (1999). Reversible activation of c-Myc in skin: induction of a complex neoplastic phenotype by a single oncogenic lesion. *Molecular cell*, *3*(5), 565-77.

Pelengaris, S., Khan, M., and Evan, G. I. (2002). Suppression of Myc-induced apoptosis in beta cells exposes multiple oncogenic properties of Myc and triggers carcinogenic progression. *Cell*, *109*(3), 321-34.

Pelengaris, S., Khan, M., and Evan, G. I. (2002). c-MYC : more than just a matter of life and death. *Nature*, *2*(October), 764-776.

Pere-Roger, I., Kim, S. H., Griffiths, B., Sewing, A., and Land, H. (1999). Cyclins D1 and D2 mediate myc-induced proliferation via sequestration of p27(Kip1) and p21(Cip1). *The EMBO journal*, *18*(19), 5310-20.

Peukert, K, Staller, P, Schneider, a, Carmichael, G., Hänel, F, and Eilers, M. (1997). An alternative pathway for gene regulation by Myc. *The EMBO journal*, *16*(18), 5672-86.

Pollock, P. M., and Hayward, N. (2002). Mutations in exon 3 of the beta-catenin gene are rare in melanoma cell lines. *Melanoma research*, *12*(2), 183-6.

Pollock, P. M, Harper, U. L., Hansen, K. S., Yudt, L. M., Stark, M., Robbins, C. M., et al. (2003). High frequency of BRAF mutations in nevi. *Nature genetics*, *33*(1), 19-20.

Polsky, D., and Cordon-Cardo, C. (2003). Oncogenes in melanoma. *Oncogene*, *22*(20), 3087-91.

Pritchard, C. A., Bolin, L., Slattery, R., Murray, R., and McMahon, M. (1996). Post-natal lethality and neurological and gastrointestinal defects in mice with targeted disruption of the A-Raf protein kinase gene. *Current biology. 6*(5), 614-7.

Qin, J. Z., Stennett, L., Bacon, P., Bodner, B., Hendrix, M. J. C., Seftor, R. E. B., et al. (2004). p53-independent NOXA induction overcomes apoptotic resistance of malignant melanomas. *Molecular cancer therapeutics*, *3*(8), 895-902.

Rimoldi, D., Salvi, S., Liénard, D., Lie, D., Lejeune, F. J., Speiser, D., et al. (2003). Lack of BRAF Mutations in Uveal Melanoma Lack of BRAF Mutations in Uveal Melanoma. *Cancer Research*, 5712-5715.

Robinson, M. J., and Cobb, M. H. (1997). Mitogen-activated protein kinase pathways. *Curr Opin Cell Biol*. Apr;9(2):180-6.

Ross, D. A., and Wilson, G. D. (1998). Expression of c-myc oncoprotein represents a new prognostic marker in cutaneous melanoma. *The British journal of surgery*, *85*(1), 46-51.

Ryan, K. M., and Birnie, G. D. (1996). Myc oncogenes: the enigmatic family. *The Biochemical journal*, *314 (Pt 3*, 713-21.

Sambrook, J., Fritsch, E.F., and Maniatis, T. (1989). Molecular Cloning: a laboratory manual. 2nd ed. N.Y., *Cold Spring Harbor Laboratory, Cold Spring Harbor Laboratory Press*. 1659 p. ISBN 0-87969-309-6

Santoni-Rugiu, E., Preisegger, K. H., Kiss, a, Audolfsson, T., Shiota, G., Schmidt, E. V., et al. (1996). Inhibition of neoplastic development in the liver by hepatocyte growth factor in a transgenic mouse model. *Proceedings of the National Academy of Sciences of the United States of America*, *93*(18), 9577-82.

Santoriello, C., Gennaro, E., Anelli, V., Distel, M., Kelly, A., Köster, R. W., et al. (2010). Kita driven expression of oncogenic HRAS leads to early onset and highly penetrant melanoma in zebrafish. *PloS one*, *5*(12), e15170.

Santos, C. I., and Costa-Pereira, A. P. (2011). Signal transducers and activators of transcription-from cytokine signalling to cancer biology. *Biochimica et biophysica acta*, *1816*(1), 38-49.

Schartl, M., Hornung, U., Gutbrod, H., Volff, J. N., and Wittbrodt, J. (1999). Melanoma loss-of-function mutants in Xiphophorus caused by Xmrk-oncogene deletion and gene disruption by a transposable element. *Genetics*, *153*(3), 1385-94.

Schartl, M., Wilde, B., Laisney, J. A., Taniguchi, Y., Takeda, S., and Meierjohann, S. (2010). A mutated EGFR is sufficient to induce malignant melanoma with genetic background-dependent histopathologies. *The Journal of investigative dermatology*, *130*(1), 249-58.

Schlagbauer-Wadl, H., Griffioen, M., Elsas, A. van, Schrier, P. I., Pustelnik, T., Eichler, H. G., et al. (1999). Influence of increased c-Myc expression on the growth characteristics of human melanoma. *The Journal of investigative dermatology*, *112*(3), 332-6.

Schreiber-Agus, Nicole. Horner, Jim. Torres, Richerd. Chiu, Fung-Chow. DePinho, R. A. (1993). Zebra Fish myc Family and max Genes: Differential Expression and Oncogenic Activity throughout Vertebrate Evolution. *Microbiology*, *13*(5), 2765-2775.

Sears, R. C. (2004). The life cycle of C-myc: from synthesis to degradation.. *Cell Cycle*, Sep;3(9):1133-7.

Sears, R., Nuckolls, F., Haura, E., Taya, Y., Tamai, K., and Nevins, J. R. (2000). Multiple Ras-dependent phosphorylation pathways regulate Myc protein stability. *Genes and Development*. Oct 1;14(19):2501-14.

Sharma, S. G., and Gulley, M. L. (2010). BRAF mutation testing in colorectal cancer. *Archives of pathology and laboratory medicine*, *134*(8), 1225-8.

Sharma, A., Tran, M. A., Liang, S., Sharma, A. K., Amin, S., Smith, C. D., Dong, C., Robertson, G. P. (2006). Targeting mitogen-activated protein kinase/extracellular signal-regulated kinase in the mutant (V600E) B-Raf signaling cascade effectively inhibits melanoma lung metastases. *Cancer Res*. Aug 15;66(16):8200-9.

Shima, A., and Mitani, H. (2004). Medaka as a research organism: past, present and future. *Mechanisms of Development*, *121*, 599-604.

Smalley, K. S. M. (2009). Understanding Melanoma Signaling Networks as the Basis for Molecular Targeted Therapy. *Journal of Investigative Dermatology*, (April), 1-10.

Snow, J. W., Abraham, N., Ma, M. C., Herndier, B. G., Pastuszak, A. W., and Goldsmith, M. a. (2003). Loss of tolerance and autoimmunity affecting multiple organs in STAT5A/5B-deficient mice. *Journal of immunology. 171*(10), 5042-50.

Socolovsky, M., Fallon, A. E., Wang, S., Brugnara, C., and Lodish, H. F. (1999). Fetal anemia and apoptosis of red cell progenitors in Stat5a-/-5b-/- mice: a direct role for Stat5 in Bcl-X(L) induction. *Cell*, *98*(2), 181-91.

Solit, D. B., Garraway, L. a, Pratilas, C. a, Sawai, A., Getz, G., Basso, A., et al. (2006). BRAF mutation predicts sensitivity to MEK inhibition. *Nature*, *439*(7074), 358-62.

Spencer, C. A., Groudine, M. (1991). Control of c-myc regulation in normal and neoplastic cells. *Adv Cancer Res*. 56:1-48.

Steiner, P., Philipp, a, Lukas, J., Godden-Kent, D., Pagano, M., Mittnacht, S., et al. (1995). Identification of a Myc-dependent step during the formation of active G1 cyclin-cdk complexes. *The EMBO journal*, *14*(19), 4814-26.

Steingrímsson, E., Copeland, N. G. and Jenkins, N. A. (2004). Melanocytes and the microphthalmia transcription factor network. *Annual review of genetics*, *38*, 365-411.

Staller, P., Peukert, K., Kiermaier, A., Seoane, J., Lukas, Ji, Karsunky, H., et al. (2001). Repression of p15 INK4b expression by Myc through association with Miz-1. *Cell*. May 3;109(3):321-34.

Stoletov K, Klemke R. (2008). Catch of the day: zebrafish as a human cancer model. *Oncogene,* Jul 31;27(33):4509-20.

Storm, S. M., Cleveland, J. L., Rapp, U. R. (1990). Expression of raf family proto-oncogenes in normal mouse tissues. Oncogene. Mar;5(3):345-51.

Strasser, A., Harris, A. W., Bath, M. L., and Cory, S. (1990). Novel primitive lymphoid tumours induced in transgenic mice by cooperation between myc and bcl-2. *Nature*. Nov 22;348(6299):331-3.

Strickland, F. M., Muller, H. K., Stephens, L. C., Bucana, C. D., Donawho, C. K., Sun, Y. et al. (2000). Induction of primary cutaneous melanomas in C3H mice by combined treatment with ultraviolet radiation, ethanol and aloe emodin. *Photochem Photobiol*. 72:407–414.

Sung, S.-C., Fan, T.-J., Chou, C.-M., Leu, J.-H., Hsu, Y.-L., Chen, S.-T., et al. (2003). Genomic structure, expression and characterization of a STAT5 homologue from pufferfish (Tetraodon fluviatilis). *European Journal of Biochemistry*, *270*(2), 239-252.

Takeda, H., and Shimada, A. (2010). The art of medaka genetics and genomics: what makes them so unique? *Annual review of genetics*, *44*, 217-41.

Tan, S.-H., and Nevalainen, M. T. (2008). Signal transducer and activator of transcription 5A/B in prostate and breast cancers. *Endocrine-Related Cancer*. 15, 367-390.

Taniguchi, Y., Takeda, S., Furutani-Seiki, M., Kamei, Y., Todo, T., Sasado, T., et al. (2006). Generation of medaka gene knockout models by target-selected mutagenesis. *Genome biology*, *7*(12), R116.

Thermes, V., Grabher, C., Ristoratore, F., Bourrat, F., and Wittbrodt, J. (2002). I-SceI meganuclease mediates highly efficient transgenesis in fish. *Mechanisms of Development*, *118*, 91-98.

Thomas P. Hopp, Kathryn S. Prickett, Virginia L. Price, Randell T. Libby, Carl J. March, Douglas Pat Cerretti, D. L. U. and P. J. C. (1988). A Short Polypeptide Marker Sequence Useful for Recombinant Protein Identification and Purification. *Nature*, *6*, 1088-1204.

Thomas, A. J. and Erickson, C. A. (2008). The making of a melanocyte: the specification of melanoblasts from the neural crest. *Pigment cell and melanoma research*, *21*(6), 598-610.

Thomas, N. E. (2006). BRAF somatic mutations in malignant melanoma and melanocytic naevi. *Melanoma research*, *16*(2), 97-103.

Thompson, J. D., Higgins, D. G., and Gibson, T. J. (1994). CLUSTAL W: improving the sensitivity of progressive multiple sequence alignment through sequence weighting, position-specific gap penalties and weight matrix choice. *Nucleic acids research*, *22*(22), 4673-80.

Tian, Y., James, S., Zuo, J., Fritzsch, B., and Beisel, K. W. (2006). Conditional and inducible gene recombinering in the mouse inner ear. *Brain Res*. May 26;1091(1):243-54.

Triozzi, P. L., Eng, C. and Singh, A. D. (2008). Targeted therapy for uveal melanoma. *Cancer treatment reviews*, *34*(3), 247-58.

Trumpp, A., Refaeli, Y., Oskarsson, T., Gasser, S., Murphy, M., Martin, G. R., et al. (2001). c-Myc regulates mammalian body size by controlling cell number but not cell size. *Nature*, *414*(6865), 768-73.

Tsai, J., Lee, J. T., Wang, W., Zhang, Jiazhong, Cho, H., Mamo, S., et al. (2008). Discovery of a selective inhibitor of oncogenic B-Raf kinase with potent antimelanoma activity. *Proceedings of the National Academy of Sciences of the United States of America*, *105*(8), 3041-6.

Udy, G. B., Towers, R. P., Snell, R. G., Wilkins, R. J., Park, S. H., Ram, P. A., et al. (1997). Requirement of STAT5b for sexual dimorphism of body growth rates and liver gene expression. *Proceedings of the National Academy of Sciences of the United States of America*, *94*(14), 7239-44.

Uong, A., Zon, L. I. (2010). Melanocytes in development and cancer. *J Cell Physiol*. Jan;222(1):38-41.

Vervoorts J, Lüscher-Firzlaff JM, Rottmann S, Lilischkis R, Walsemann G, Dohmann K, Austen M, Lüscher B. (2003). Stimulation of c-MYC transcriptional activity and acetylation by recruitment of the cofactor CBP. *EMBO Rep.* May;4(5):484-90.

Wagner, A. J., Meyers, C., Laimins, L. A., Hay, N. (1993). c-Myc induces the expression and activity of ornithine decarboxylase. *Cell Growth and Differentiation*, *4*(November), 879-883.

Wagner, K.-U., and Rui, H. (2008). Jak2/Stat5 signaling in mammogenesis, breast cancer initiation and progression. *Journal of mammary gland biology and neoplasia*, *13*(1), 93-103.

Wang, C., Tai, Y., Lisanti, M. P., and Liao, D. J. (2011). c-Myc induction of programmed cell death may contribute to carcinogenesis: A perspective inspired by several concepts of chemical carcinogenesis. *Cancer Biology and Therapy*, *11*(7), 615-626.

Wanzel, M., Herold, S., and Eilers, M. (2003). Transcriptional repression by Myc. *Trends in Cell Biology*, *13*(3), 146-150.

Watnick, R. S., Cheng, Y. N., Rangarajan, A., Ince, T. A., Weinberg, R. A. (2003) Ras modulates Myc activity to repress thrombospondin-1 expression and increase tumor angiogenesis. *Cancer Cell.* Mar;3(3):219-31.

Weis, S., Schartl, M., (1998). The macromelanophore locus and the melanoma oncogene Xmrk are separate genetic entities in the genome of Xiphophorus. *Genetics* 149, 1909–1920.

Wellbrock, C., Schartl, M. (1999). Multiple binding sites in the growth factor receptor Xmrk mediate binding to p59fyn, GRB2 and Shc. Eur. *J. Biochem*. 260, 275–283.

Wellbrock, C., Schartl, M. (2000). Activation of phosphatidylinositol 3- kinase by a complex of p59fyn and the receptor tyrosine kinase Xmrk is involved in malignant transformation of pigment cells. *Eur. J. Biochem*. 267, 3513–3522.

Wellbrock, C., Geissinger, E., Gómez, A., Fischer, P., Friedrich, K., and Schartl, M.. (1998). Signalling by the oncogenic receptor tyrosine kinase Xmrk leads to activation of STAT5 in Xiphophorus melanoma. *Oncogene*. Jun 11;16(23):3047-56.

Wellbrock, C., and Hurlstone, A. (2010). BRAF as therapeutic target in melanoma. *Biochemical pharmacology*, *80*(5), 561-7.

Wellbrock, C., Karasarides, M., and Marais, R. (2004). The raf proteins take centre stage. *Nat Rev Mol Cell Biol. Nov;5(11):875-85.*

Wellbrock, C., Weisser, C., Geissinger, E., Troppmair, J., Schartl, M., (2002). Activation of p59(Fyn) leads to melanocyte dedifferentiation by influencing MKP-1-regulated mitogen-activated protein kinase signal- ing. *J. Biol. Chem.* 277, 6443–6454.

Westermarck, J. (2010). Regulation of transcription factor function by targeted protein degradation: an overview focusing on p53, c-Myc, and c-Jun. *Methods Mol Biol.* 2010;647:31-6.

White, R. M., Cech, J., Ratanasirintrawoot, S., Lin, C. Y., Rahl, P. B., Burke, C. J., Langdon, E., Tomlinson, M. L., Mosher, J., Kaufman, C. *et al* (2011). DHODH modulates transcriptional elongation in the neural crest and melanoma. *Nature.* 2011 Mar 24;471(7339):518-22.

White, R. M. and Zon, L. I. (2008). Melanocytes in Development, Regeneration, and Cancer. *Cell.* Sep 11;3(3):242-52.

Wittbrodt J., Adam, D., Malitschek, B., Mäueler, W., Raulf, F., Telling, A., Robertson, S. M., Schartl, M. (1989). Novel putative receptor tyrosine kinase encoded by the melanoma-inducing Tu locus in Xiphophorus. *Nature.* Oct 5;341(6241):415-21.

Wittbrodt, J., Lammers, R., Malitschek, B., Ullrich, A., and Schartl, M. (1992). The Xmrk receptor tyrosine kinase is activated in Xiphophorus malignant melanoma. *The EMBO journal*, *11*(11), 4239-46.

Wittbrodt, J., Shima, A., and Schartl, M. (2001). Medaka — a model organism from the far east. *Nat Rev Genet. 2002 Jan;3(1):53-64.*

Wojnowski, L., Zimmer, A. M., Beck, T. W., Hahn, H., Bernal, R., Rapp, U.R., Zimmer. A. (1997). Endothelial apoptosis in Braf-deficient mice. *Nature.* Jul;16(3):293-7.

Woods, D., Parry, D., Cherwinski, H., Bosch, E., Lees, E., and Mahon, M. M. C. (1997). Raf-Induced Proliferation or Cell Cycle Arrest Is Determined by the Level of Raf Activity with Arrest Mediated by p21 Cip1. *Microbiology*, *17*(9), 5598-5611.

Wu, H., Goel, V., and Haluska, F. G. (2003). PTEN signaling pathways in melanoma. *Oncogene*, *22*(20), 3113-22.

Wu, X., Noh, S. J., Zhou, G., Dixon, J. E., and Guan, K. L. (1996). Selective activation of MEK1 but not MEK2 by A-Raf from epidermal growth factor-stimulated Hela cells. *The Journal of biological chemistry*, *271*(6), 3265-71.

Xing, M. (2005). BRAF mutation in thyroid cancer. *Endocrine-related cancer*, *12*(2), 245-62.

Yang, H., Higgins, B., Kolinsky, K., Packman, K., Go, Z., Iyer, R., Kolis, S., Zhao, S., Lee, R., Grippo, J. F. *et al* (2010). RG7204 (PLX4032), a selective BRAFV600E inhibitor, displays potent antitumor activity in preclinical melanoma models. *Cancer Res.* Jul 1;70(13):5518-27.

Yasumoto, K., Yokoyama, K., Shibata, K., Tomita, Y., Shibahara, S. (1994). Microphthalmia-associated transcription factor as a regulator for melanocyte-specific transcription of the human tyrosinase gene. *Mol. Cell. Biol*. 14:8058–8070.

Yokota, J., Tsunetsugu-Yokota, Y., Battifora, H., Le Fevre, C., and Cline, M. J. (1986). Alterations of myc, myb, and rasHa proto-oncogenes in cancers are frequent and show clinical correlation. *Science*. 231(4735), 261-5.

Yu, H., and Jove, R. (2004). The stats of cancer — new molecular targets come of age. *Nat Rev Cancer*, Feb;4(2):97-105.

Zeller, K. I., Jegga, A. G., Aronow, B. J., O`Donnell, K. a, and Dang, Chi V. (2003). An integrated database of genes responsive to the Myc oncogenic transcription factor: identification of direct genomic targets. *Genome biology*, *4*(10), R69.

Zhang, J. (2003). Evolution by gene duplication: an update. *Trends in Ecology and Evolution*, *18*(6), 292-298.

Zhang, K., Faiola, F., and Martinez, E. (2005). Six lysine residues on c-Myc are direct substrates for acetylation by p300. *Biochemical and biophysical research communications*, *336*(1), 274-80.

Zhu, J., Woods, D, McMahon, M, and Bishop, J. M. (1998). Senescence of human fibroblasts induced by oncogenic Raf. *Genes and development*, *12*(19), 2997-3007.

Zon, L. I, and Peterson, R. T. (2005). In vivo drug discovery in the zebrafish. *Nature reviews. Drug discovery*, *4*(1), 35-44.

7. APPENDIX
7.1 Abbreviation

Terms

4-OHT	4-Hydroxytamoxifen
BrdU	5-bromo-2`-deoxyuridine
ddH$_2$O	Deionized water
DN	Dominant negative
DNA	Deoxyribonucleic acid
DNTPs	Deoxynucleotides triphosphate
Fig.	Figure
IF	Immunefluorescence
IPTG	Isopropyl β-D-1-thiogalactopyranoside
I-SceI	meganuclease
NaCl	sodium chloride
ON	overnight
PFA	paraformaldehyde
RNA	Ribonucleic acid
rpm	Rotations per min
RT	Room temperature
SDS	sodium dodecyl sulfate
UV	ultraviolet
WB	Western blot
X-gal	5-bromo-4-chloro-3-indolyl-beta-D-galactopyranoside

Units

|	
°C	degrees Celscius
bp	base pairs
h	hour
kb	kilobase
l	liter
M	molar
μ	micro
m	mili
min	min
ml	mililiters
mM	milimolar
rpm	revolutions per minute
s	seconds
U	unit
vol	volume

7.2 Vectors

7.2.1 BRAF pCR2.1 vector map

This vector contains full length medaka braf cloned by the strategy described in section 4.1.1.1
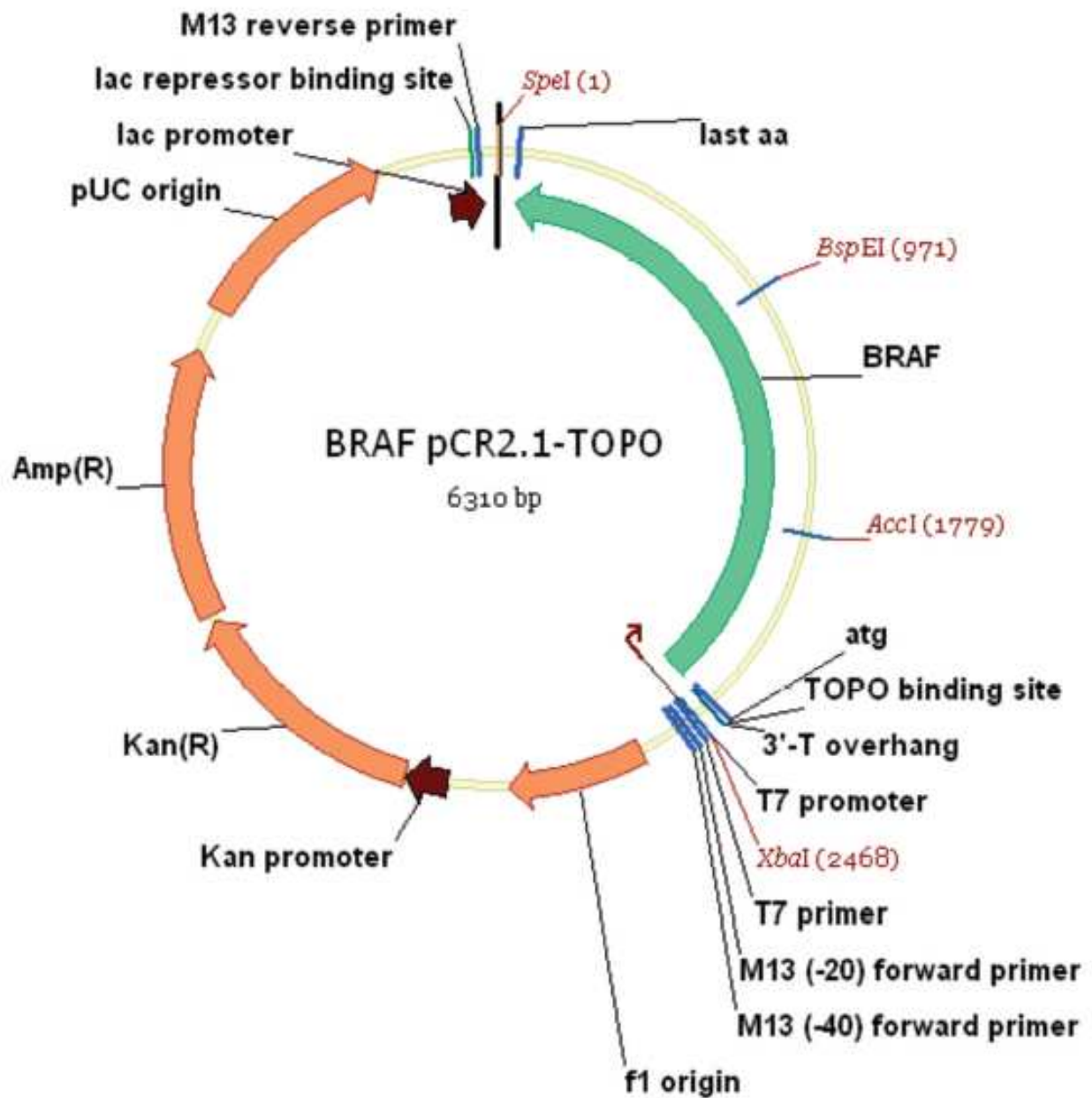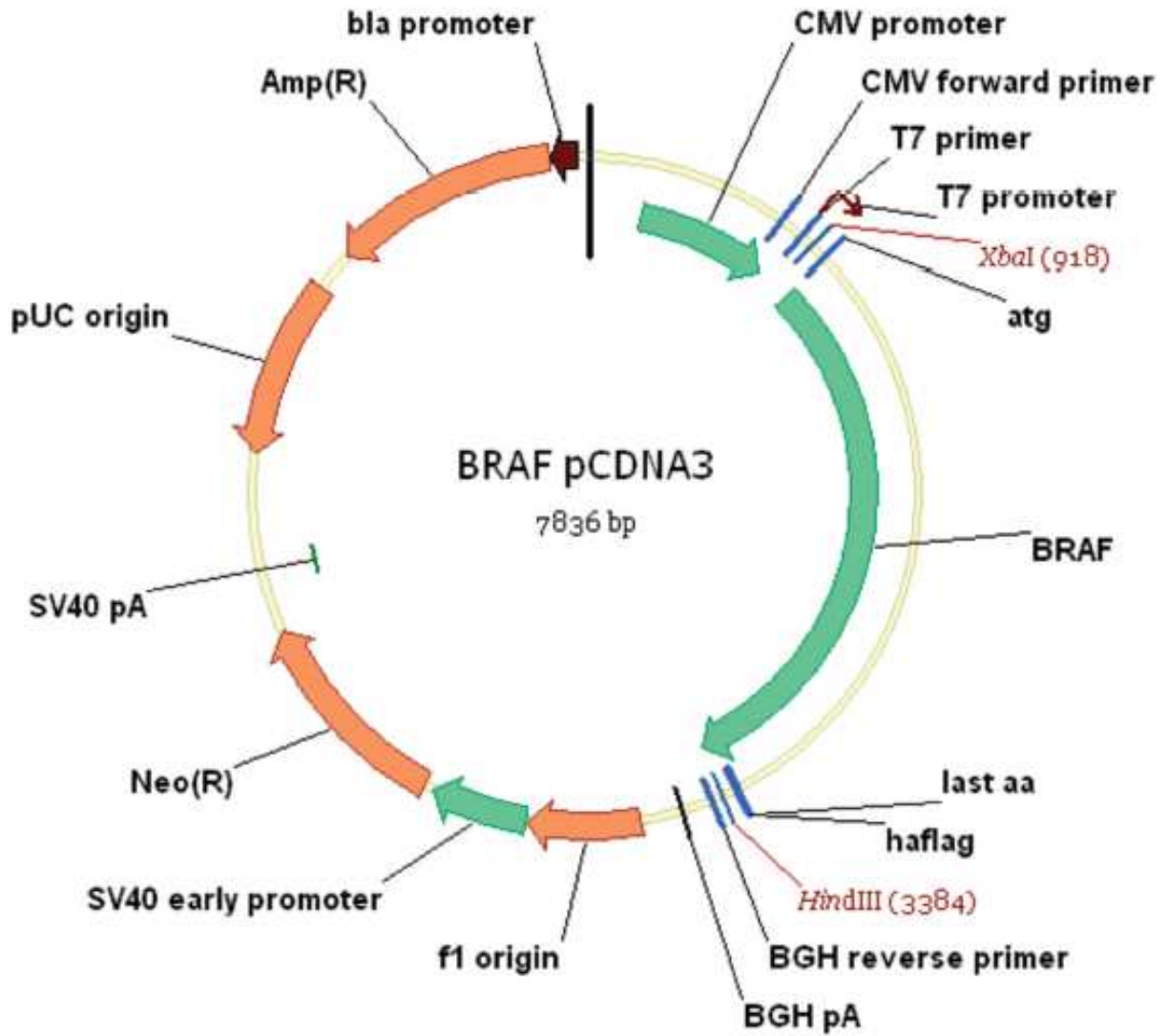
7.2.2 BRAF pSceI MITF vector map

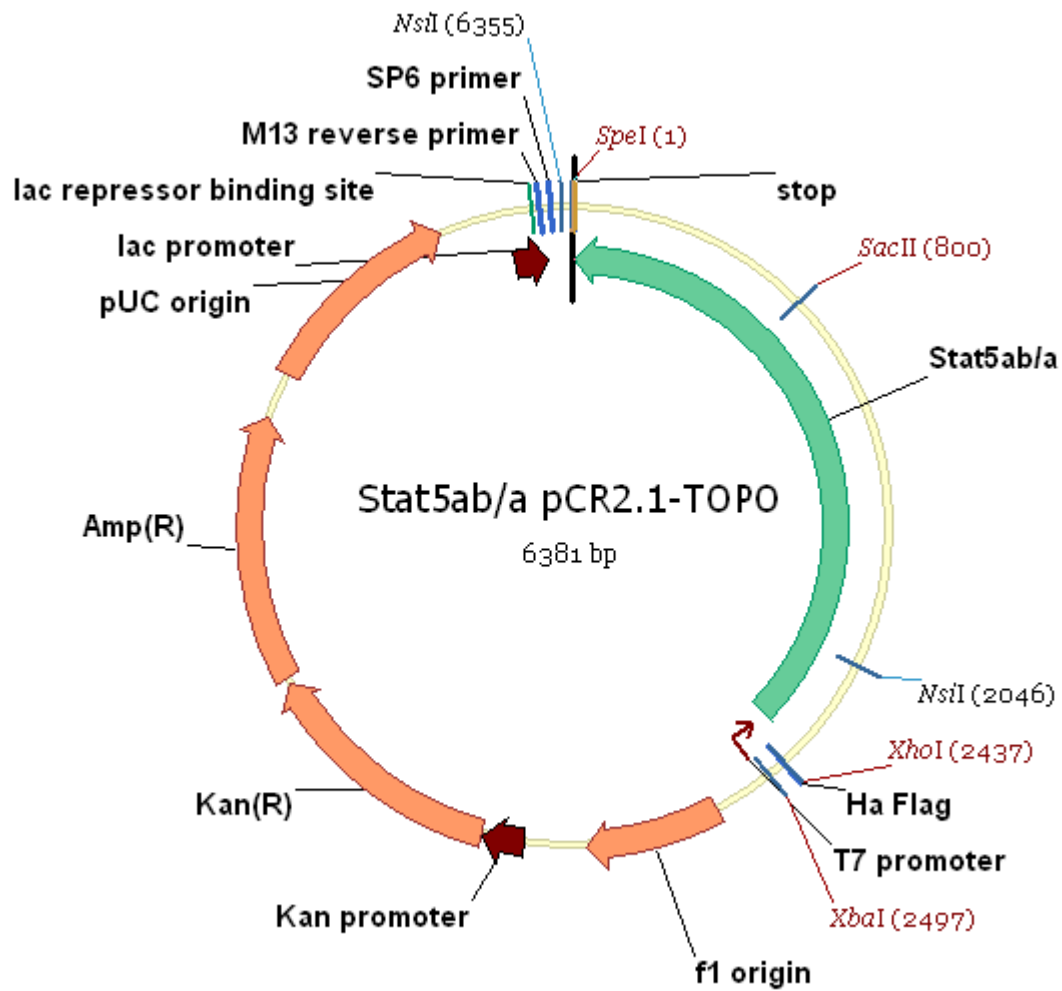This vector contains full length medaka braf sub-cloned by the strategy described in section 4.1.1.3
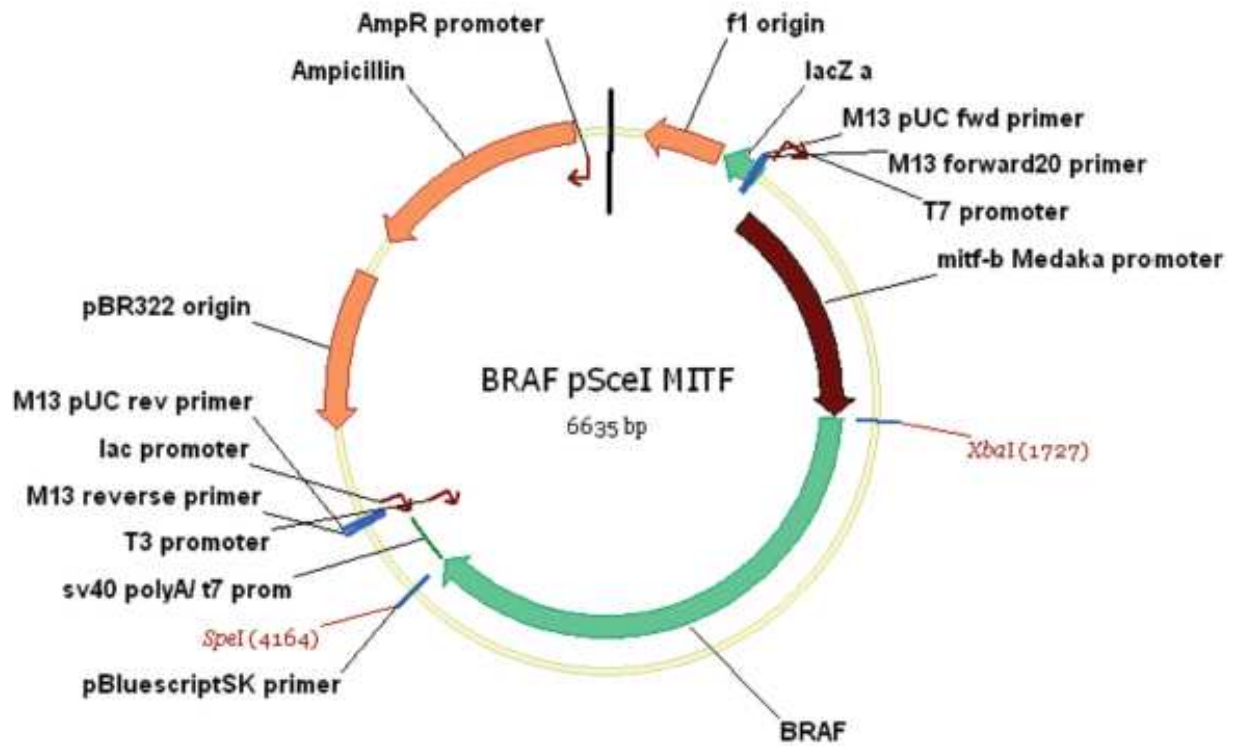
7.2.3 BRAF pCDNA3 vector map

This vector contains full length medaka braf sub-cloned by the strategy described in section 4.1.1.3
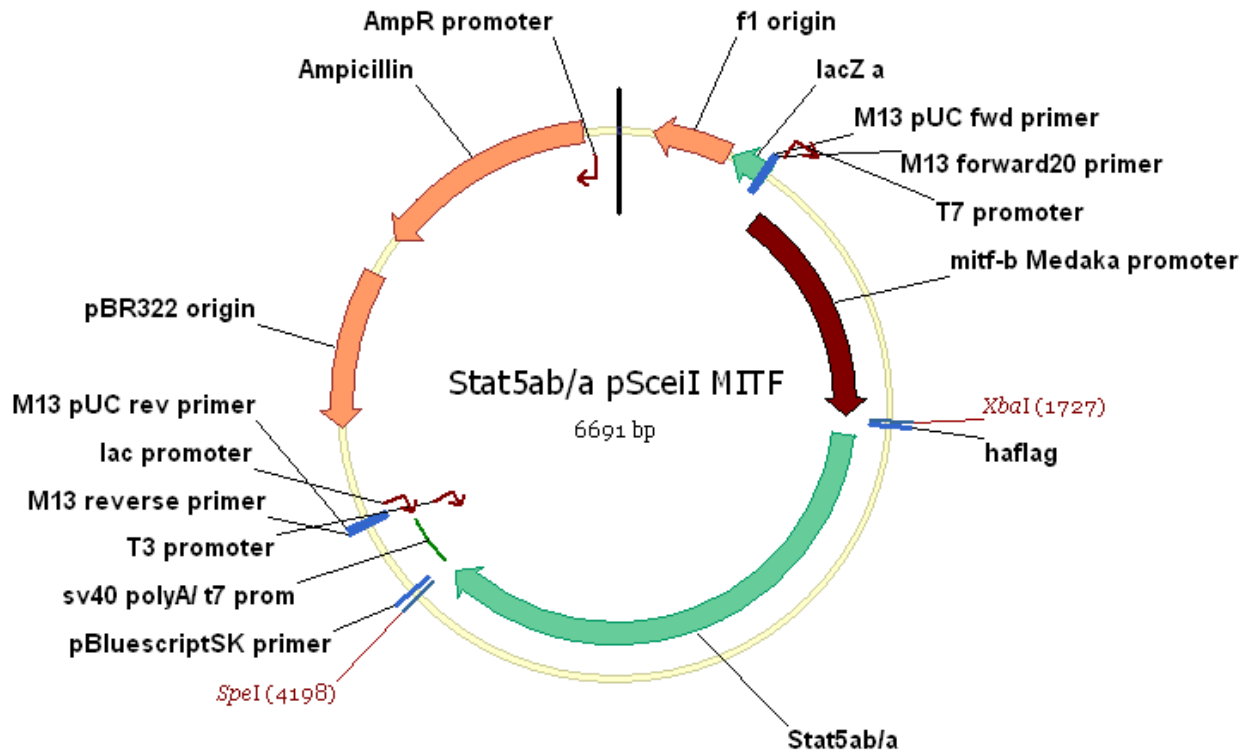
7.2.4 Stat5ab/a pCR2.1 vector map

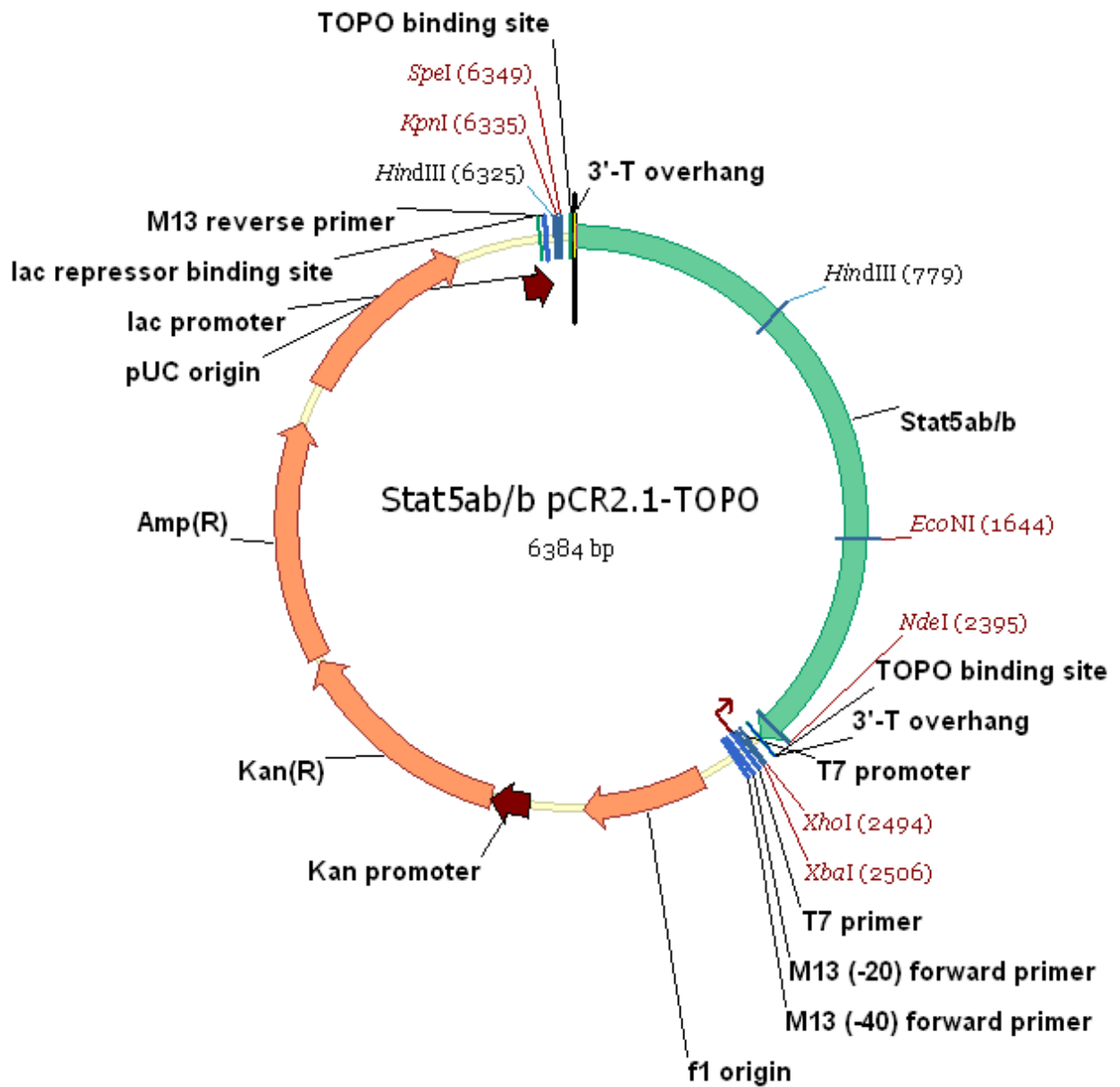This vector contains full length medaka Stat5ab/a cloned by the strategy described in section 4.2.1.1

7.2.5 Stat5ab/a pSceI MITF vector map

This vector contains full length medaka Stat5ab/a sub-cloned by the strategy described in section 4.2.1.4
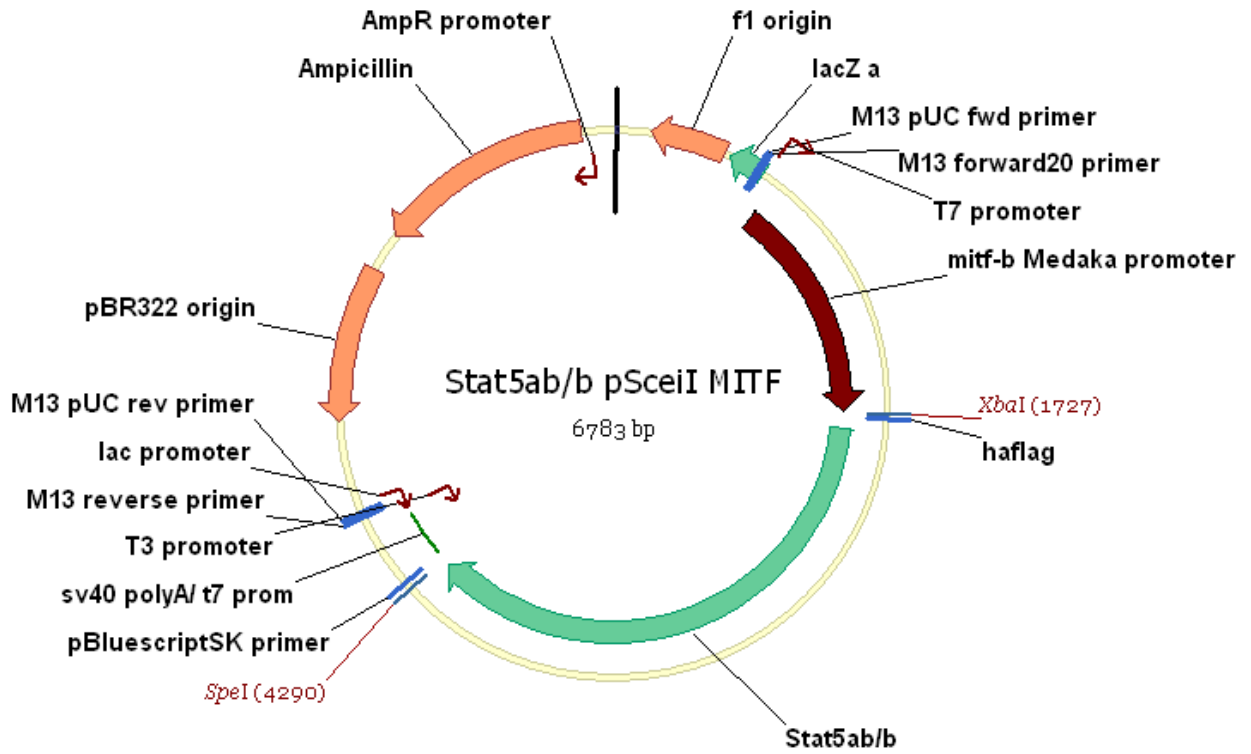

Stat5ab/a pSceI MITF
6691 bp

7.2.6 Stat5ab/b pCR2.1 vector map

This vector contains full length medaka Stat5ab/a cloned by the strategy described in section
4.2.1.2

7.2.7 Stat5ab/b pSceI MITF vector map

This vector contains full length medaka Stat5ab/a cloned by the strategy described in section 4.2.1.4

7.3 Curriculum vitae

<u>Personal details</u>

Name	Luciana Alcantarino Menescal
Address	Tiepolostrasse 4. 97070. Würzburg, Germany.
Telephone	
E-mail	lumenescal@yahoo.com.br

<u>Education</u>

Oct 07 - present   University of Würzburg, Germany
Physiological Chemistry I Department
PhD thesis: "*In vivo* characterization of genetic factors involved in Xmrk driven melanoma formation in Medaka *(Oryzias latipes):* a closer look at *braf, Stat5* and *c-myc*"

Jun 04 - Jun 06   Federal University of Pará, Brazil
Master in Genetics and Molecular Biology
Thesis title: "Myostatin gene expression analyses in different muscles in Nelore cow breed"

Mar 00 - Mar 04   Federal University of Pará, Brazil
Diploma in Biomedicine
Final work title: "Genetic diversity of red-bellied Titis (*Callicebus moloch*) from Eastern Amazonia based on microsatellite markers"

<u>Other Academic and Professional Activities</u>

Dec 06 - Jun 07   Lecturer in the University of Vale do Acaraú, Brazil (cytology and genetics)

Jun 03 - Mar 04   Research trainee at the DNA Polymorphisms Laboratory at the Federal University of Pará, Brazil (population genetics in primates)

Dec 02 - Apr 03   Internship at the Casa Marina Resort. Key West, USA.

Nov 01 to Oct 02   Research trainee at the Evandro Chagas Institute, Brazil (malaria research)

<u>Fellowships</u>

Apr 11 - Sep 11   STIBET Abschlußbeihilfen from DAAD

Oct 07 - Mar 11   Deutsche Forschungsgemeinschaft (DFG) PhD fellowship

Mar 04 - Jun 06   Master fellowship from CAPES (government agency linked to the Brazilian Ministry of Education)

Languagues

Mother tongue   **Portuguese** (fluent)

Second languages   **English** (fluent)
                        German (proficient)
                        Spanish (good)

Conference Abstracts

2010 - Autumm School 2010 – The Puzzling World of Cancer by the Integrated Graduate College (IGC) of the SFB Transregio 17 "Ras-dependent pathways in human cancer" exposing "A novel *in vivo* model for Braf function in the Medaka fish (Oryzias latipes)". Würzburg, Germany.

2010 - 5th International Symposium of the Graduate School of Life Sciences of the University of Würzburg exposing "A novel *in vivo* model for Braf function in the Medaka fish (Oryzias latipes)". Würzburg, Germany.

2010 - 16th Meeting of the European Society for Pigment Cell Research exposing "A novel *in vivo* model for Braf function in the Medaka fish (Oryzias latipes)". Hinxton, England.

2009 - 4th International Symposium of the Graduate School of Life Sciences of the University of Würzburg exposing "Insights on Stat5 and Braf function in malignant melanoma". Würzburg, Germany.

2004 - 50th National Genetics Congress exposing "Genetic Variability in Red-Bellied Titi Monkey (*Callicebus moloch*) from Tucurui's Environmental Protection Area in North Brazil using DNA microsatellite analysis". Florianopolis, Brazil.

Luciana Menescal

Würzburg, 26th February, 2012

7.4 Publications

Menescal, L. A. , Gonçalves, E. C., Silva, A., Ferrari, S. F. , Schneider, M. P. Genetic diversity of red-bellied Titis (Callicebus moloch) from Eastern Amazonia based on microsatellite markers. Biochem Genet. 2009**.** Apr;47(3-4):235-40

Menescal, L. A., Schmidt, C., Liedtke, D., Schartl, M. Liver Hyperplasia after tamoxifen induction of Myc in a transgenic medaka model. 2012. Diseases, Models and Mechanisms. (In revision)